

AD-774 142

A REVIEW OF THE X-22A VARIABLE STABILITY
AIRCRAFT AND RESEARCH FACILITY

J. Victor Labacqz, et al

Calspan Corporation

Prepared for:

Naval Air Systems Command

February 1974

DISTRIBUTED BY:

NTIS

National Technical Information Service
U. S. DEPARTMENT OF COMMERCE
5285 Port Royal Road, Springfield Va. 22151

UNCLASSIFIED

Security Classification

AD-774142

DOCUMENT CONTROL DATA - R & D

(Security classification of title, body of abstract and indexing annotation must be entered when the overall report is classified)

1. ORIGINATING ACTIVITY (Corporate author) Calspan Corporation Box 235 Buffalo, New York 14221	2a. REPORT SECURITY CLASSIFICATION
	2b. GROUP

3. REPORT TITLE
A Review of the X-22A Variable Stability Aircraft and Research Facility

4. DESCRIPTIVE NOTES (Type of report and inclusive dates)
Final Report

5. AUTHOR(S) (First name, middle initial, last name)
J. Victor Lebacqz, Rogers E. Smith, Robert C. Radford

6. REPORT DATE February 1974	7a. TOTAL NO. OF PAGES 92 98	7b. NO. OF REFS 10
---------------------------------	---------------------------------	-----------------------

8a. CONTRACT OR GRANT NO. N00019-72-C-0417 b. PROJECT NO. c. d.	9a. ORIGINATOR'S REPORT NUMBER(S) AK-5130-F-2
	9b. OTHER REPORT NO(S) (Any other numbers that may be assigned this report)

10. DISTRIBUTION STATEMENT
Approved for Public Release; Distribution Unlimited

11. SUPPLEMENTARY NOTES	12. SPONSORING MILITARY ACTIVITY Naval Air Systems Command Department of the Navy
-------------------------	---

13. ABSTRACT

The variable stability X-22A aircraft and associated research facilities represent a unique capability to perform V/STOL flying qualities research. The demonstrated fixed-operating point capabilities of the aircraft's variable stability system are reviewed, and the recent extension of these capabilities for hover and transition is documented in detail. The report also contains summary descriptions of the ground simulator facility, the X-22A aircraft systems, and data processing and analysis procedures.

Reproduced by
NATIONAL TECHNICAL
INFORMATION SERVICE
U S Department of Commerce
Springfield VA 22151

DD FORM 1 NOV 65 1473

UNCLASSIFIED

Security Classification

14 KEY WORDS	LINK A		LINK B		LINK C	
	ROLE	WT	ROLE	WT	ROLE	WT
	X-22A Variable Stability Aircraft					
V/STOLL Flying Qualities						
X-22A Ground Simulator						
Fixed-Operating Point						
Hover Capabilities						
Transition Capabilities						
X-22A Data Processing						

is

FOREWORD

This report was prepared for the United States Naval Air Systems Command, the National Aeronautics and Space Administration Langley Research Center, the Federal Aviation Agency, and the United States Air Force Flight Dynamics Laboratory under Contract Number N00019-72-C-0417 by Calspan Corporation (formerly Cornell Aeronautical Laboratory, Inc.), Buffalo, New York.

The research reported herein was performed by the Flight Research Department of Calspan. Mr. J. L. Beilman was the Program Manager for the programs discussed. Technical monitoring was performed by the X-22A Flight Research Steering Group, chaired by Mr. R. Siewert of the Naval Air Systems Command. The authors are grateful to Mr. Siewert and the members of the Steering Group for their interest and support, and wish to acknowledge their appreciation to: Mr. C. Mazza, NADC; Messrs. R. J. Tapscott, J. Garren, and J. Brewer, NASA; Mr. J. Teplitz, FAA; and Mr. T. L. Neighbor, USAF.

The authors are particularly grateful to Mr. E. W. Aiken, who performed the control augmentation design discussed in Section II, Mr. J. L. Beilman, who aided in and reviewed the w-LORAS calibrations discussed in Section II, and Mrs. J. A. Martino, who was Technical Editor for this report. We also extend our appreciation to all the individuals at Calspan involved in the X-22A programs for their many outstanding contributions.

TABLE OF CONTENTS

<u>Section</u>		<u>Page</u>
I	INTRODUCTION.	1
II	FLIGHT SIMULATION CAPABILITY.	3
	2.1 Review of Fixed-Operating Point Flight Simulation Capabilities.	3
	2.2 Development of Transition/Hover Flight Simulation Capability.	7
	2.3 Flight Demonstrations.	19
III	GROUND SIMULATION CAPABILITY.	38
	3.1 Equipment and Mechanization.	38
	3.2 Experimental Applications.	43
IV	CONCLUDING REMARKS AND RECOMMENDATIONS.	46
 <u>Appendix</u>		
I	X-22A VARIABLE STABILITY AIRCRAFT	47
II	DATA ACQUISITION AND PROCESSING SYSTEM.	66
III	IDENTIFICATION OF SIMULATED CHARACTERISTICS	71
IV	FLIGHT DEMONSTRATIONS	83
	REFERENCES	87
	GLOSSARY OF SYMBOLS AND ABBREVIATIONS.	88

LIST OF ILLUSTRATIONS

<u>Figure</u>		<u>Page</u>
2-1	Summary of Short Term Dynamics for Evaluation Configurations in Task I	4
2-2	Deceleration Transition, Level Flight 30° ⇒ 90°, Flight F-87	20
2-3	Deceleration Transition, $\theta = -10^\circ$, 30° ⇒ 90°, Flight F-92	23
2-4	Decelerating Transition, $\theta = -10^\circ$, 30° ⇒ 90°, Flight F-92	26
2-5	Decelerating Transition, $\theta = -10^\circ$, 15° ⇒ 90°, Flight F-92	29
2-6	Decelerating Transition, $\theta = -10^\circ$, 15° ⇒ 90°, Flight F-92	32
2-7	Decelerating Transition, $\theta = -10^\circ$, 0° ⇒ 90°, Flight F-92.	35
3-1	X-22A Ground Simulator	39
3-2	X-22A Ground Simulator Functional Block Diagram.	40
3-3	X-22A Ground Simulator Cockpit	41
3-4	X-22A Ground Simulator Instrument Display.	44

Section I
INTRODUCTION

The X-22A variable stability V/STOL aircraft is a versatile and unique research tool which can be used to investigate the flying qualities of a wide range of both STOL and V/STOL aircraft. Since the initiation of flying qualities experiments using this aircraft, the demonstrated capabilities of the machine itself, of the data gathering and analysis procedures, and of the supporting research facility have been continuously increased. Chronologically, the major developments may be summarized as follows:

- Task I: first use of the variable stability system (VSS) in a flying qualities program, at two fixed operating points ($\lambda = 50^\circ$, $V_0 = 65$ kts; $\lambda = 30^\circ$, $V_0 = 80$ kts), in which a wide range of longitudinal dynamics was investigated (Reference 1).
- Task I: development and implementation of a comprehensive digital data acquisition and flight safety monitoring system (Reference 2).
- Task I: first use on a flying qualities program of a digital identification technique developed expressly for the X-22A (Reference 3).
- Task II: extensive range of lateral-directional dynamic characteristics investigated at fixed operating point ($\lambda = 50^\circ$, $V_0 = 65$ kts), plus greatly increased reliance on digital identification and data reduction procedures (References 4 and 5).
- Task II: investigation and expansion of the flight envelope for VSS operation in transition and hover which led to full decelerating transitions and a vertical landing while operating on the VSS (documented in this report).
- Ground Simulator: design and development of a fixed-base ground simulator of the X-22A and a subsequent exploratory research experiment investigating transition (References 6 and 7).

This report has the two following purposes:

1. To provide summary descriptions of the X-22A aircraft and the research facilities associated with it.
2. To document specifically the sub-experiment conducted during the Task II flight program aimed at demonstrating capabilities of the X-22A to perform transition and hover flying qualities experiments using the variable stability system (VSS).

The body of the report is concerned with the simulation capability of the aircraft and the ground simulator, while the appendices present supporting data and information. Specifically, Section II presents a review of the dynamic characteristics at fixed operating point that have been simulated during the first two flying qualities experiments, and describes in detail the development of the hover and transition capabilities of the X-22A while operating on the VSS. Section III presents a review of the recently developed X-22A ground simulation facility. Appendix I discusses the characteristics of the basic X-22A and its variable stability system in detail, Appendix II describes the Digital Data Acquisition System and associated data processing capabilities, and Appendix III reviews the digital identification technique developed for the X-22A. Appendix IV documents the flight test plan used to demonstrate the X-22A variable stability capability to pilots selected by the X-22A Flight Research Steering Group.

Section II

FLIGHT SIMULATION CAPABILITY

This section reviews the simulation capabilities of the variable stability X-22A aircraft, with the emphasis of the discussion being on dynamics and capabilities that have been demonstrated in flight and, where appropriate, the range of gains in the VSS required to achieve these dynamics. The discussion is divided into two parts. The first part reviews briefly the ranges of dynamics investigated in the first two STOL flying qualities experiments performed using the X-22A (Tasks I and II, References 1 and 4). The second part documents in detail the sub-experiment performed during the Task II flight program to investigate and develop the capabilities of the aircraft for hover and transition work using the VSS; this documentation is not included elsewhere, and hence this part of this section constitutes the requisite "final report" on the sub-experiment.

2.1 REVIEW OF FIXED-OPERATING POINT FLIGHT SIMULATION CAPABILITIES

The first flying qualities program using the X-22A concentrated on exploring the influence of the longitudinal short term response dynamics on flying qualities for STOL landing approach (Reference 1). Two flight conditions were investigated ($\lambda = 50^\circ$, $V_o = 65$ kts and $\lambda = 30^\circ$, $V_o = 80$ kts), with approach angles varying from $\gamma = -6^\circ$ to $\gamma = -9^\circ$. The short term response dynamics are primarily a function of the stability derivatives M_w and M_q , and hence variations in these derivatives constituted the basic investigation; in addition, the speed stability M_u was varied if necessary to maintain the long-term response nearly stable, and the pilot selected the control sensitivity $M_{\delta_{ES}}$. Of the total number of response-feedback variables available in the X-22A (Appendix I), then, this experiment investigated ranges of Δ_{ES}/α_v , Δ_{ES}/q , Δ_{ES}/u , and Δ_{ES}/δ_{ES} .

Using these gains the resulting range of short-term dynamics achieved for both flight conditions investigated is shown on Figure 2-1. The numbers correspond to the configuration identifier used in Reference 1. As can be seen, the resulting dynamics varied over $0.8 \text{ rad/sec} \leq \omega_{ST} \leq 2.6 \text{ rad/sec}$, $0.04 < \zeta_{ST} < 0.8$, and $0.21 \text{ rad/sec} \leq 2 \zeta_{ST} \omega_{ST} \leq 1.9 \text{ rad/sec}$. No limitations of the VSS in these channels were observed for this range of gains. These results represent the range of dynamics achieved to date and should not be viewed as limiting values of the VSS.

The second X-22A flying qualities program, conducted as the primary experiment for Task II, extended the demonstrated capability of the lateral-directional VSS channels significantly. This experiment investigated the effects of lateral-directional flying qualities parameters and their interaction with control power requirements on STOL flying qualities in landing approach ($V_o = 65$ kts, $\lambda = -7.5^\circ$) (Reference 4). Of primary interest in the investigation were roll mode time constant, Dutch roll undamped natural frequency, roll-to-sideslip ratio at the Dutch roll frequency, and yaw due to

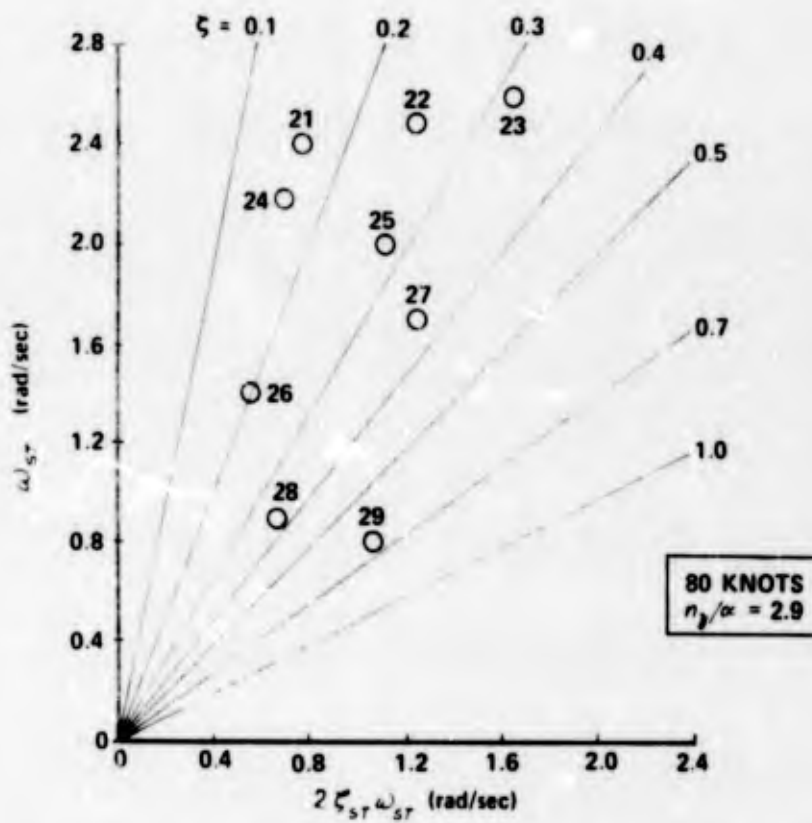
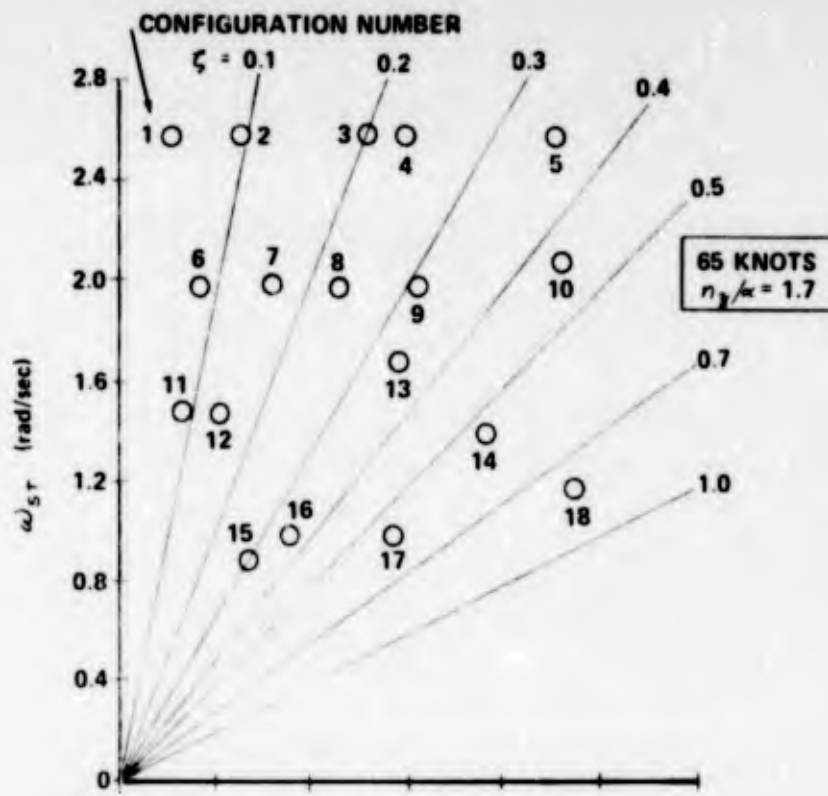


Figure 2-1 SUMMARY OF SHORT TERM DYNAMICS FOR EVALUATION CONFIGURATIONS IN TASK I

aileron, as well as the effects of limited roll control power for various combinations of these parameters. These parameters are nonlinear functions of all the stability derivatives in the lateral-directional characteristic matrix, and hence almost all of the available channels in the VSS were used.

The range of achieved dynamics is shown in Table 2-1. The dynamic characteristics vary from roll modes highly augmented over that of the basic X-22A (Configurations 1-3) to ones that are deaugmented (Configurations 6 and 7), from dihedral effect (L'_p) near that of the basic aircraft (Configuration 3) to highly deaugmented (Configuration 6), and from directional stiffnesses that are well augmented (Configurations 2-7) to one that is somewhat deaugmented (Configuration 1). In this experiment as in Task I, no limitations of VSS capability were observed for the feedback gain ranges used. Again these results represent achieved values and should not be viewed as the limit of the VSS.

Table 2-1

CHARACTERISTIC MODAL PARAMETER VALUES

Base Config.	ζ_r	ζ_s	ω_d	ζ_d	$ \phi/\beta _d$
1	.57	11	.40	.16	1.54
2	.39	-128	1.43	.22	.46
3	.31	9	1.30	.17	1.28
4	.72	-34	1.55	.23	.30
5	.78	-37	1.27	.18	1.42
6	1.57	-26	1.45	.20	.40
7	1.31	23	1.27	.23	1.27

At the 65 knots, $\lambda = 50$ deg flight conditions, the X-22A has the following control powers:

$$M'_{ES\ MAX} = 1.8 \text{ rad/sec}^2$$

$$L'_{AS\ MAX} = 1.8 \text{ rad/sec}^2$$

$$N'_{RP\ MAX} = 0.8 \text{ rad/sec}^2$$

The possible range of force gradients is extensive for all the evaluation pilot's controls, ranging from ~ 1.5 lb/in. to a stiff stick for pitch and roll control and from 7 lb/in. to no displacement rudders (stiff) for the pedals. Frequency response data for the feel system shows that the systems are approximately second order with $\omega_{FS} \doteq 2$ Hz and $\zeta_{FS} \doteq 0.6$, which is considered sufficiently fast so as not to be a factor for low speed simulation work.

In summary, then, the two flying qualities experiments at fixed-operating point that have been performed using the X-22A have exercised most of the capabilities of the aircraft's variable stability system. These capabilities were used to simulate a wide range of dynamic characteristics which span the range of those that might reasonably be expected to occur in STOL aircraft at the constant flight conditions investigated. No limitations in any of the VSS channels were observed in either flight program, and it may be concluded that the flight conditions are sufficiently extensive to investigate in depth STOL flying qualities.

2.2 DEVELOPMENT OF TRANSITION/HOVER FLIGHT SIMULATION CAPABILITY

The Task II X-22A flight program involved two experiments conducted concurrently. The primary experiment was the lateral-directional flying qualities experiment discussed in Section 2.1 and reported upon in Reference 4. In addition to this primary experiment, a flight investigation of limited extent was performed to expand the X-22A capabilities to perform flying qualities research in transition and hover. The primary objectives of this investigation may be summarized as follows:

- Installation and checkout of a w -LORAS to provide vertical damping simulation capability at low speeds and hover.
- Redefinition of the allowable altitude for hovering while controlling the aircraft through the VSS to allow realistic flying qualities experiments in hover.
- Preliminary assessment of stability and control augmentation schemes for hover using the VSS to provide background data for future flying qualities experiments in hover.
- Definition through flight test of reference transition profiles within the operational boundaries of the aircraft to provide a guide for variable stability research in transition.

These objectives defined the four phases of the experiment, and this section of the report reviews the reasons for each of them, discusses the methods of investigation used, and documents the results that were obtained for future reference.

2.2.1 Installation of w -LORAS

In order to perform useful flying qualities research in the hover and near-hover flight regimes, it is necessary to be able to investigate the effects of vertical velocity damping (Z_w) and pitching moment due to vertical velocity (M_w). Conventional aerodynamic sensors of vertical velocity (angle of attack vanes) become useless for generating feedback signals as forward velocity approaches zero because, even if they continue to track the local air flow correctly, the measured angles become too large. It is therefore necessary to generate a w -velocity signal in some other way.

One possibility that has been suggested, and which was originally included in the X-22A VSS, involves integration of the normal acceleration signal to obtain an approximate "inertial" vertical velocity signal. This approach has several disadvantages, however: (1) the accelerometer signal is subject to stiction biases, (2) the signal must be corrected on-line for pitch and roll attitudes in order to generate the correct velocity information, and (3) the response to w -gusts of the simulated aircraft will not be properly modeled (Appendix IV, Reference 1).

The necessity for an accurate measurement of vertical airspeed therefore resulted in the installation on the nose boom of the aircraft of a LORAS II airspeed system oriented in the y - z plane of the aircraft during the course of this experiment. The LORAS II is an improved version of the u -LORAS mounted on the vertical tail of the airplane (see Figures I-14 and I-15 of Appendix I), and uses essentially the same operating principles to measure and resolve relative airspeeds with linear resolution down to zero airspeed (Reference 8). The y - z orientation was selected for checkout in order to provide an additional measurement of body-axis lateral velocity; it was known that the lateral velocity information from the u -LORAS on the tail is compromised by the tail flow-field, and since the location of the LORAS II (w -LORAS) on the nose boom should be relatively free of such local flow effects, this orientation was chosen as being more useful than an x - z orientation, which would provide an additional measurement of longitudinal airspeed.

Calibration data for the w -LORAS at low forward velocities were obtained primarily on Flights 86F and 87F during the Task II flight program. The procedure used to obtain these data involved setting up trimmed forward velocities of approximately 0, 10, 20 and 30 kts at a constant altitude above the runway (~ 100 ft), and then performing forced pitching oscillations. If the velocity and altitude are maintained constant, this procedure results in simple and straightforward calibrations of both the angle of attack vane and of the w -LORAS. The calibration calculation results should be viewed as substantiating the fact that the w -LORAS is functioning correctly, however, and should not be considered final. The reason for this qualification involves the orientation of the w -LORAS, as installed and checked out, in the y - z plane.

The w -LORAS flight data at longitudinal velocities above approximately 20 kts show marked degradations in signal-to-noise ratio and inconsistencies with the angle of attack measurement. These inconsistencies are attributable to the fact that the primary component of the velocity is normal to the plane of the w -LORAS rotation in forward flight; the out-of-plane inflow angles at the heads of the instrument therefore become large as forward velocity increases and likely lead to flow separation and consequent pressure fluctuations and distortions. While it is true that the angle of attack measurement from the vane is of good quality for these higher velocities, it is apparent that some form of complementary filtering as a function of airspeed would be required to use the appropriate measurement in the VSS. A more desirable alternative is to change the installation of the w -LORAS to the x - z plane, in which case the forward velocity vector would be in the plane of rotation and the excessive out-of-plane inflow angles would be eliminated.

Changing the orientation to the x - z plane, of course, results in measurements of body-axis longitudinal and vertical velocities, and so an additional measurement of lateral velocity is no longer available. As was noted in Reference 4, however, the flow effects around the tail not only affect the lateral velocity measurement but also compromise the longitudinal

velocity measurement with the u -LORAS, in sideslipped flight conditions. An additional measurement of longitudinal velocity from the w -LORAS would therefore be beneficial.

The primary results relevant to this phase of the experiment may be summarized as follows:

- A w -LORAS was installed on the nose-boom of the X-22A to provide a useable measure of air velocity relative to the aircraft vertical body axis at forward velocities down to zero.
- Calibration data taken at low forward velocities demonstrated that the w -LORAS functioned correctly and measured relative vertical velocity as desired.
- Degradations of the quality of the vertical velocity measurements as forward speed increased were found, and it is recommended that the orientation of the w -LORAS be changed to the x-z plane.

2.2.2 Flight Envelope for Hover on VSS

During the Task I program and at the beginning of the Task II program, the X-22A aircraft was restricted to hovering above a minimum altitude of 1000 feet AGL when operating on the variable stability system (Reference 9). This restriction was based primarily on lack of information concerning two areas of difficulty which might compromise safe ejection capability:

1. Re-engagement of the primary artificial feel and trim (PAFT) system upon VSS disengagement. Information was required on the difficulty of controlling the aircraft PAFT-off in hover and on re-engaging the PAFT (in forward flight, the stick must essentially be released to re-engage the PAFT).
2. Effect of a feedforward system (FFS) actuator hardover. (See Appendix I for a discussion of the FFS.) In hover, the critical situation would be a blade FFS actuator hardover ($\pm 3^\circ$ full authority), which would produce rolling and/or pitching disturbances. Information was required on the extent of these disturbances prior to correction by the safety pilot, as well as concomitant altitude loss, rate of sink, etc.

This altitude restriction would be unacceptable for any flying qualities research program in hover with a representative task, and hence the objective of the second phase of the experiment was to investigate the two areas of difficulty in order to ascertain their effects and thereby reduce if possible the altitude restriction.

To investigate these areas, practice PAFT engage/disengagements and simulated FFS hardovers in hover were initiated at altitudes above 1000 ft AGL; transient characteristics such as altitude loss and attitude changes were monitored on-line in the Mobile Telemetry Van, and, in combination with the comments of the pilots, used as a decision basis for reducing the altitude progressively. The PAFT disengagement/engagement procedure was straightforward, in that the VSS was "dumped" at arbitrary times by the evaluation pilot, which gave the aircraft to the safety pilot with the PAFT disengaged. The FFS hardovers were simulated by wiring auxiliary switches to the FFS servos to command either one-half or full authority inputs. Four of these switches were installed in the cockpit to provide the following inputs:

Evaluation Pilot (EP): $\pm 1.5^\circ$ left aft duct blades
 $\pm 3^\circ$ right front duct blades
 $\pm 1.5^\circ$ left front duct blades
 $\pm 3^\circ$ right aft duct blades

In addition to investigating these areas in hovering flight, this phase of the experiment performed preliminary investigations relevant to the two remaining phases. Practice inbound ($\lambda \Rightarrow 90^\circ$) and outbound ($\lambda \Rightarrow 0^\circ$) transitions in level flight were initiated at safe altitudes to investigate the effects of VSS disengagements midway through a decelerating transition, and the non-aerodynamic VSS feedback gains (i.e., rates and attitudes) were exercised in hover.

The following listing documents the results obtained during this phase in a chronological fashion by flight number.

- Flight F-55
- engage fly-by-wire (FBW) in hover at 1000 ft AGL
 - engage VSS in hover at 1000 ft AGL. All VSS feedback gains at zero except:
 $\Delta \epsilon / q = -3.9$ in./rad/sec
 $\Delta \eta / p = -2.2$ in./rad/sec
 $\Delta \xi / r = -6.4$ in./rad/sec
 - VSS transition outbound at 1000 ft AGL, $90^\circ \Rightarrow 30^\circ$.

Flight F-56

- VSS transition inbound at 800 ft AGL, $50^\circ \Rightarrow 90^\circ$, with VSS gains as above.
- VSS hover, EP inputs to give 3° blade deflections followed by intentional dump of system. SP recovered with no difficulty, no altitude loss.
- SP hovered aircraft with PAFT off, encountered no difficulties although had some tendency to over-control.
- VSS hover at 500 ft AGL, EP inputs followed by dumps, up to 15° roll and 10° pitch attitudes, SP had no difficulty in recovering immediately, no loss of altitude.
- VSS hover for FFS hardover simulation:
 - a) SP inputs $+1.5^\circ \beta_{LF}$, EP overpowers
 - b) SP inputs $+3^\circ \beta_{RA}$, EP overpowers
 - c) EP inputs $+3^\circ \beta_{RF}$ and dumps system, EP recovers with no difficulty or altitude loss, max roll attitude $\sim 5^\circ$, negligible pitch attitude.
- VSS transition outbound, $90^\circ \Rightarrow 15^\circ$.

Flight F-65

- VSS transition inbound, gains as in F-55, $15^\circ \Rightarrow 45^\circ$ followed by EP dump of system. No noticeable transients, SP transitioned outbound to 30° .
- VSS transition inbound, $30^\circ \Rightarrow 70^\circ$ followed by EP dump of system. No noticeable transients, SP transitioned outbound to 30° with loss of ~ 150 ft altitude.
- VSS transition inbound, $30^\circ \Rightarrow 80^\circ$ followed by EP dump of system. No noticeable transients, SP transitioned inbound to 90° with no difficulties.
- VSS hover, descend to 200 ft AGL, EP dump of system, SP re-engages PAFT with no difficulty.
- VSS hover, descend to 50 ft AGL, maneuvers on system, dump of system with no transients, SP re-engages PAFT with no difficulty, no altitude loss.
- VSS hover, descend to 35 ft AGL, dump of system with no transients, SP performs vertical landing.

Flight F-69

- VSS transition outbound, $50^\circ \Rightarrow 30^\circ$, gains as in 87F.
- VSS transition inbound on final approach, $30^\circ \Rightarrow 50^\circ$.
- VSS transition inbound at 200 ft AGL along runway $50^\circ \Rightarrow 81^\circ$.
- VSS transition inbound while moving to runway intersection with taxiway Q, $81^\circ \Rightarrow 90^\circ$.

- VSS investigation of feedback gain authorities in hover, 200 ft AGL (the numbers indicate digitrol values for standard unit gains of Task II; 50 = no gain)
 - Δ_{ES}/q : 50 \Rightarrow 20, definite change in damping
 - $\Delta_{AS}/\dot{\phi}$: 50 \Rightarrow 20, definite change in damping
 - $\Delta_{RP}/\dot{\psi}$: 50 \Rightarrow 30, definite change in damping
 - Δ_{ES}/θ : 50 \Rightarrow 20, very powerful attitude hold
 - $\Delta_{AS}/\dot{\theta}$: 50 \Rightarrow 00, noticeable but weak attitude hold
 - Δ_{RP}/ψ : 50 \Rightarrow 55, very powerful directional stability
 - $\Delta_{RP}/\dot{\psi}$: 50 \Rightarrow 70, aircraft rotated to heading of VSS engagement.
- VSS LANDING IN HOVER with gains:
 - $\Delta_{ES}/q = -3.9$ in/rad/sec
 - $\Delta_{AS}/\dot{\phi} = -2.2$ in/rad/sec
 - $\Delta_{RP}/\dot{\psi} = -6.4$ in/rad/sec

These results may be summarized by the following conclusions determined in this phase of the experiment:

- FSS hardovers in hover present no difficulties for safe recovery with minimum altitude loss, and do not induce large attitude changes.
- The fact that the PAFT does not automatically re-engage upon a VSS dump does not cause difficulties in recovery when in hover. In fact, it was found that the PAFT may be re-engaged more easily in hover than in forward flight; for example, it is not necessary to release the safety pilot's stick in hover as it is in forward flight.
- The minimum altitude of 1000 ft AGL for hover on the VSS was unrealistic. Safe operation is possible all the way down to touchdown on the VSS in hover, and a vertical landing was performed on the system.
- Level flight transitions on the VSS cause no difficulties when the system is dumped. It was found that the safety pilot should continue the transition inbound if the dump occurs at a duct angle greater than 65-70 degrees. The constant rate-only feedback gains were sufficient to perform VSS transitions.
- No difficulties were found in exercising the appropriate VSS feedback gains in hover, and all those investigated functioned properly.

2.2.3 Control Augmentation in Hover

The third phase of this experiment involved the implementation on the VSS of preliminary designs of stability and control augmentation for hover after the flight envelope for hover on the VSS had been expanded. This implementation, although qualitative in nature, was desirable in order to demonstrate the VSS capabilities in this flight regime to aid the design of future programs. In addition, the feedback gains synthesized for this investigation were also to be used for the transition investigation discussed in the next subsection.

Three basic hover augmentation schemes were designed for implementation: (1) rate augmentation and command in pitch, roll, and yaw, (2) attitude command in pitch and roll, and (3) a quasi-velocity command for the three translation body axis velocities. As these designs were exploratory in nature, the model of the basic X-22A used in the design process was that which is implemented on the X-22A Ground Simulator (Reference 7); this model is a fairly accurate representation on the X-22A in hover, and the use of it obviated the necessity for calibration records and subsequent identification of the actual aircraft, in the hover, on this flight program. The model, the selected gains and the resulting approximate transfer functions are given in Tables II-2 and II-3. Note specifically that the attitude and velocity command systems employ vertical velocity damping (the w/s_c transfer function) to test the use of the w -LORAS in the VSS. The notation in the tables implies that $K(s+a) \Rightarrow K(a)$ and $K(s^2+2\zeta\omega s+\omega^2) \Rightarrow K[\zeta; \omega]$.

Table II-2

LONGITUDINAL HOVER TRANSFER FUNCTIONS
FOR HOVER AUGMENTATION SCHEMES

CONFIGURATION	FEEDBACK GAINS REQUIRED (IN/RAD)	TRANSFER FUNCTIONS		
		θ/s_c	u/s_c	w/s_c
BASIC X-22A MODEL ($\lambda = 90^\circ$)	NONE	$\frac{M_{\delta_{es}}(.25)}{(1.0)[-38; 0.8]}$	$\frac{-g M_{\delta_{es}}}{(1.0)[-38; 0.8]}$	$\frac{Z_{\delta_c}}{(.17)}$
RATE CONTROL	$\Delta_{es}/q = -6.5$	$\frac{M_{\delta_{es}}(.25)}{(2.34)[.11; .52]}$	$\frac{-g M_{\delta_{es}}}{(2.34)[.11; .52]}$	$\frac{Z_{\delta_c}}{(.17)}$
ATTITUDE CONTROL	$\Delta_{es}/q = -6.5$ $\Delta_{es}/\theta = -12.5$ $\Delta_c/w = 0.35$	$\frac{M_{\delta_{es}}(.25)}{(.45)[.53; 1.9]}$	$\frac{-g M_{\delta_{es}}}{(.45)[.53; 1.9]}$	$\frac{Z_{\delta_c}}{(.94)}$
VELOCITY CONTROL	$\Delta_{es}/q = -6.5$ $\Delta_{es}/\theta = -6.5$ $\Delta_c/w = 0.35$	$\frac{M_{\delta_{es}}(.25)}{(1.0)[.68; 1.1]}$	$\frac{-g M_{\delta_{es}}}{(1.0)[.68; 1.1]}$	$\frac{Z_{\delta_c}}{(.94)}$

Table II-3

**LATERAL-DIRECTIONAL HOVER TRANSFER FUNCTIONS
FOR HOVER AUGMENTATION SCHEMES**

CONFIGURATION	FEEDBACK GAINS REQUIRED (INCH/RAD)	TRANSFER FUNCTIONS		
		ϕ/δ_{as}	v/δ_{as}	r/δ_{rp}
BASIC X-22A MODEL ($\lambda = 90^\circ$)	NONE	$\frac{L_{\delta_{as}} (.12)(.23)}{(1.19)(.098)[-35; 0.92]}$	$\frac{gL_{\delta_{as}} s}{(1.19)(.098)[-35; 0.92]}$	$\frac{N_{\delta_{rp}} (1.15)[-35; 0.89]}{(1.19)(.098)[-35; 0.92]}$
RATE CONTROL	$\Delta_{as/p} = -3.7$ $\Delta_{rp/r} = -6.15$	$\frac{L_{\delta_{as}} (.23)}{(1.8)[-0.01; 0.7]}$	$\frac{gL_{\delta_{as}}}{(1.8)[-0.01; 0.7]}$	$\frac{N_{\delta_{rp}} (1.95)[-0.03; 0.68]}{(1.2)(1.8)[-0.01; 0.7]}$
ATTITUDE CONTROL	$\Delta_{as/p} = -3.7$ $\Delta_{as/\phi} = -4.8$ $\Delta_{rp/r} = -6.15$	$\frac{L_{\delta_{as}} (.23)}{(.82)[.35; 1.2]}$	$\frac{gL_{\delta_{as}}}{(.82)[.35; 1.2]}$	$\frac{N_{\delta_{rp}} (1.0)[.39; 1.13]}{(1.4)(.82)[.35; 1.2]}$
VELOCITY CONTROL	$\Delta_{as/p} = -3.7$ $\Delta_{as/\phi} = -4.8$ $\Delta_{rp/r} = -6.15$	SAME AS ATTITUDE CONTROL		

It should be emphasized that these feedback gains are not the maximum available in the VSS, and the resulting transfer function control characteristics are therefore not optimized. The emphasis of the investigation was on the practicality of achieving these types of control systems on the X-22A.

The use of these control systems in flight was demonstrated on Flight F-86. Based on pilot commentary and on-line monitoring of the flight records, the following characteristics were evident. The rate control system provided approximately the same hover characteristics as the basic X-22A with $\frac{1}{2}$ SAS, which is to be expected since the gains chosen for the demonstration were approximately one half the SAS gains in pitch and roll. The attitude command system for pitch and roll provided good frequency characteristics, but the damping ratio was less than expected in roll, indicating that the roll damping derivative used in the ground simulator is too low. The attempt to increase the vertical velocity damping using ω -LORAS measurement was only marginally successful, primarily due to inadequate filtering of the high frequency noise on the measurement signal. Only about 1/5 of the planned gain authority was used, therefore, and so the effects of increased vertical damping could not be properly assessed. The longitudinal and lateral velocity command systems provided the first order responses desired to some extent, but they were compromised by a fairly lightly damped second order oscillation superposed on them.

The following conclusions relevant to this phase of the experiment may be drawn:

- The capability of the X-22A VSS to simulate rate and attitude control command systems was demonstrated satisfactorily.
- Feeding back the ω -LORAS signal to the collective stick to simulate different amounts of vertical damping requires more extensive filtering of the measurement signal to decrease noise in the system.
- The velocity command system requires more damping feedback than was used for this demonstration.

2.2.4 Reference Transition Profile

The objective of the final phase of this experiment was to obtain an appropriate reference transition profile to aid design studies for flying qualities research programs in transition. The definition of a reference profile for design studies is necessary in order to properly choose control augmentation strategy and command signals that will not force the aircraft out of its permissible flight envelope.

The decelerating transition flight envelope ($\lambda \Rightarrow 90^\circ$) is constrained primarily by combinations of many control and response variables that may lead to duct buffet. These variables include rate of descent, angle of attack (or pitch attitude), collective (δ_c) control position, duct angle (λ)

and reconversion rate ($\dot{\lambda}$), and forward velocity, as well as others which have less effect on the duct buffet. On a flight program of limited extent, it is clearly impossible to investigate the effects of all these variables independently. For this experiment, therefore, many of them were constrained to values that are representative of decelerating transition profiles that may be used for future research. Glide slope angle was constrained to $\theta = -7.5^\circ$ and $\theta = -10^\circ$ by performing visual approaches using the mirror-light landing aid discussed in Reference 4. The velocity-duct angle relationship was kept within reasonable bounds by performing the transitions at less than the maximum reconversion rate ($|\dot{\lambda}_{avg}| < 5$ deg/sec). In maximum rate reconversions, the velocity lags far behind the correct velocity-duct angle relationship for trim at a given λ ; by performing the reconversions through "beeping" the ducts to achieve an average rate of $\dot{\lambda} \approx -2$ to -3 degrees/sec, this relationship is more nearly satisfied. To aid in control of pitch attitude, the bulk of the transition work was performed on the VSS, both to demonstrate its capabilities and to provide the pilot with the attitude command system used in the hover investigation.

The bulk of the transition work was performed on two flights, with the first one including exploratory level-flight decelerating transitions on the VSS in level flight and then VFR descending decelerating partial transitions (VSS) at $\theta = -7.5^\circ$, while the second one investigated VFR descending decelerating transitions on the VSS at $\theta = -10^\circ$ all the way up to a full transition from $\lambda = 0$ deg to $\lambda = 90$ deg, and even attempted simulated IFR partial transitions. Representative time histories of the aircraft responses and control motions are shown in Figures 2-2 through 2-7. An annotated and abbreviated documentation of the results of the flights, including summarized pilot comments, is given in the following listing. Transition ranges are given in degrees of duct angle.

- Flight F-87
- Level flight, $15^\circ \Rightarrow 50^\circ$, VSS, rate command, continuous
"Airspeed lags way behind correct duct angle for continuous rate decelerating transitions. Got to $\lambda = 50^\circ$, still had 90 kts airspeed."
 - Level flight, $15^\circ \Rightarrow 50^\circ$, VSS, rate command, "beeping"
"Beeping the ducts allows closer correlation of airspeed and duct angle, and seems better."
 - Level flight, $50^\circ \Rightarrow 15^\circ$, VSS, attitude command, beeping
"There's a tremendous trim change required to get the nose up for $\lambda = 15^\circ$, and it's harder to do it with attitude command. Need more pitch sensitivity" (Note: the pitch gearing was not increased for this flight.)
 - Level flight, $50^\circ \Rightarrow 30^\circ$, VSS, attitude command, beeping.
 - Level flight, $30^\circ \Rightarrow 50^\circ$, VSS, attitude command, beeping.

- Level flight, $30^\circ \Rightarrow$ hover, VSS, attitude command, beeping. (Figure 2-2)
"Airplane feels very good in hover. Quick response, good forces. No problems on the transition. It went very smoothly. Forces for attitude command are not good for gross maneuvering, but are all right for transition and good in hover."
- Level flight, hover $\Rightarrow 30^\circ$, VSS, attitude command, beeping.
- $\delta = -7.5^\circ$, $30^\circ \Rightarrow 50^\circ$, VSS, attitude command.
- "No problem with the transition. I blurred off the ball -- have to be more forceful with stick and collective. For small transition maneuvers, the attitude command system is fine."
- Level, $50^\circ \Rightarrow 30^\circ$, VSS, attitude command.
- $\delta = -7.5^\circ$, $30^\circ \Rightarrow 50^\circ$, VSS, attitude command, on ball whole time.
"Must manhandle airplane a bit, and can then really fly the ball."
- $\delta = -7.5^\circ$, $50^\circ \Rightarrow$ hover, VSS, attitude command, held ball most of way down. Hover at 80 ft AGL, hands off.

Flight F-92

- All transitions on VSS with attitude command
- $\delta = -10^\circ$, $15^\circ \Rightarrow 30^\circ$, started too high.
- $\delta = -10^\circ$, $30^\circ \Rightarrow 50^\circ$, on meatball most of the time. VFR.
"The most confusing thing is knowing what to do with the collective lever. Have two controls doing the same thing."
- $\delta = -10^\circ$, $30^\circ \Rightarrow$ hover, on meatball most of the time. VFR. (Figure 2-3)
"No problems. Noticeable trim change in wrong direction: have to use nose down to slow down, no real sweat. Backed off on collective until end when must increase for hover. (Note: this technique gives some duct buzz for $60^\circ < \lambda < 80^\circ$). Should come in with collective a little sooner. Airplane is very stable."
- $\delta = -10^\circ$, $30^\circ \Rightarrow$ hover, lost ball somewhat, back on at 300 ft AGL for hover. VFR. (Figure 2-4)
- $\delta = -10^\circ$, $15^\circ \Rightarrow \sim 45^\circ$. Started in too close. VFR
"Very difficult to stay on ball at $\lambda = 15^\circ$. Much more push force required. Were below the ball most of the time."
- $\delta = -10^\circ$, $15^\circ \Rightarrow$ hover, lost ball right at end. VFR (Figure 205)
"Hard to hold nose down and collective up."

- $\gamma = -10^{\circ}, 15^{\circ} \Rightarrow$ hover, VFR, on ball whole time. (Figure 2-6)
"Am getting better. Don't like having to push to slow down -- that's backwards to what I'd like to see."
- $\gamma = -10^{\circ}, 15^{\circ} \Rightarrow \sim 45^{\circ}$ IFR. Could not do task.
"Much more difficult task. Have both longitudinal and lateral to worry about. Started late, don't know what altitude to start transition at. Push force is even more uncomfortable."
- Simulated IFR to attempt transition.
- $\gamma = -10^{\circ}, 15^{\circ} \Rightarrow \sim 30^{\circ}$. IFR. Couldn't do task.
"Don't have enough information to know where I am on the approach."
- Back to VFR for full transition.
- $\gamma = -10^{\circ}, 0^{\circ} \Rightarrow$ hover, VFR. On ball most of way. (Figure 2-7)

As can be seen from the figures, the transitions were generally performed at an average reconversion rate of $\dot{\lambda} \doteq -2.5$ deg/sec (see Figure 2-6). Duct buffet was not a problem through the transition except generally around $\lambda = 70^{\circ}$. As can be seen from the figures, the pilot has a tendency to be decreasing the collective and pulling the nose up in this region to slow the airplane down, as the velocity decrease due to duct rotation tends to lag the correct duct angle; as a result, the angle of attack increases markedly and leads to the onset of duct buzz. This characteristic does not compromise the capability to make full decelerating transitions at the moderate average reconversion rates investigated, as the buffet is minor. It is clear however, that transitions at maximum reconversion rate require a more precise scheduling of collective stick and pitch attitude commands, and, in fact, it appears that the reconversion rate would have to be decreased through this region.

The conclusions that may be drawn from this final phase of the experiment are summarized below:

- Decelerating transitions controlled through the VSS have been demonstrated for glide slope angles of $\gamma = -7.5$ deg and $\gamma = -10$ deg.
- Reconversion rates of $\dot{\lambda} \doteq -2$ to -3 deg/sec on the average allow complete decelerating transitions ($\lambda = 0^{\circ} \Rightarrow \lambda = 90^{\circ}$) to be performed at these descent angles with only minor duct buzz effects. Transitions at the maximum rate ($\dot{\lambda} = -5$ deg/sec), however, require precise commands for the pilot on collective stick and pitch attitude control positions, and may still lead to large amounts of duct buffet.
- The $\lambda = 0$ deg condition investigated for initiation of a full transition requires extremely high nose-up attitudes for trim ($\theta_0 \doteq 15$ deg). This characteristic, in combination with the requirement through most of the transition for a nose-down

attitude of $\theta_0 = -15^0$ to minimize buffet, results in a large attitude change which the pilots do not like. It may be more desirable to initiate the transitions at $\lambda = 15^0$, $V = 110$ kts for future work.

- No fundamental limitations of the X-22A VSS were observed that might compromise future transition research.

2.3 Flight Demonstrations

The fixed-operating point and transition capabilities of the X-22A variable stability aircraft have been demonstrated in flight to interested pilot personnel from the services which comprise the X-22A Flight Research Steering Group. These demonstrations provide a graphic illustration of the capabilities discussed in this section. A sample flight plan and summary is given in Appendix IV as an example of this capability.

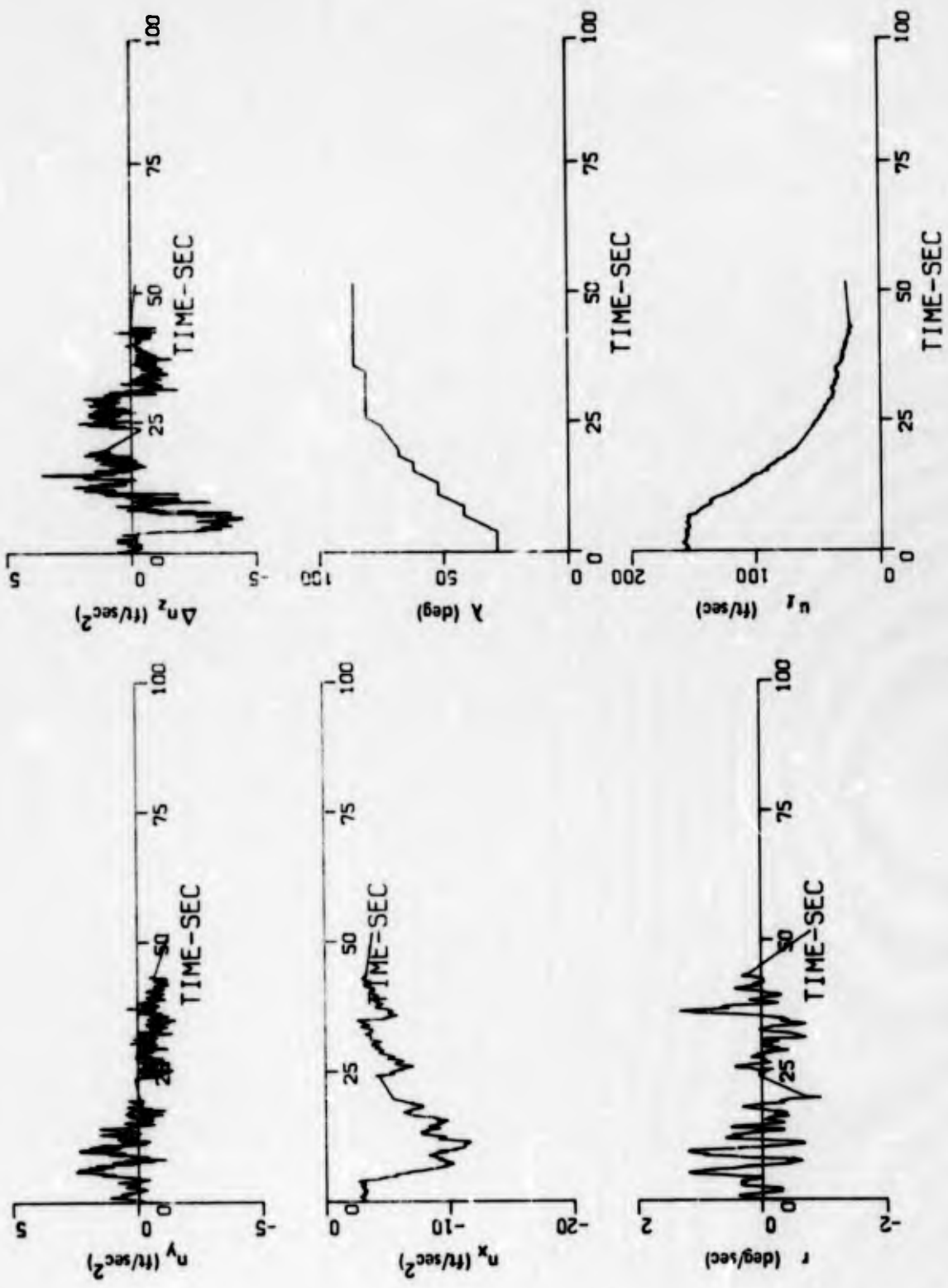


Figure 2-2 DECELERATING TRANSITION, LEVEL FLIGHT, 30° ⇒ 90°, FLIGHT F-87 (Sheet 1 of 3)

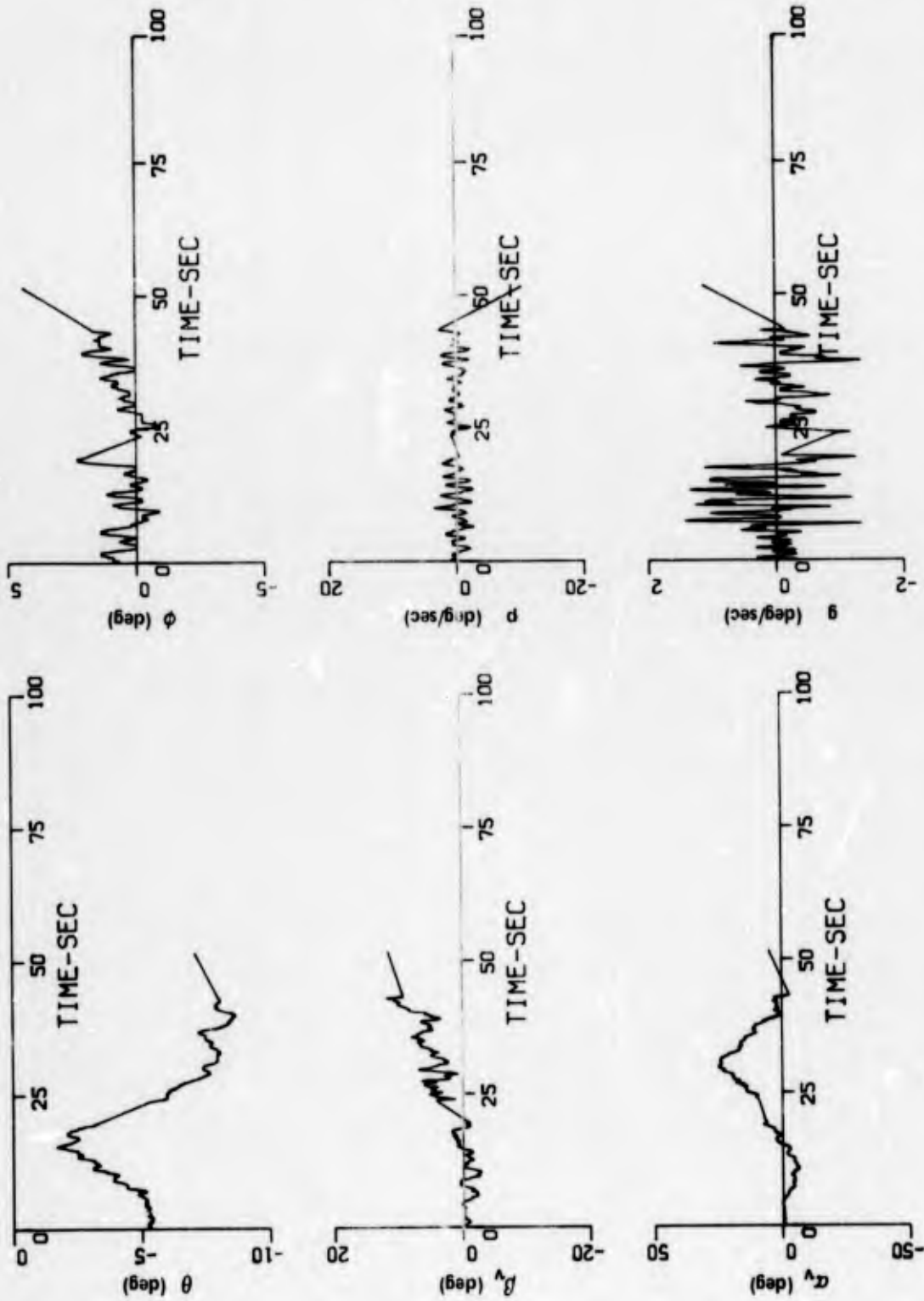
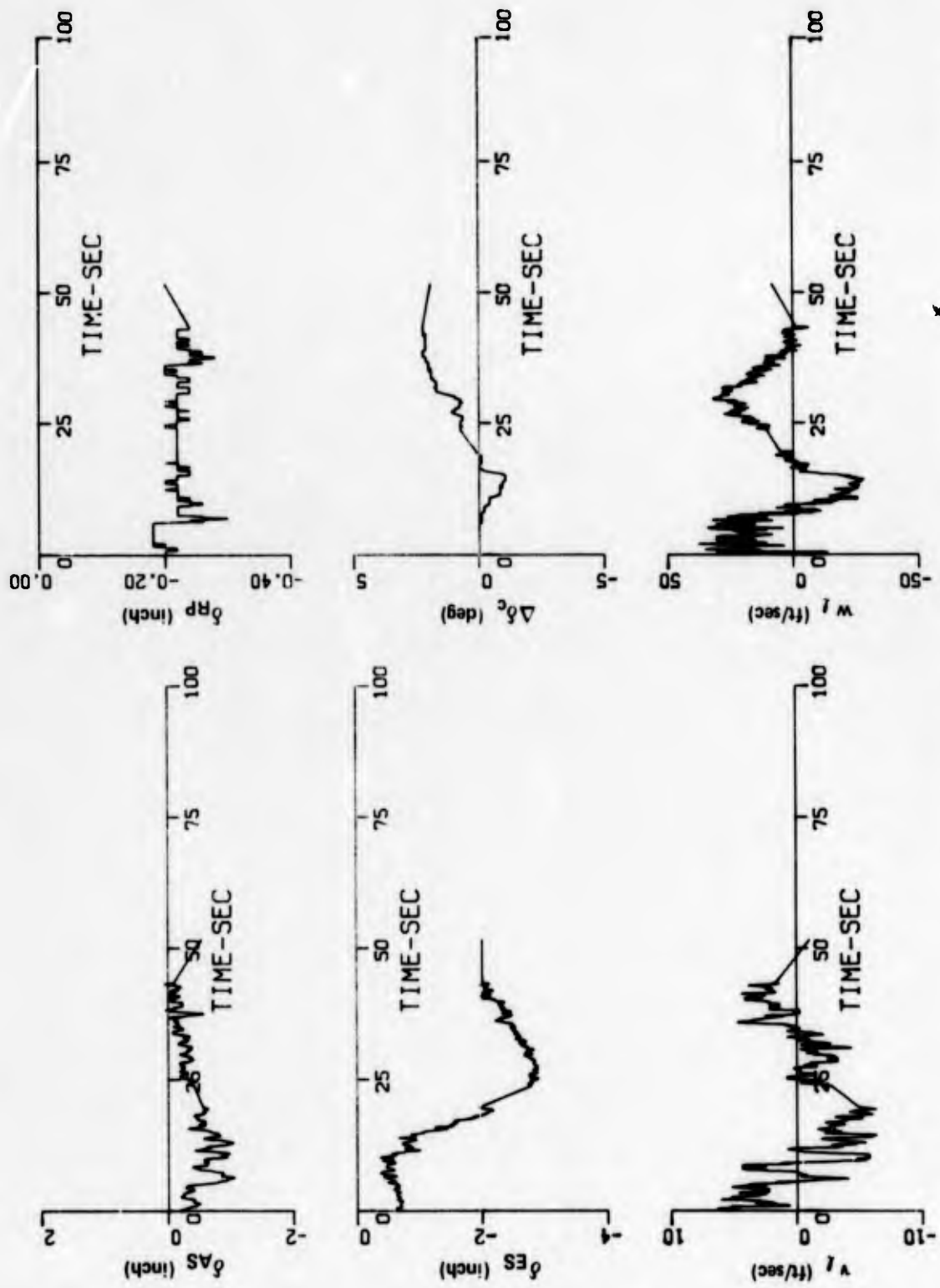


Figure 2-2 DECELERATING TRANSITION, LEVEL FLIGHT, $30^\circ \Rightarrow 90^\circ$, FLIGHT F-87 (Sheet 2 of 3)



*

Figure 2-2 DECELERATING TRANSITION, LEVEL FLIGHT, $30^\circ \Rightarrow 90^\circ$, FLIGHT F-87 (Sheet 3 of 3)

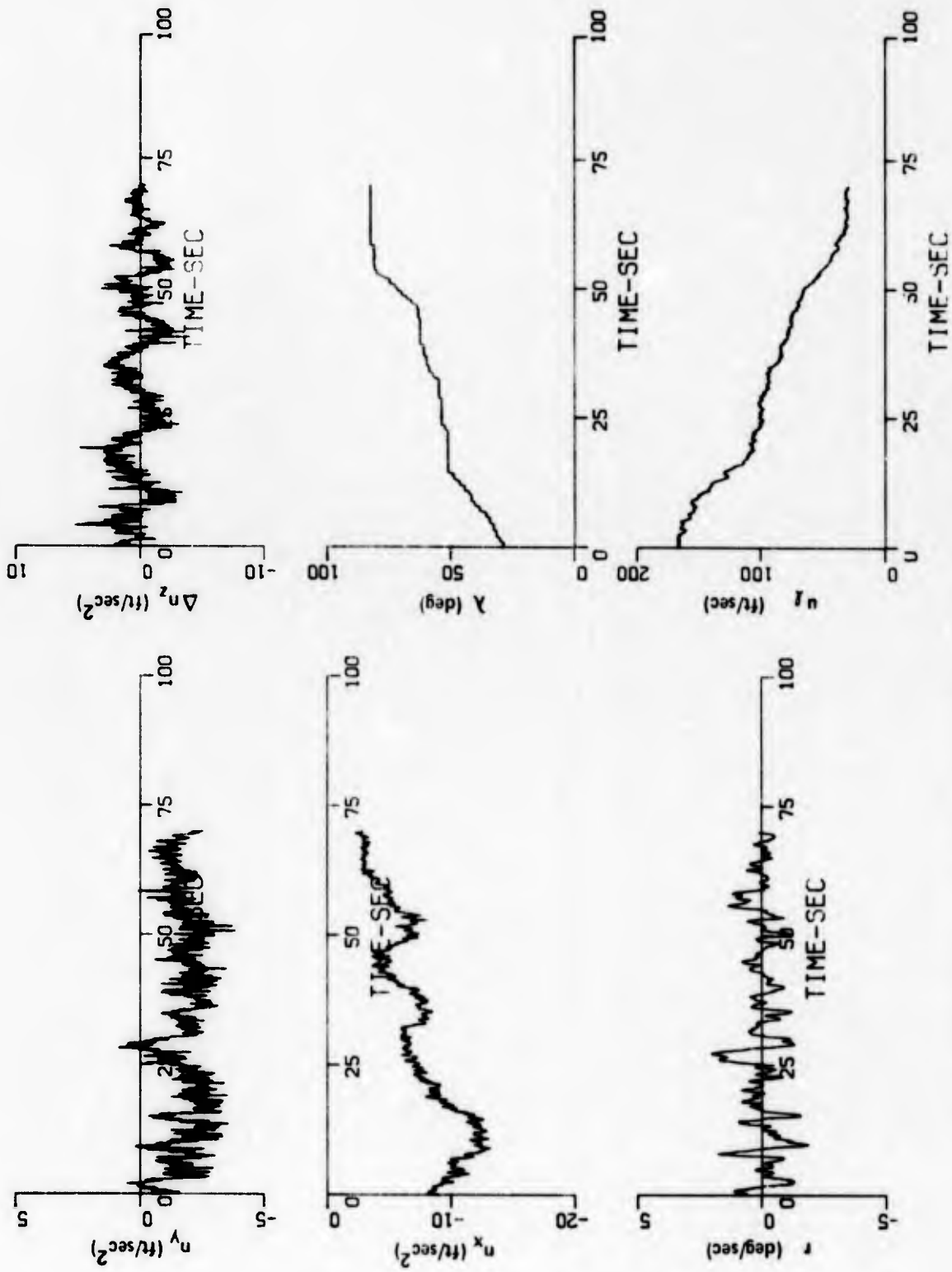


Figure 2-3 DECELERATING TRANSITION, $\gamma = -10^\circ, 30^\circ \Rightarrow 90^\circ$, FLIGHT F-92 (Sheet 1 of 3)

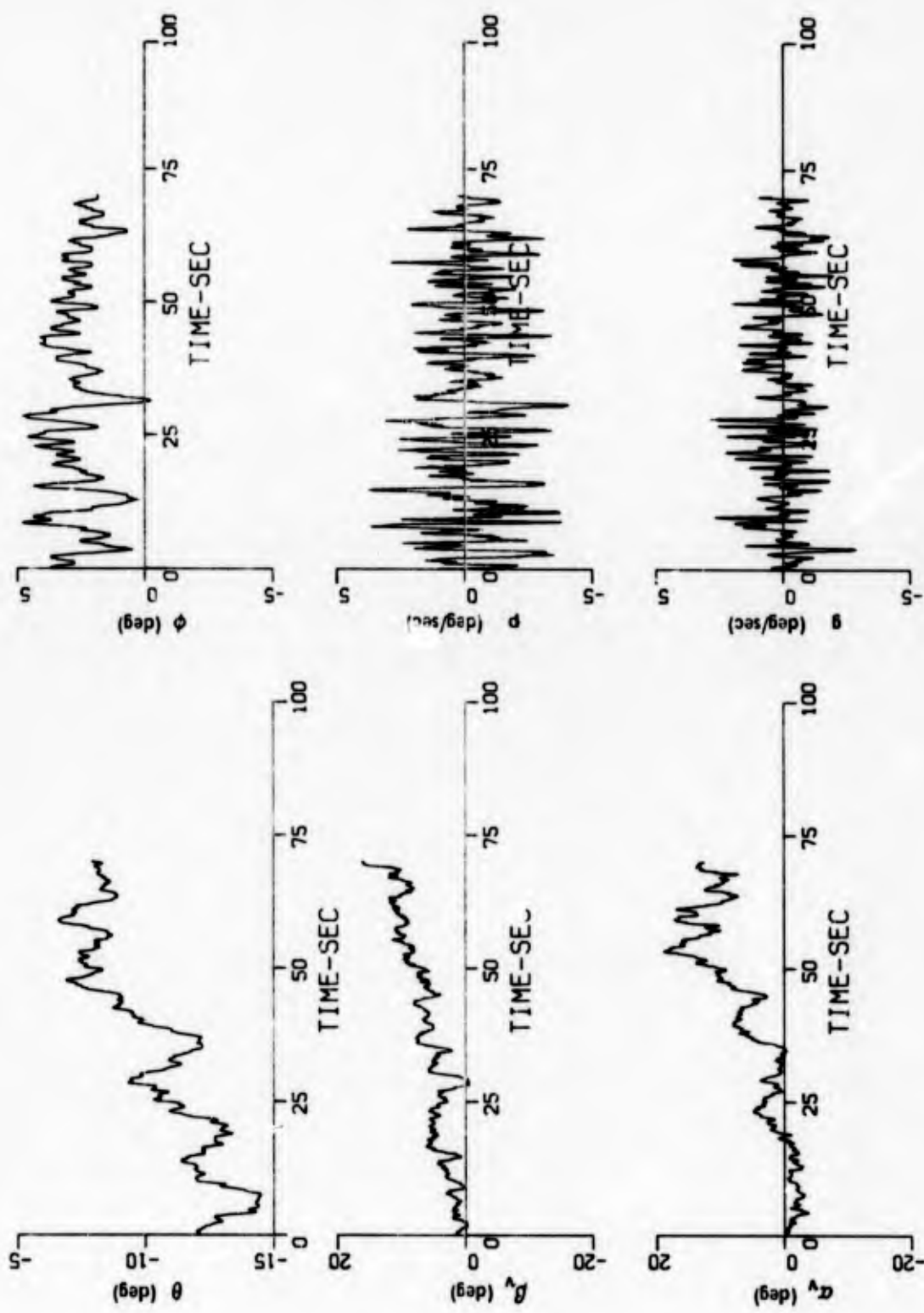


Figure 2-3 DECELERATING TRANSITION, $\gamma = -10^\circ, 30^\circ \Rightarrow 90^\circ$, FLIGHT F-92 (Sheet 2 of 3)

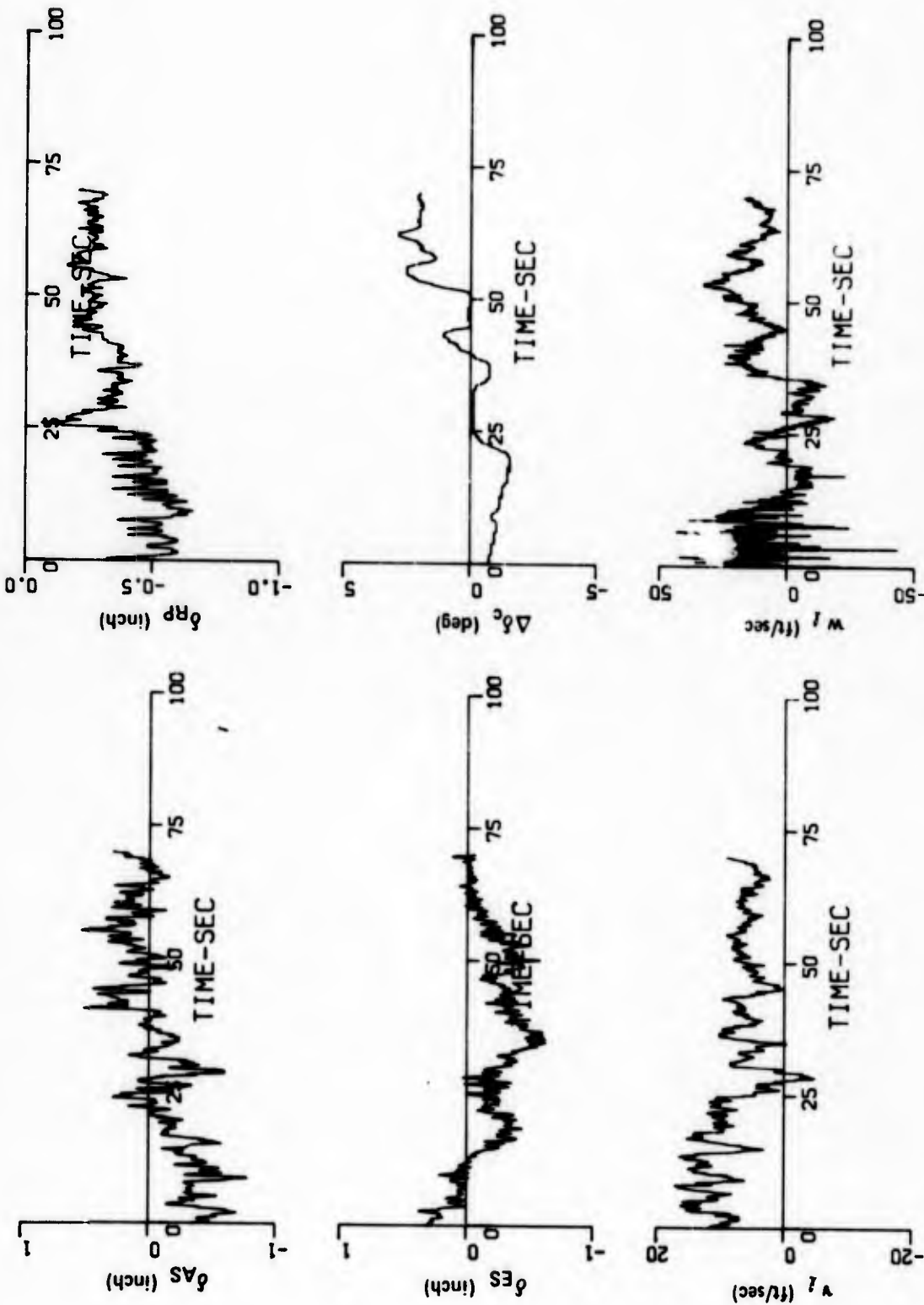


Figure 2-3 DECELERATING TRANSITION, $\gamma = -10^\circ, 30^\circ \Rightarrow 90^\circ$, FLIGHT F-92 (Sheet 3 of 3)

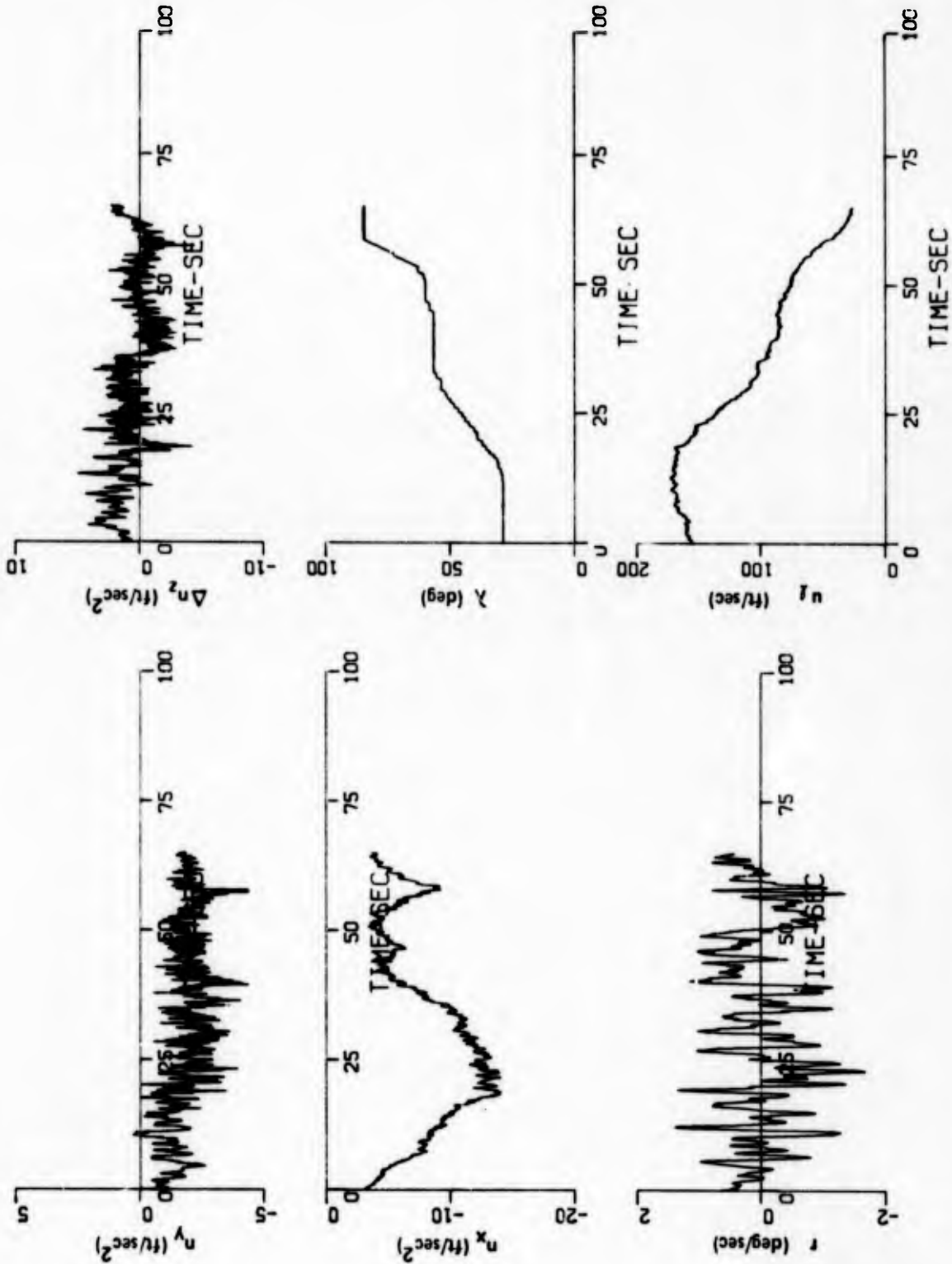


Figure 2-4 DECELERATING TRANSITION, $\gamma = -10^\circ, 30^\circ \Rightarrow 90^\circ$, FLIGHT F-92 (Sheet 1 of 3)

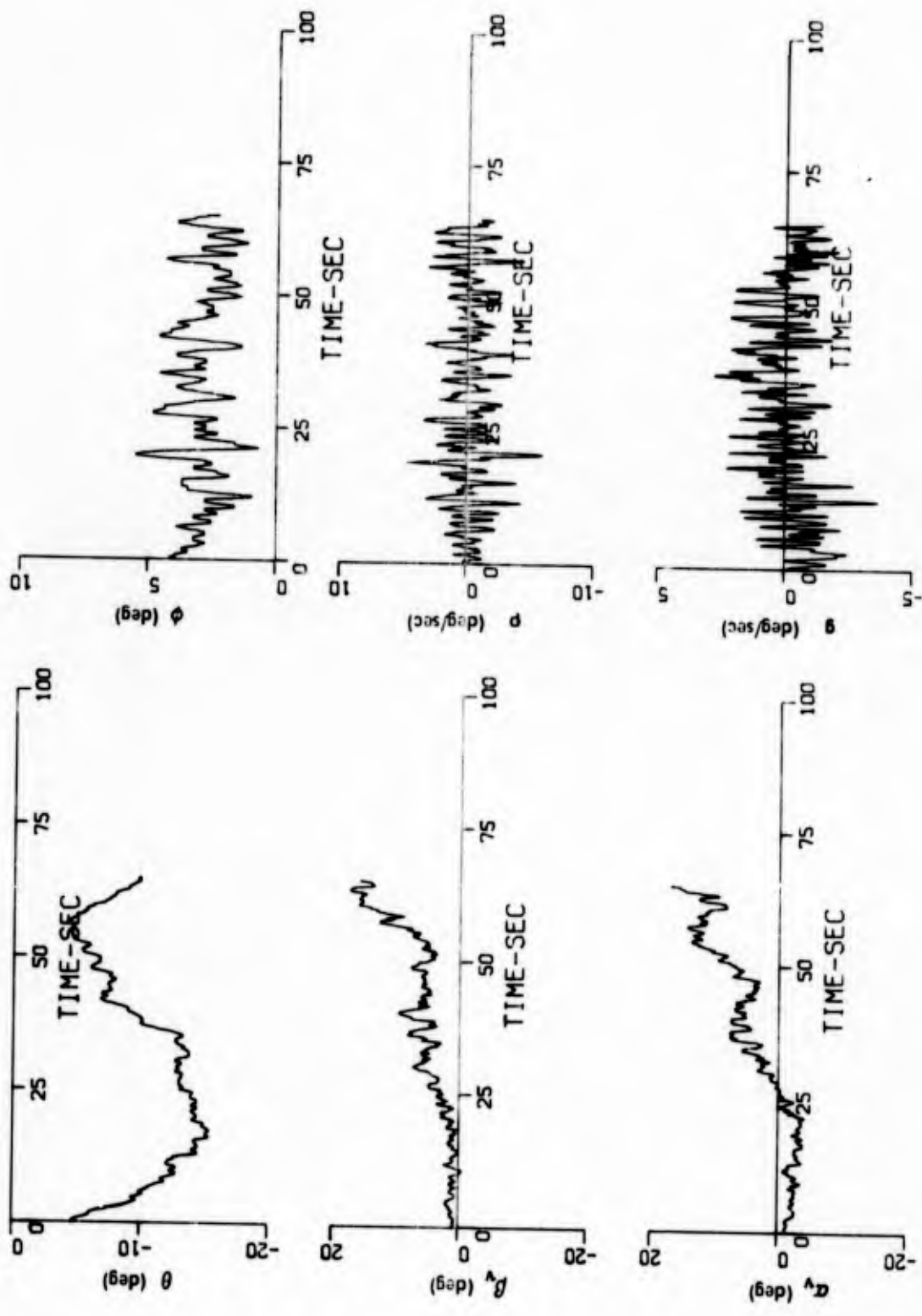


Figure 2-4 DECELERATING TRANSITION, $\gamma = -10^\circ, 30^\circ \Rightarrow 90^\circ$, FLIGHT F-92 (Sheet 2 of 3)

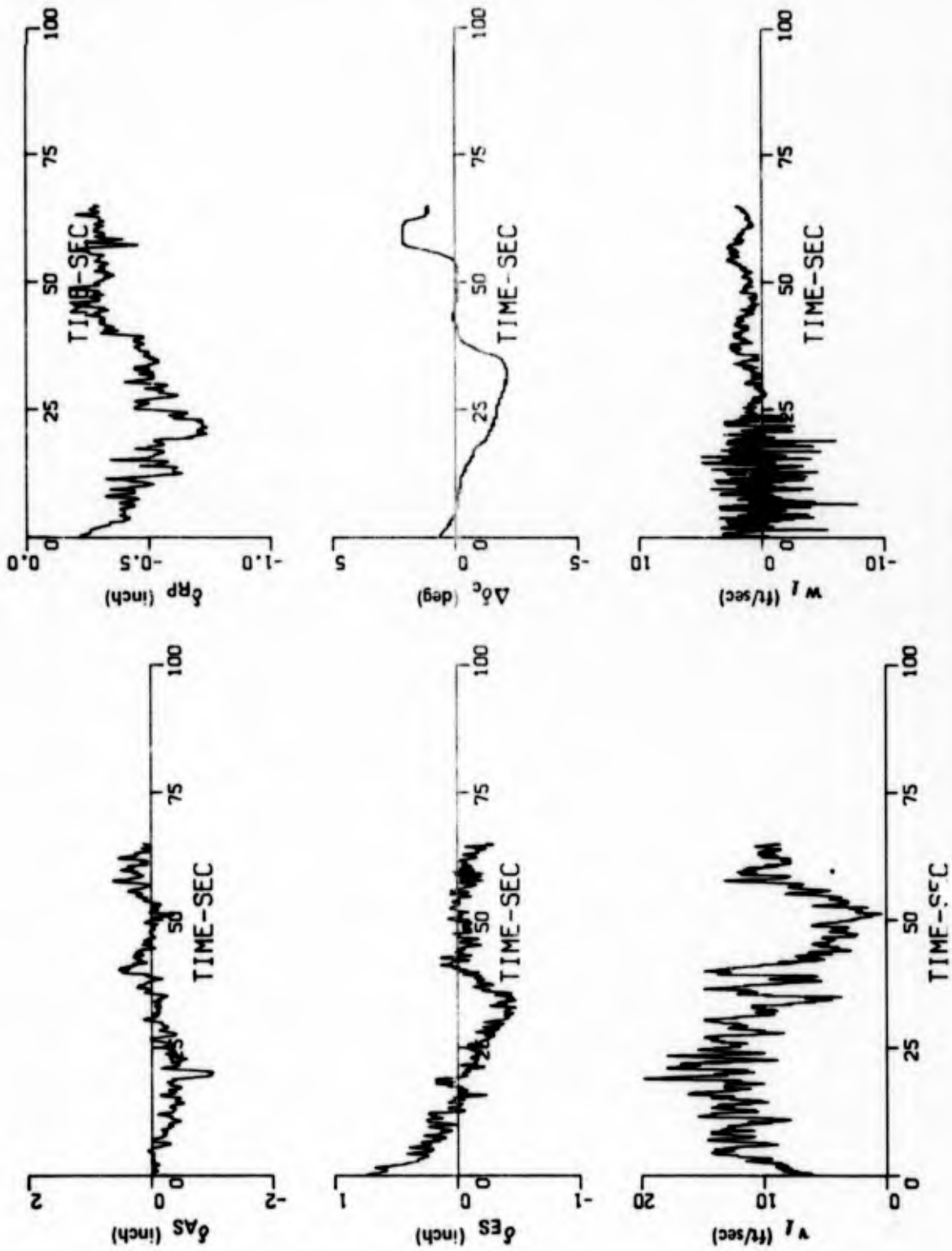


Figure 2-4 DECELERATING TRANSITION, $\gamma = -10^\circ, 30^\circ \Rightarrow 90^\circ$, FLIGHT F-92 (Sheet 3 of 3)

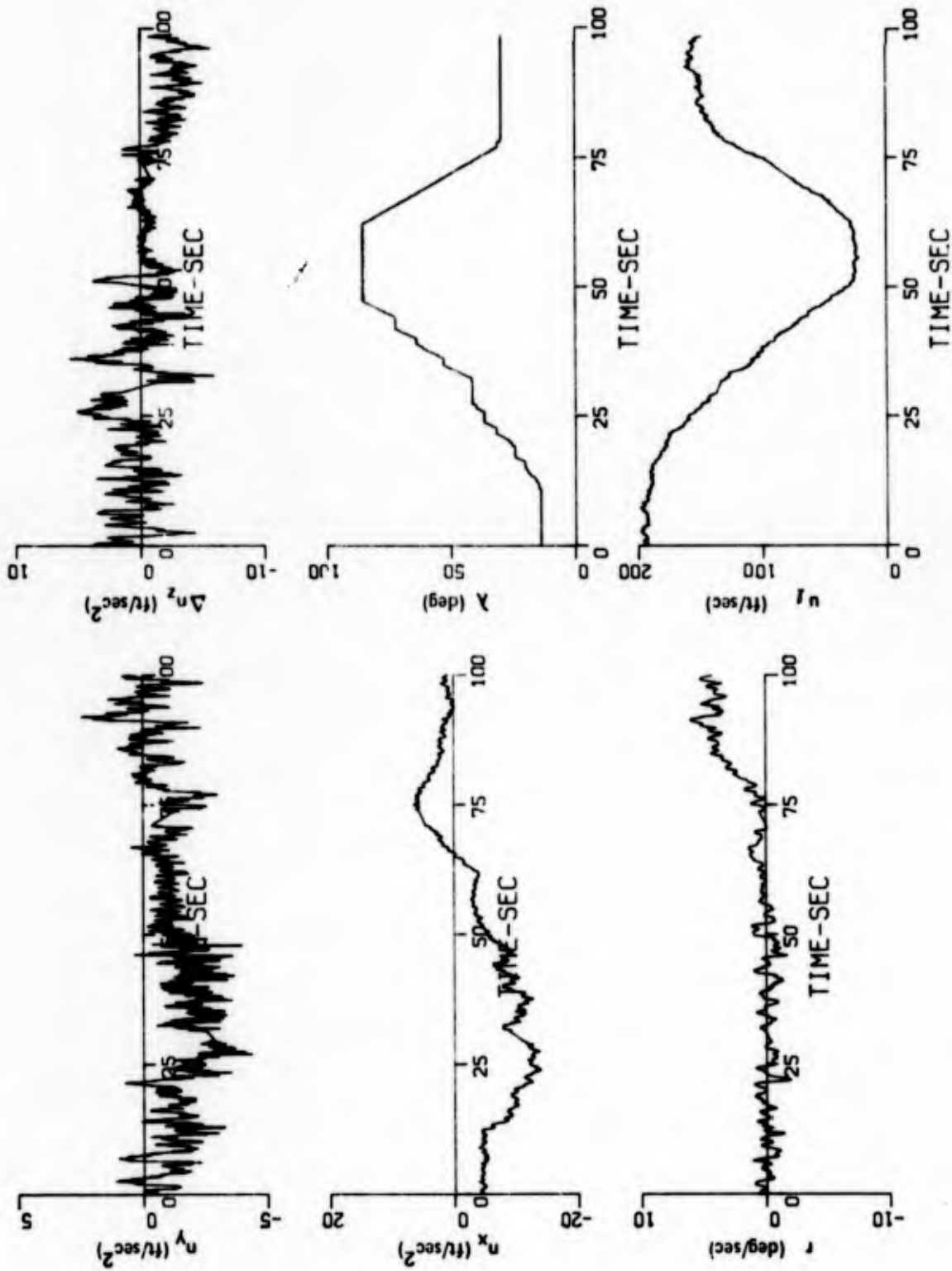


Figure 2-5 DECELERATING TRANSITION, $\gamma = -10^\circ, 15^\circ \Rightarrow 90^\circ$, FLIGHT F-92 (Sheet 1 of 3)

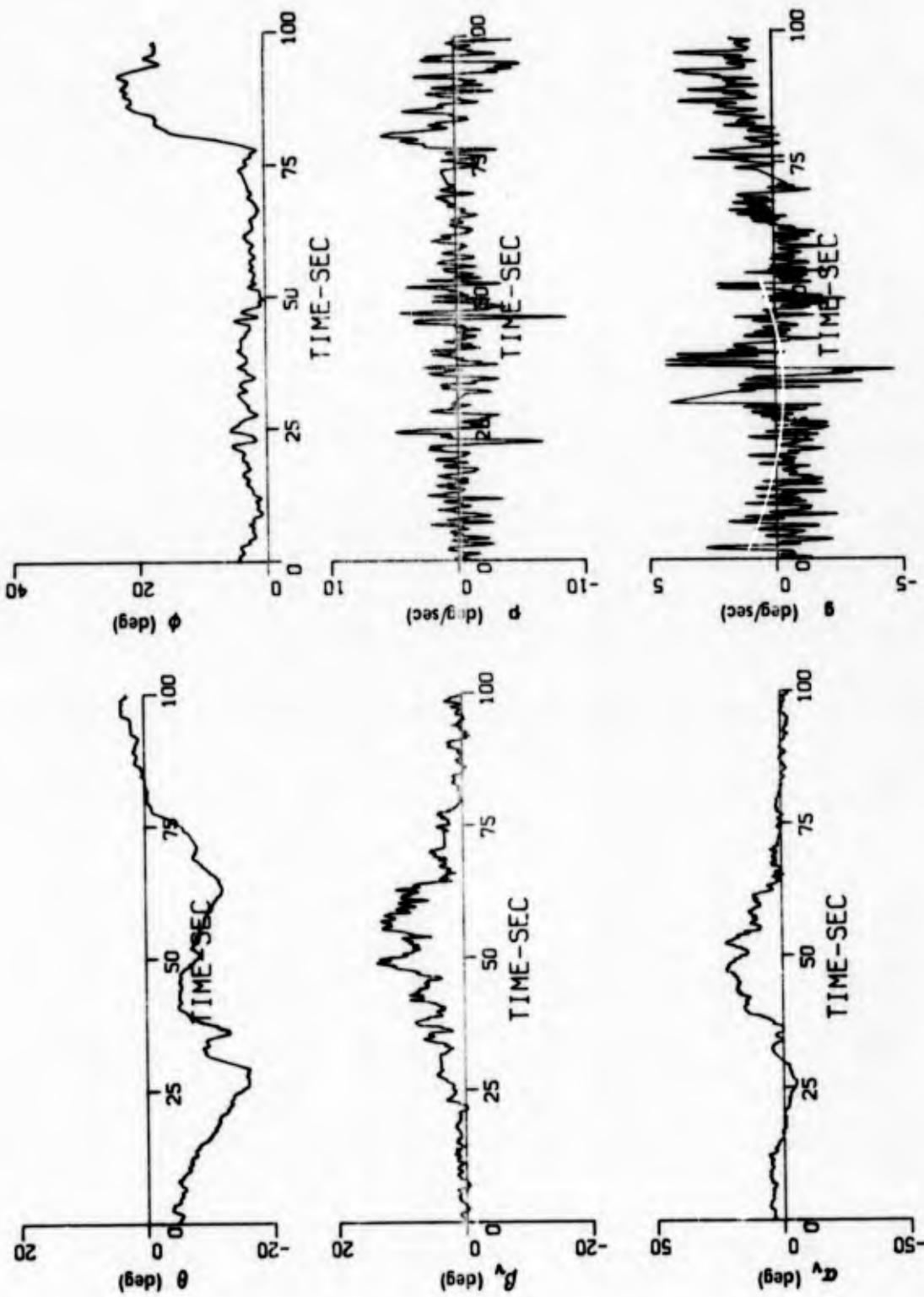


Figure 2-5 DECELERATING TRANSITION, $\gamma = -10^\circ$, $15^\circ \Rightarrow 90^\circ$, FLIGHT F-92 (Sheet 2 of 3)

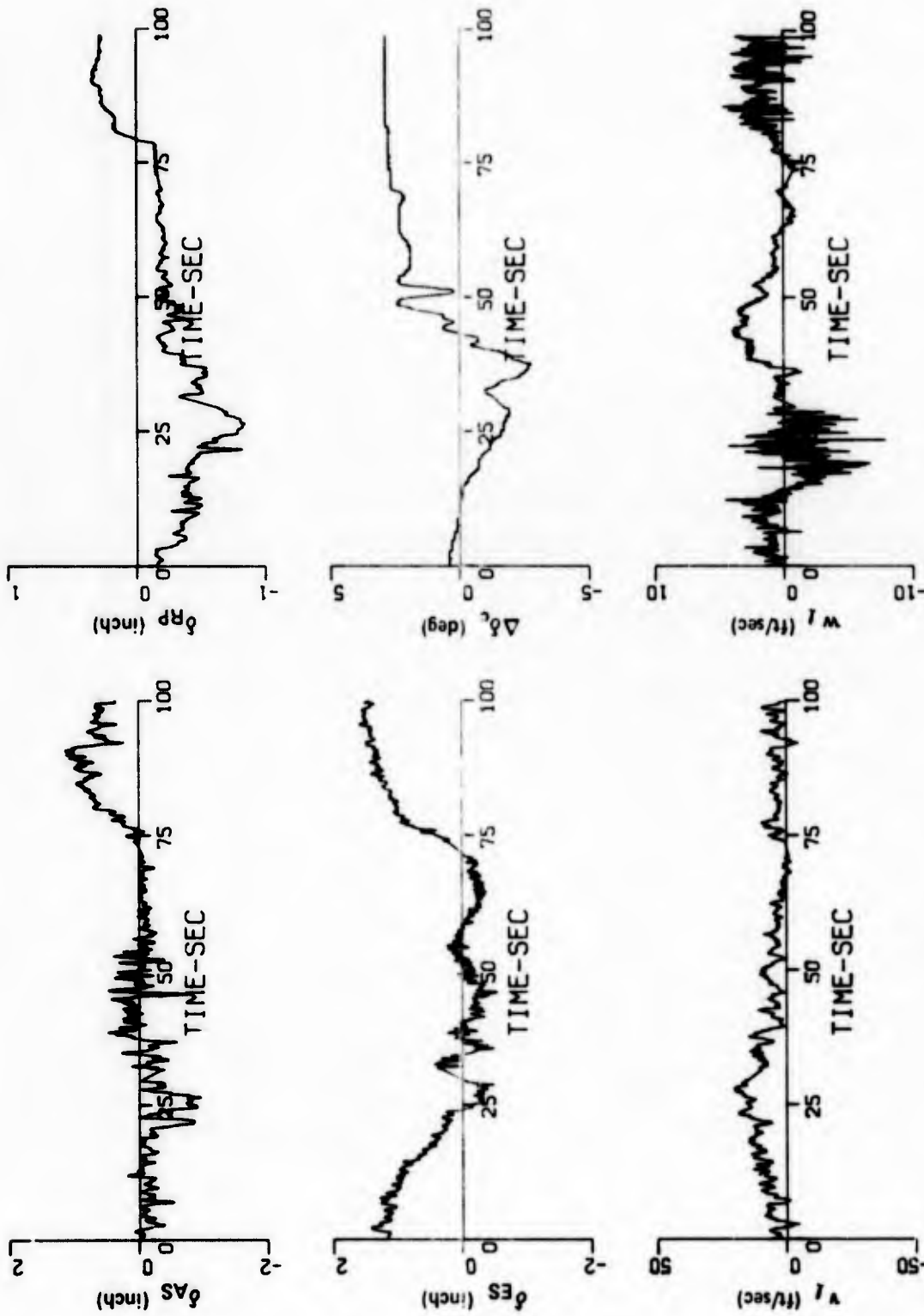


Figure 2-5 DECELERATING TRANSITION, $\gamma = -10^\circ, 15^\circ \Rightarrow 90^\circ$, FLIGHT F-92 (Sheet 3 of 3)

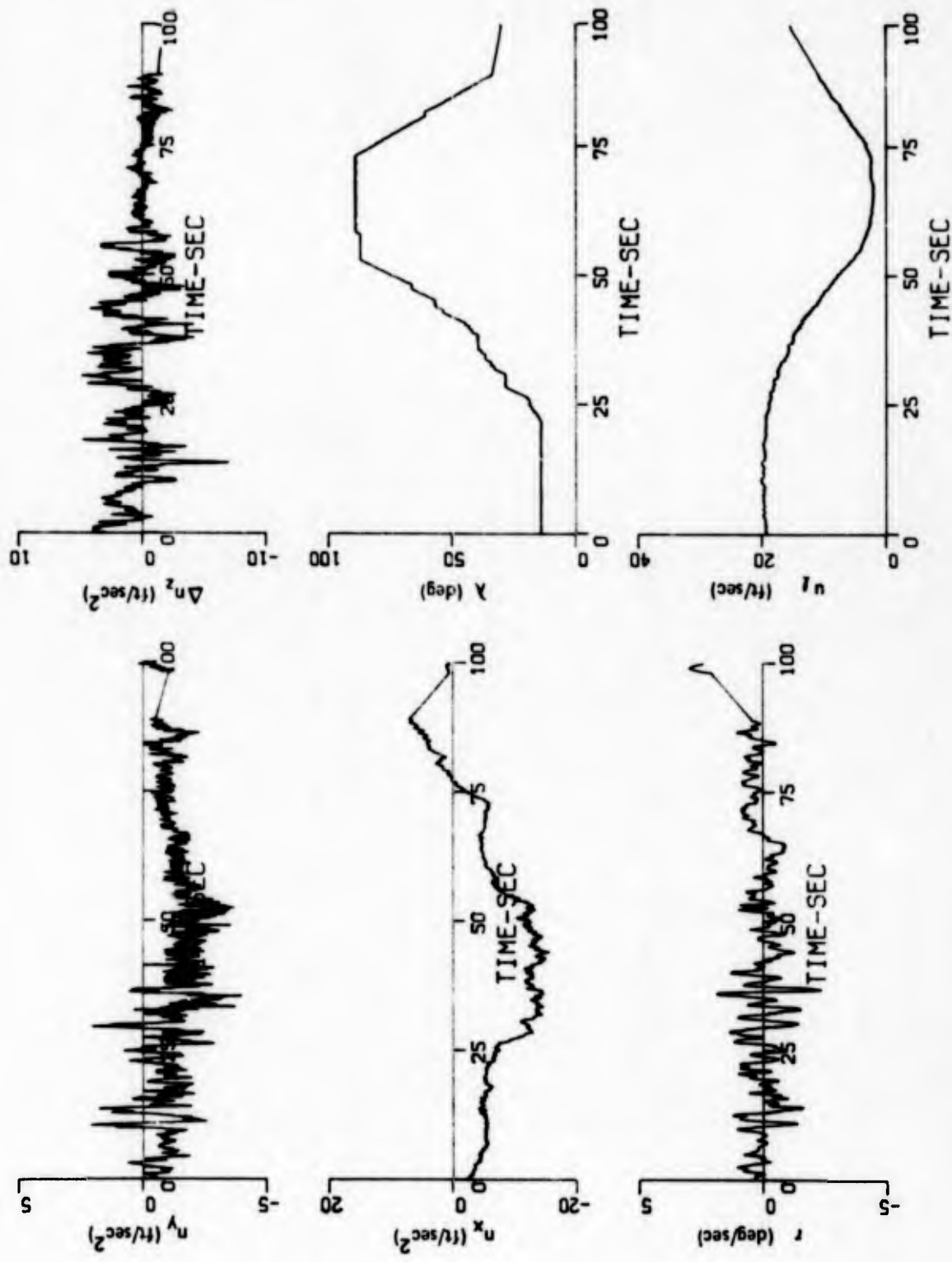


Figure 2-6 DECELERATING TRANSITION, $\gamma = -10^\circ, 15^\circ \Rightarrow 90^\circ$, FLIGHT F-92 (Sheet 1 of 3)

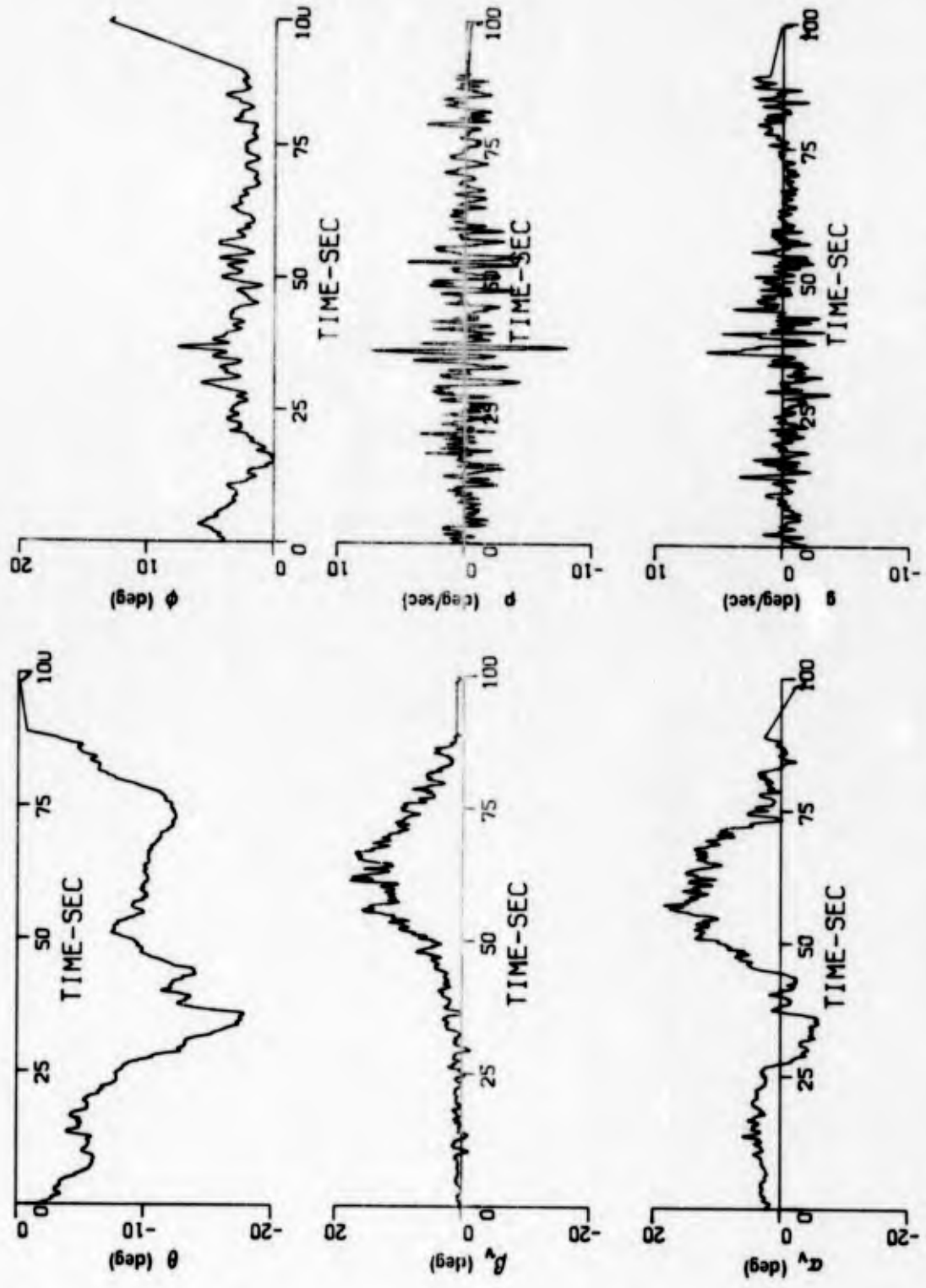


Figure 2-6 DECELERATING TRANSITION, $\gamma = -10^\circ, 15^\circ \Rightarrow 90^\circ$, FLIGHT F-92 (Sheet 2 of 3)

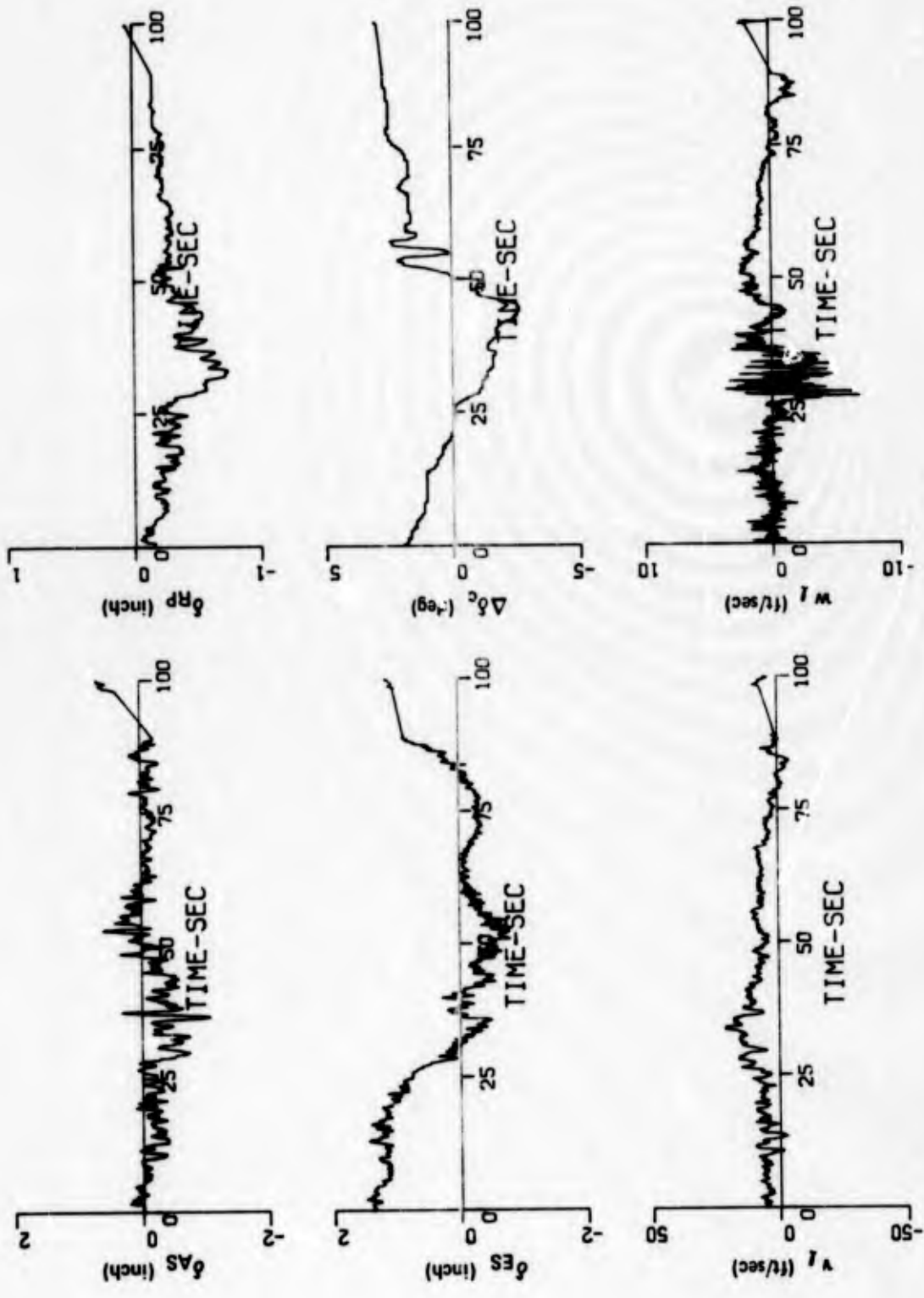


Figure 2-6 DECELERATING TRANSITION, $\gamma = -10^\circ, 15^\circ \Rightarrow 90^\circ$, FLIGHT F-92 (Sheet 3 of 3)

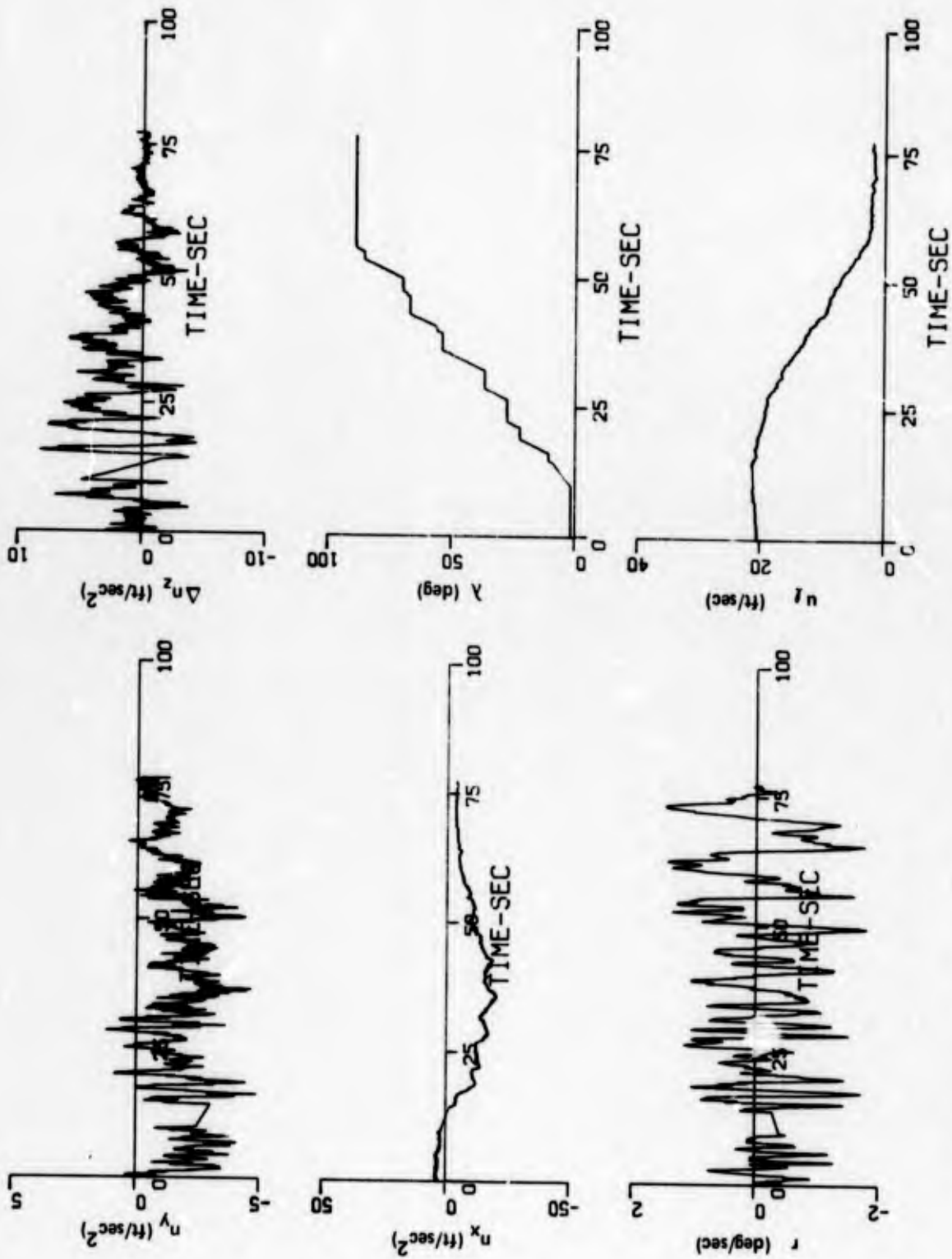


Figure 2-7 DECELERATING TRANSITION, $\gamma = -10^\circ, 0^\circ \Rightarrow 90^\circ$, FLIGHT F-92 (Sheet 1 of 3)

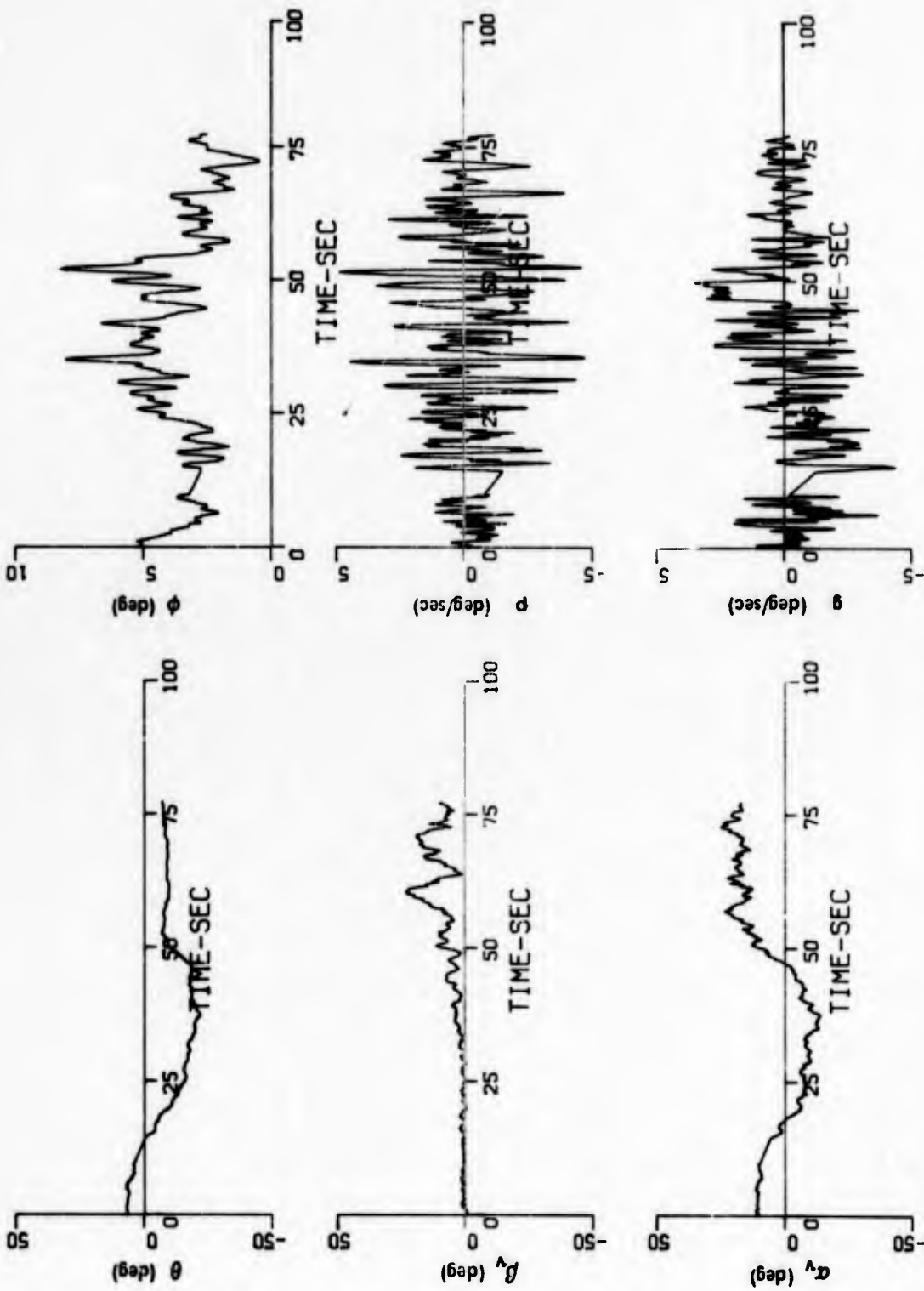


Figure 2-7 DECELERATING TRANSITION, $\gamma = -10^\circ$, $0^\circ \Rightarrow 90^\circ$, FLIGHT F-92 (Sheet 2 of 3)

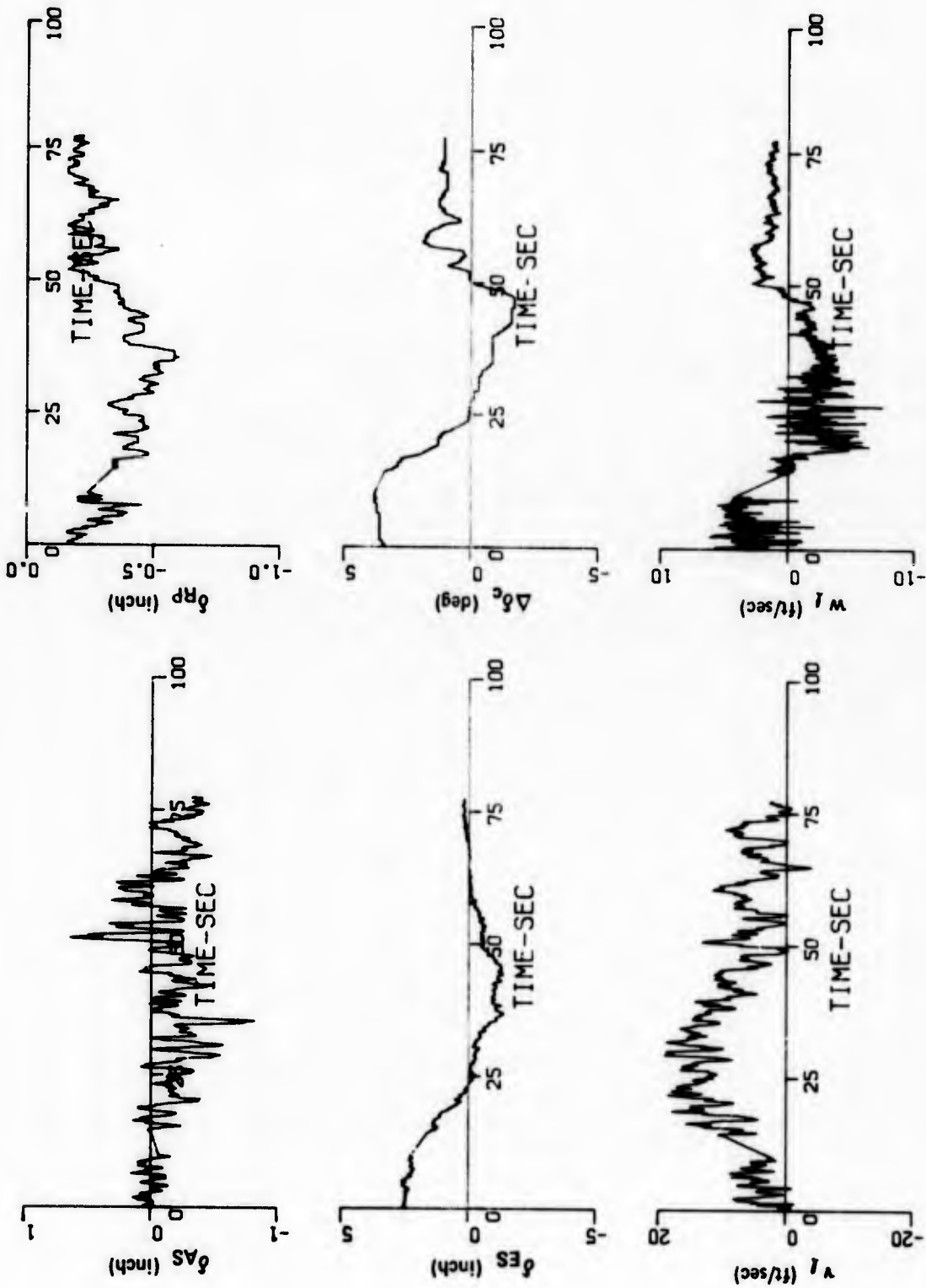


Figure 2-7 DECELERATING TRANSITION, $\gamma = -10^\circ, 0^\circ \Rightarrow 90^\circ$, FLIGHT F-92 (Sheet 3 of 3)

Section III

GROUND SIMULATION CAPABILITY

The purpose of this section is to present a brief description of the ground simulation facility which effectively complements the X-22A variable stability aircraft operation. This fixed-base ground simulator, shown in Figure III-1, is designed to supplement the X-22A aircraft operation in the following manner:

- Perform preliminary tests of experimental programs prior to flight tests in the actual aircraft.
- Develop new experimental hardware and systems, such as control systems and displays prior to installation in the actual aircraft.
- Ground test new equipment and check experimental setups in the aircraft prior to actual flight test.
- Provide pilot training as required.

A more detailed description of the facility is given in References 6 and 7 while the following section summarizes the equipment used and the overall capability of the ground simulator.

3.1 EQUIPMENT AND MECHANIZATION

The ground simulator is composed of the following functional components, with their relationship indicated in the block diagram of Figure III-2.

- Digital computer - solves the computer model equations (housed in X-22A Mobile Van - Appendix II).
- Variable feel system - provides force-position characteristics for pilot's stick and rudder pedal controls.
- Variable stability system electronics - combines inputs from pilot's controls with feedback of computed responses to provide control inputs to computer model.
- Cockpit displays - flight instruments used by pilot to fly under instrument conditions. (see Figure III-3)
- Interface - patch boards, signal conversion, filtering, and scaling between simulator components.

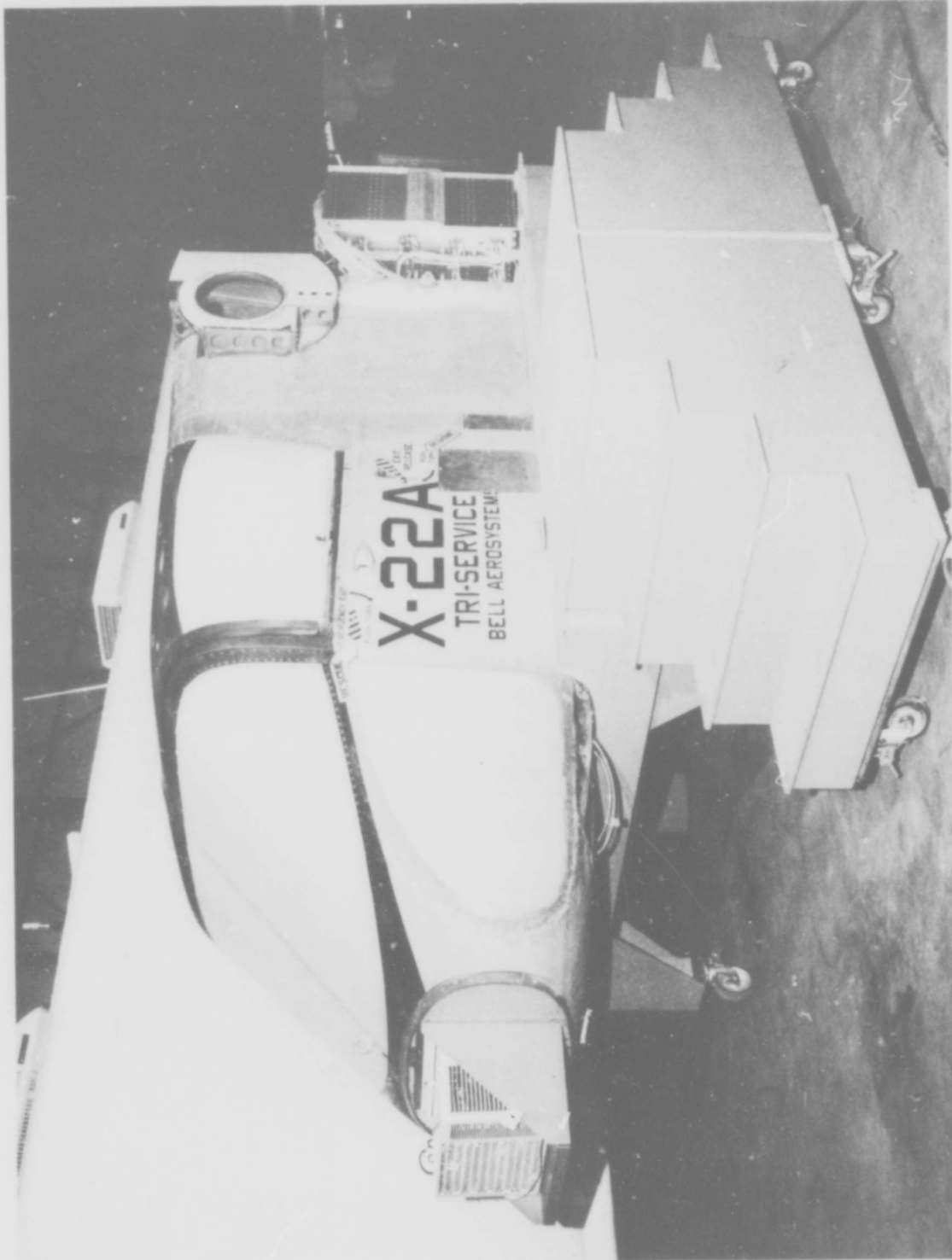


Figure 3-1 X-22A GROUND SIMULATOR

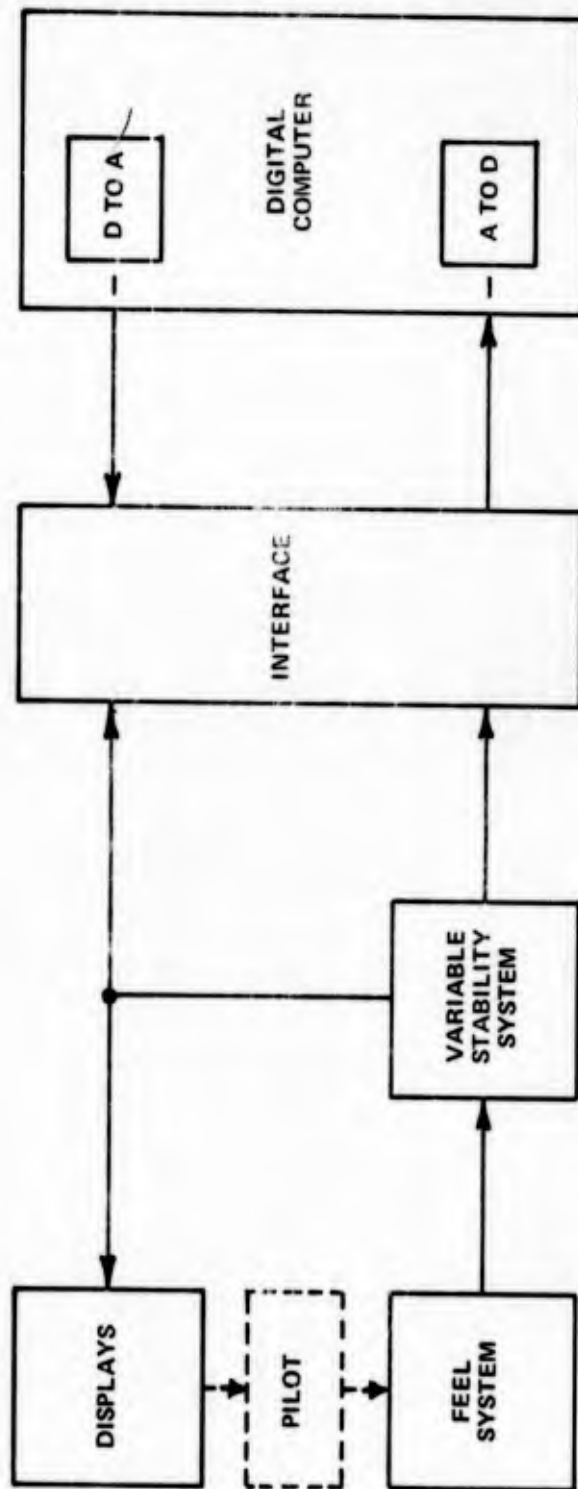


Figure 3-2 X-22A GROUND SIMULATOR FUNCTIONAL BLOCK DIAGRAM

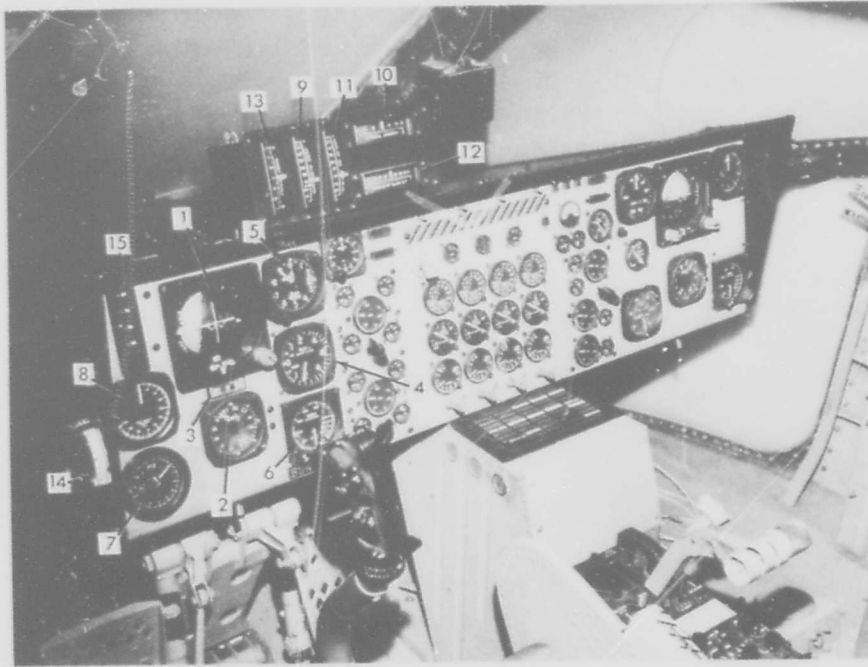


Figure 3-3 X-22A GROUND SIMULATOR COCKPIT

- 1) Attitude Director Indicator
- 2) Bearing, Distance, Heading Indicator
- 3) Slip Indicator
- 4) Rate of Climb Indicator
- 5) Altimeter
- 6) Radar Altimeter
- 7) RPM Indicator
- 8) Duct Angle Indicator
- 9) Longitudinal Airspeed Indicator (-30 to +60 kt)
- 10) Lateral Airspeed Indicator
- 11) Angle of Attack Meter
- 12) Angle of Sideslip Indicator
- 13) Normal Acceleration Indicator
- 14) Collective Stick Indicator
- 15) Forward Airspeed Indicator (-30 to +150 kt)

The feel system, variable stability system electronics, and flight instruments duplicate those found in the X-22A aircraft. All other elements associated with the aircraft including its airframe equations of motion, power plant characteristics, flight control system, and guidance system are simulated by the computer. As an option, the actual X-22A aircraft can be tied in with the simulator so that some of its components can be incorporated directly. For example, the complete flight control system can be employed with measured propeller blade and elevon signals used as inputs to the computer model for studying problems associated with the flight control system itself.

The primary use of the ground simulator is to simulate the flight operation of the X-22A variable stability aircraft in flying qualities research use. For such use, the X-22A equations of motion including its orientation with respect to a runway or landing pad, together with equations for the landing guidance system, are programmed on the digital computer. The appropriate response variables are computed and fed to the cockpit instruments and the variable stability system. The pilot's control inputs from the feel system together with the computed response variables are processed by the variable stability system electronics, just as in the X-22A aircraft, to generate the control inputs to the computer model (the X-22A equations of motion). Both constant and variable gains, using its function generators, are available in the variable stability system. Steady winds can be simulated in the computer, and a tape unit can also be used to feed simulated gusts into the computer. The feel system force-position gradients are adjustable; they can be made nonlinear, and can be varied as a function of flight condition through function generators. Thus, the simulation of different VTOL and STOL aircraft or aircraft characteristics can be performed in the ground simulator in much the same manner as it would be done in flight with the X-22A aircraft. The cockpit, flight instruments, pilot's controls, and the variable stability system electronics essentially duplicate those used in flight, thus greatly enhancing the capability to develop and test experimental techniques, procedures, and equipment in the ground simulator prior to actual use in flight. For data recording, the full digital data acquisition and processing system, used during X-22A flight programs and described in Appendix III, is available.

To simplify simulator operation and to facilitate analytical or developmental type investigations, the X-22A ground simulator may be used without the variable stability system by relegating the representation of feedback control loops to a digital computer. The feedback loops may be incorporated directly into the computer program, or even simpler, the effect of a feedback loop may be incorporated by just modifying the appropriate stability derivative or coefficient in the aircraft equations of motion. For preliminary investigation these approaches are ideal because the effect of derivative or feedback gain changes are defined precisely in the computer, i.e., no control actuator or variable stability system characteristics need be accounted for. Numerical calculation apart from the simulation, e.g., calculation of characteristic roots and transfer functions, or check solutions from a different computer, can be made with the assurance that they do precisely represent the characteristics of the simulation.

The X-22A ground simulator can also be used as a general aircraft instrument flight simulator, from helicopters, for which the collective stick would be used, to conventional airplanes, for which the engine throttles (four are available), would be used. The use of a digital computer, with complete programming flexibility and tape storing of programs, greatly enhances the capability of the ground simulator to be used for general simulation. Complex and nonlinear aerodynamic characteristics can be readily incorporated, as can nonlinear control characteristics, or simple linearized equations of motion. Auxiliary systems, such as an ILS approach system or a sophisticated digital adaptive flight control system, can be readily included in the simulation. Three factors limit the simulation capability: the problem must fit the computer storage (presently 24,000 16-bit words); it must fit the computer speed (1.2 μ s CPU and 800 nsec memory cycle times); and sufficient time must be allowed for writing the program or modifying an existing one.

In summary, the X-22A ground simulator is a flexible research tool which together with the variable stability aircraft forms a complete research facility. The next section describes a recent simulation program which demonstrates the capabilities of the simulator.

3.2 EXPERIMENTAL APPLICATIONS

The capabilities of the ground simulator as a valid and useful tool, both for independent research and as an aid in the design of flight programs, were well demonstrated in the first experiment which used this facility. The purpose of this experiment was to investigate guidance and display command logic for full decelerating transition approaches under IFR conditions (Reference 7). In particular, a NASA "moving map" horizontal situation display was studied in combination with the standard X-22A attitude indicator with ILS cross-pointers; the cross-pointers plus an auxiliary "tab" were used to display flight director information according to various control laws (see Figure III-4). Pilot evaluations of representative sets of control logic were gathered, both to obtain general research information and to pinpoint specific combinations to be investigated in a forthcoming X-22A flight program involving decelerating IFR approaches.

The following types of control augmentation were investigated:

- Attitude command system, normal X-22A thrust control, response feedback.
- Attitude command, normal X-22A thrust control, prefilter (quasi model following) system.
- Attitude command with synthesized direct velocity control.
- Automatic system.

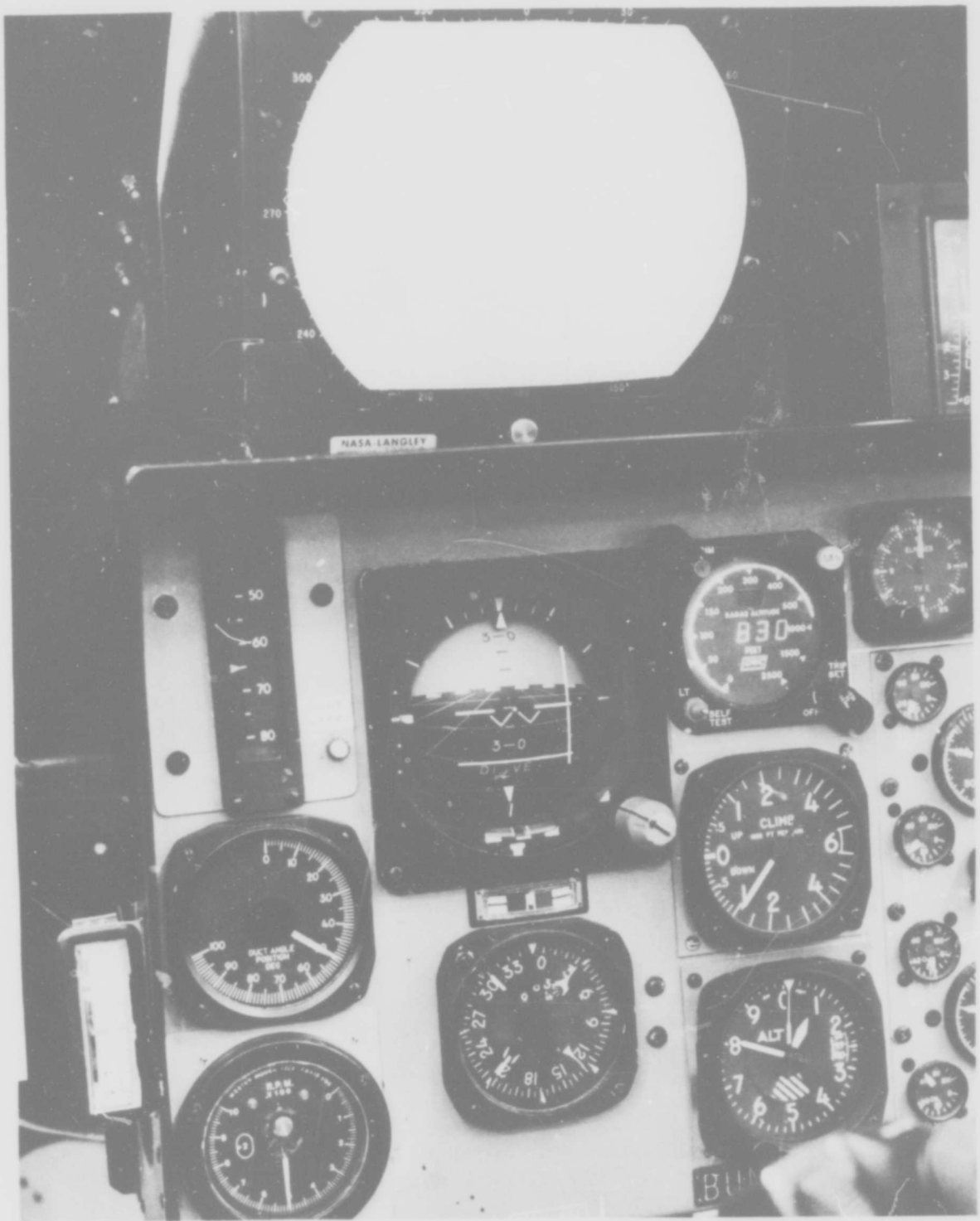


Figure 3-4 X-22A GROUND SIMULATOR INSTRUMENT DISPLAY

These control augmentation schemes and the sets of flight director command logic provided the two dimensions of the evaluation matrix. The evaluation task was a decelerating transition at ~ 0.1 g at a constant glide slope angle (10 deg) to an altitude of 100 feet, followed by a level flight deceleration to a hover; this task is representative of that which will be used in a forthcoming flight experiment. The results are documented in Reference 7. Of primary interest for this summary is the fact that the moving map display was found to be marginally acceptable for the task investigated and the experiment resulted in a recommendation that this display be replaced for future flight experiments.

Section IV

CONCLUDING REMARKS AND RECOMMENDATIONS

This report has reviewed the demonstrated capabilities of the X-22A aircraft and ground simulator, with particular emphasis on documenting the recently expanded aircraft capabilities in hover and transition. The following concluding remarks and recommendations are in order:

- The variable stability system has provided a wide range of simulated dynamics at fixed operating point, both longitudinal and lateral-directional, with no evidence of system limitations.
- The X-22A aircraft has been cleared for hover and transition on the VSS to essentially zero altitude, and a vertical landing on the VSS has been demonstrated. No limitations of the VSS for either the hover augmentation studies or the descending transitions were noted.
- It is recommended that the orientation of the w-LORAS be changed to the x-z plane to obtain both a better w-measurement for all forward speeds and a u-measurement less corrupted by local flow effects. It may also be necessary to move the u-v LORAS from its present position on the tail to obtain a less corrupted v-measurement.
- The usefulness of the ground simulator as a complement to the X-22A aircraft was demonstrated during the first experiment on this facility, which resulted in a recommendation to improve or replace the horizontal situation display (moving map) for future flight research programs.

Appendix I

X-22A VARIABLE STABILITY AIRCRAFT

This appendix presents detailed information on the basic X-22A aircraft, the Variable Stability System (VSS), and the technique employed to achieve the simulated aircraft characteristics using the VSS.

Basic X-22A

As is evident from Figure I-1, the X-22A has four ducted propellers and four engines. The engines are connected to a common system of rotating shafts which distribute propulsive power to the four propellers. Changes in the direction of the thrust vector are accomplished by rotating the ducts which are interconnected so that all rotate through the same angle and which can be varied between 0 and 95 degrees. Thrust magnitude is determined by a collective pitch lever, very similar to a helicopter. Normal looking pitch, roll and yaw controls in the cockpit (Figure I-2) provide the desired control moments by differentially positioning the appropriate control elements (propeller pitch or elevon deflection) in each duct.

In hovering flight (Figure I-3), the X-22A employs fore and aft differential blade pitch for pitching moments, left and right differential blade pitch for rolling moments, and left and right differential elevon deflection for yawing moments. In forward flight (Figure I-4), fore and aft differential elevon deflection is used for pitching moments, left and right differential blade pitch for yawing moments. A mechanical mixer directs and proportions the pilot's commands to the appropriate propellers and elevons as a function of the duct angle. Figure I-5 presents a functional diagram of the primary X-22A flight control system as well as the variable stability system which is discussed in the next section.

The rate of descent capability of the X-22A at various speed and duct angle combinations (Reference 10) is illustrated in Figure I-6, while Figure I-7 shows the transition envelope. For the STOL approach experiments performed with the X-22A, speed/duct angle combinations of 65 kt/50 deg and 80 kt/30 deg were chosen to maximize the X-22A rate of descent capabilities at the steep approach angles ($\gamma = -7.5$ and -9 deg). Maximum speed in the present configurations is 150 knots and the aircraft is capable of full transitions from this speed to a hover.

GENERAL SPECIFICATIONS

DIMENSIONS

Length	39.57 ft	
Height	20.69 ft	
Tread	8.0 ft	
Wing	Front	Aft
Area	139 sq ft	286 sq ft
Span	22.97 ft	39.24 ft
Aspect Ratio	3.86	5.38

ENGINE RATINGS

<u>SHP</u>	<u>SLS</u>	<u>Thrust</u>	<u>rpm</u>	<u>Min.</u>
1250	Mil.	154	19,500	30
1050	Nor.	132	19,500	Cont.

POWER PLANT

No. & Model	(4) YT58-GE-8D
Mfr.	General Electric Co.
Type	Free Power Turbine
Reduction	
Gear Ratio	0.133
Prop Mfr.	Hamilton Standard
Prop. Dia.	84 in.
No. of Blades	3
Tail Pipe	Fixed Area

WEIGHTS

<u>Loading</u>	<u>lb</u>
Empty	11,622
Gross	15,287
Max Takeoff	18,420
Max Landing	15,287

FUEL

<u>No.</u>	<u>Gal</u>	<u>Location</u>
<u>Tanks</u>		
1	465	Fuselage

Fuel Grade JP-4 or JP-5

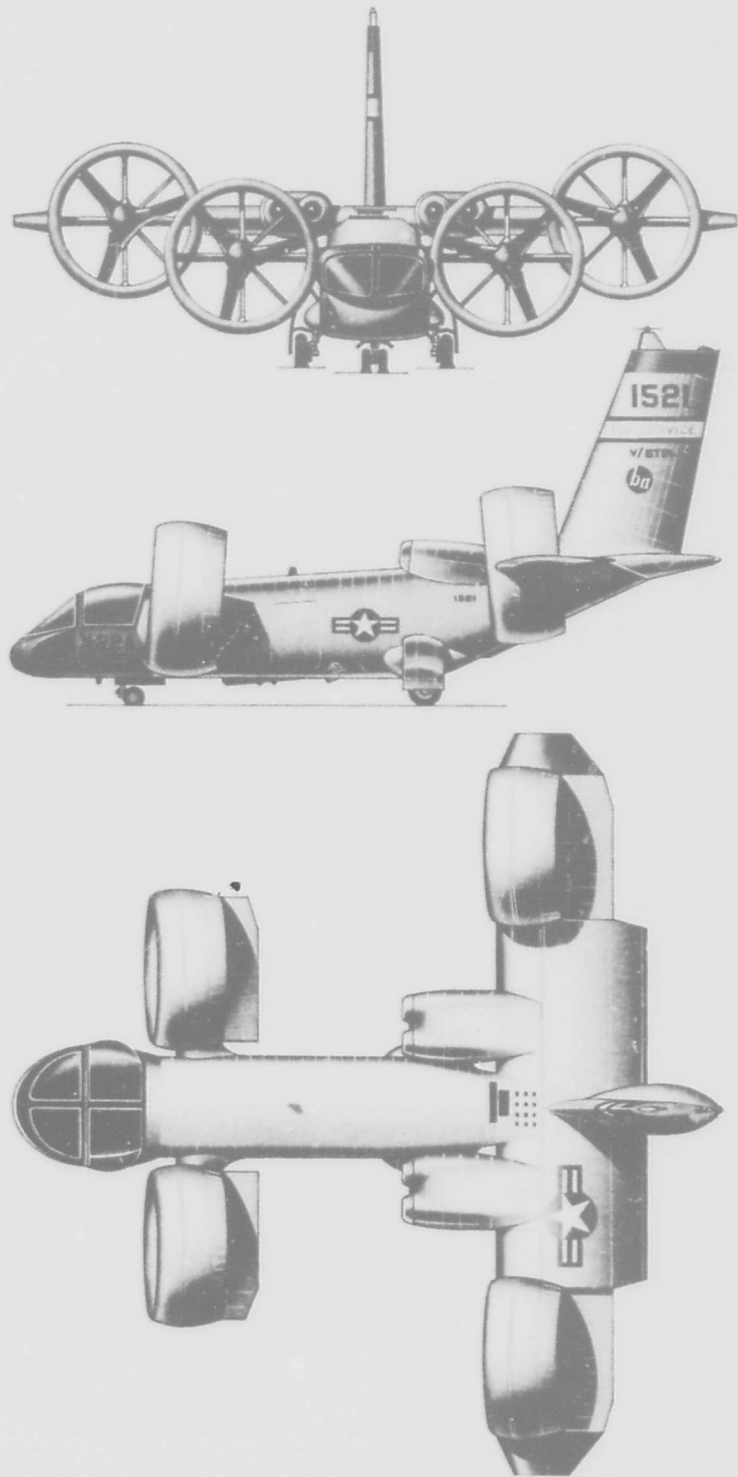


Figure I-1 X-22A AIRCRAFT, 3-VIEW

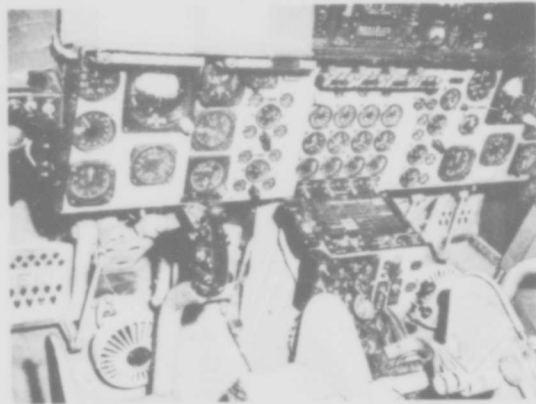


Figure I-2 INTERNAL VIEW, X-22A COCKPIT



Figure I-3 X-22A IN HOVERING FLIGHT

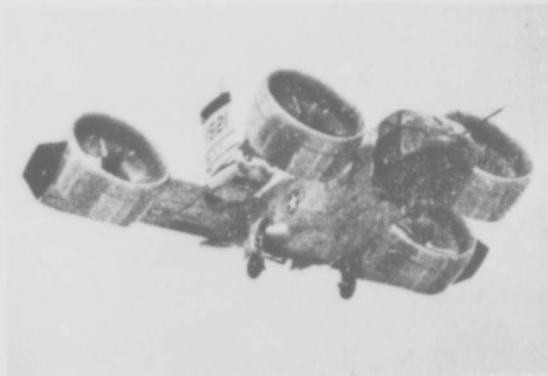


Figure I-4 X-22A IN FORWARD FLIGHT

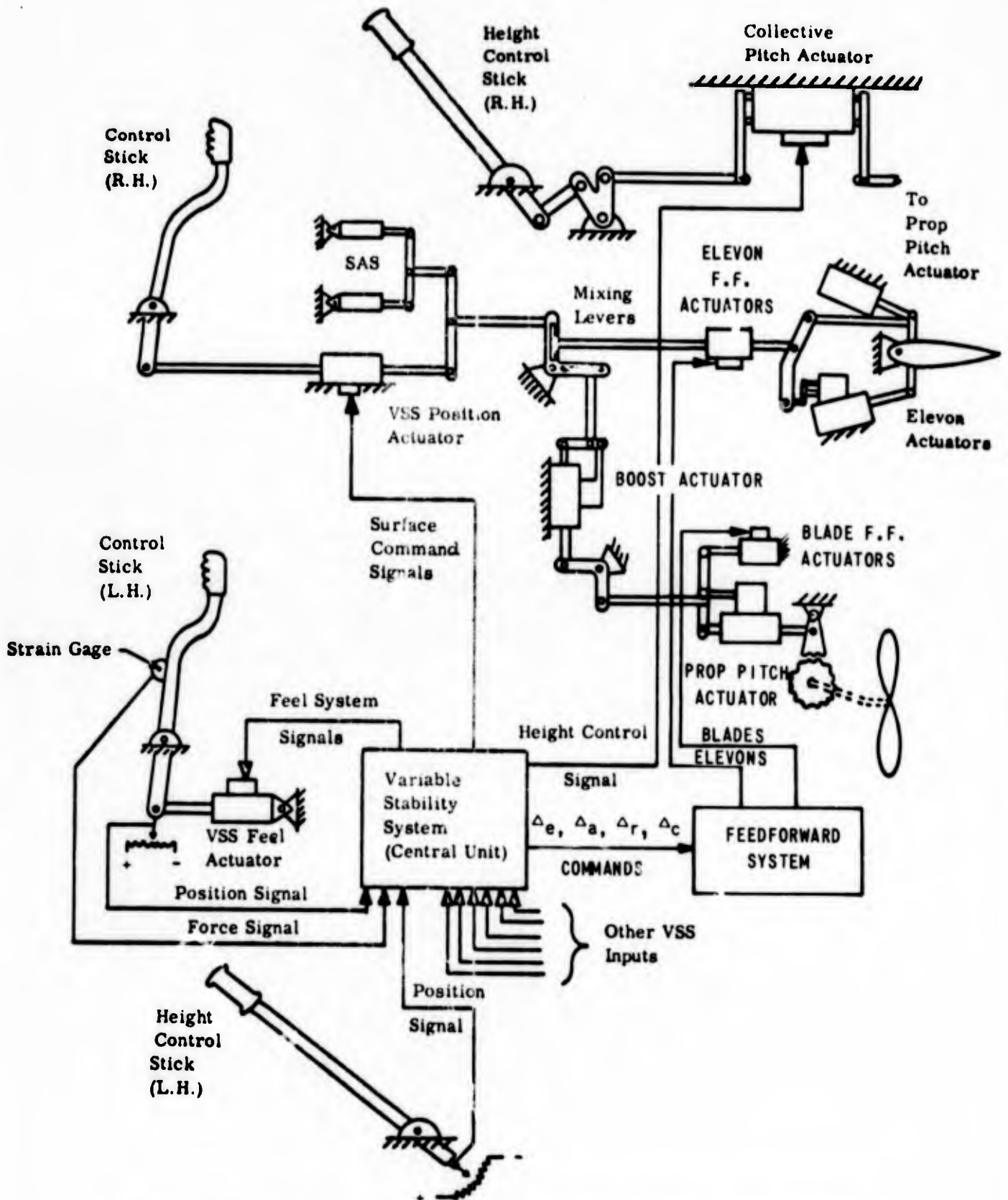


Figure I-5 FUNCTIONAL DIAGRAM OF VARIABLE STABILITY AND PRIMARY FLIGHT CONTROL SYSTEMS

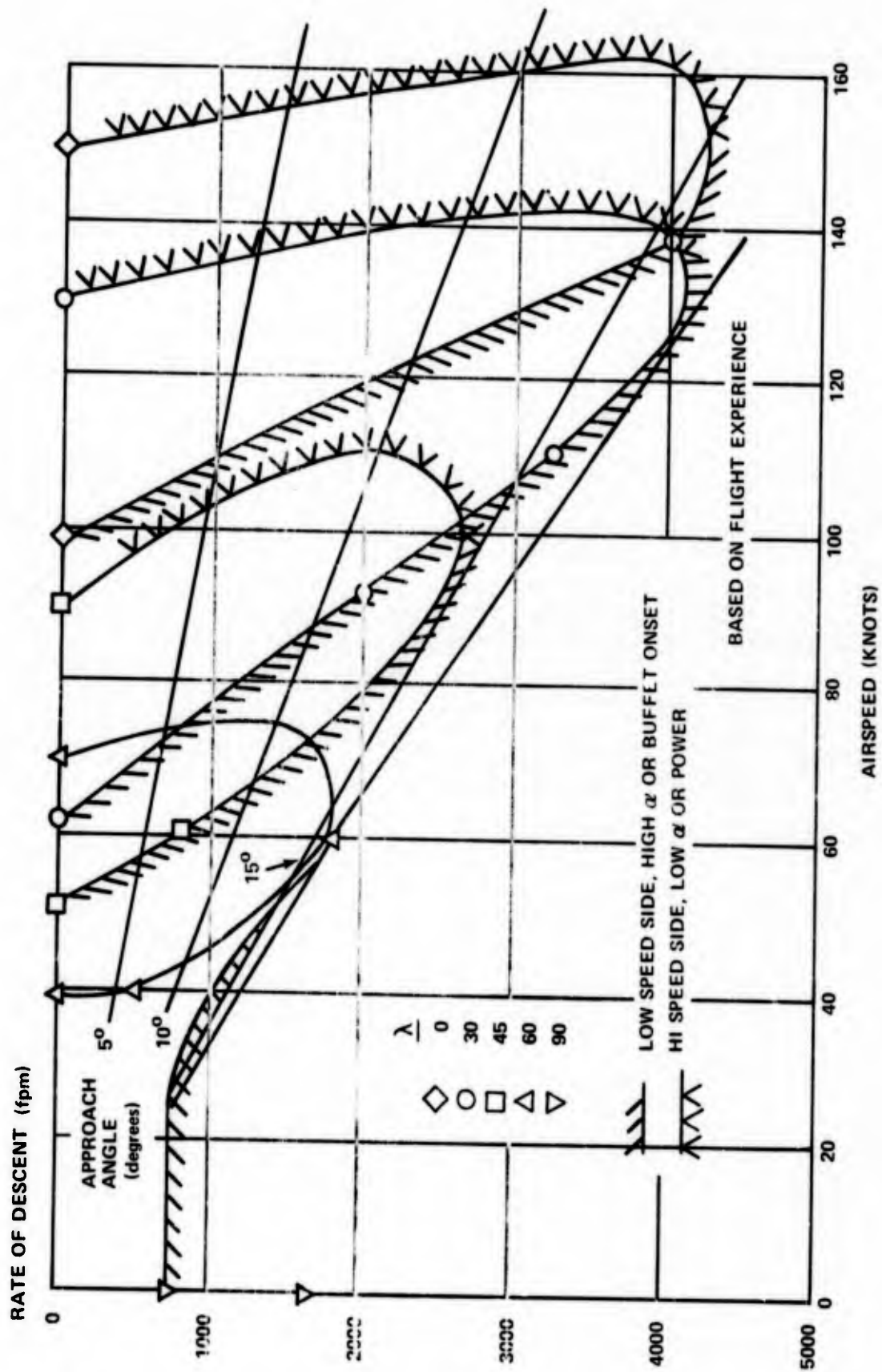


Figure I-6 RATE OF DESCENT CHARACTERISTICS

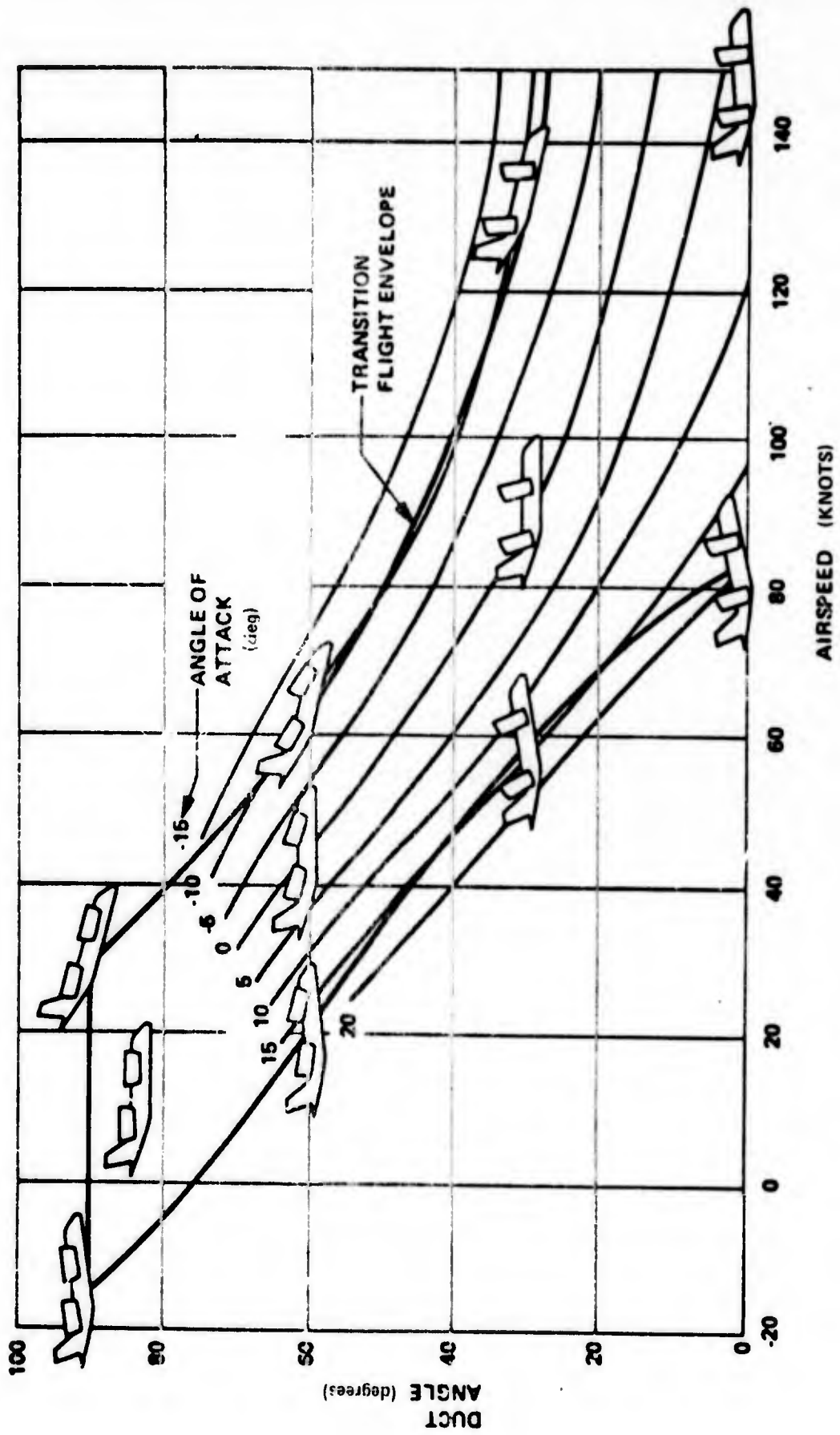


Figure 1-7 EQUILIBRIUM LEVEL FLIGHT ANGLE OF ATTACK AND TRANSITION FLIGHT ENVELOPE

X-22A Variable Stability System (VSS) and Mechanization

There are four VSS controllers - thrust, pitch, roll and yaw - and three artificial feel servos for the evaluation pilot cockpit controls, each employing electrohydraulic servos. When rigged for VSS flight the left hand flight controls are mechanically disconnected from the right hand flight controls and connected to the set of VSS pitch, roll and yaw feel servos. The VSS thrust servo operates the boost servo for the collective pitch system. VSS pitch, roll and yaw servos operate the right hand flight controls, moving the same linkages which are moved manually by the right hand pilot in normal non-VSS flight. (In fact, these same actuators serve a dual role by providing artificial feel for the primary flight control system when the VSS is not engaged.) Phasing of these control motions to the blades and elevons is accomplished by the mechanical mixer as for normal flight. A functional diagram of the variable stability flight control system is shown in Figure I-5.

During VSS operation, the evaluation pilot occupies the left hand seat in the cockpit. The system operator, who also serves as the safety pilot, occupies the right hand seat. The evaluation pilot's inputs, in the form of electrical signals, operate the appropriate right hand flight controls through the electrohydraulic servos. In addition to the evaluation pilot's inputs, signals proportional to aircraft motion and relative wind variables (for example, angle of attack or pitch rate) are fed back to move the right hand controls in the required manner and thus modify the aircraft's response characteristics as desired. The response-feedback and input gain controls are located beside the safety pilot as shown in Figure I-8 and are used to set up the simulation configurations in flight. Note that the evaluation pilot cannot feel the basic X-22A control motions caused by the variable stability system.

A simplified example of the X-22A variable stability system mechanization is shown in Figure I-9. This example illustrates how the desired values of the pitch control sensitivity, $M_{\delta_{e}}$, and the angle of attack stability, M_{α} , are achieved with this response feedback technique. For completeness, the full schematic diagrams for the pitch, roll, yaw and thrust control channels of the VSS, including the artificial feel system, are shown in Figures I-10, 11, 12 and 13.

An electronic control limiter can be inserted in any channel to systematically change the control power available to the evaluation pilot. This feature was used extensively in the lateral control power experiment reported in Reference 4.

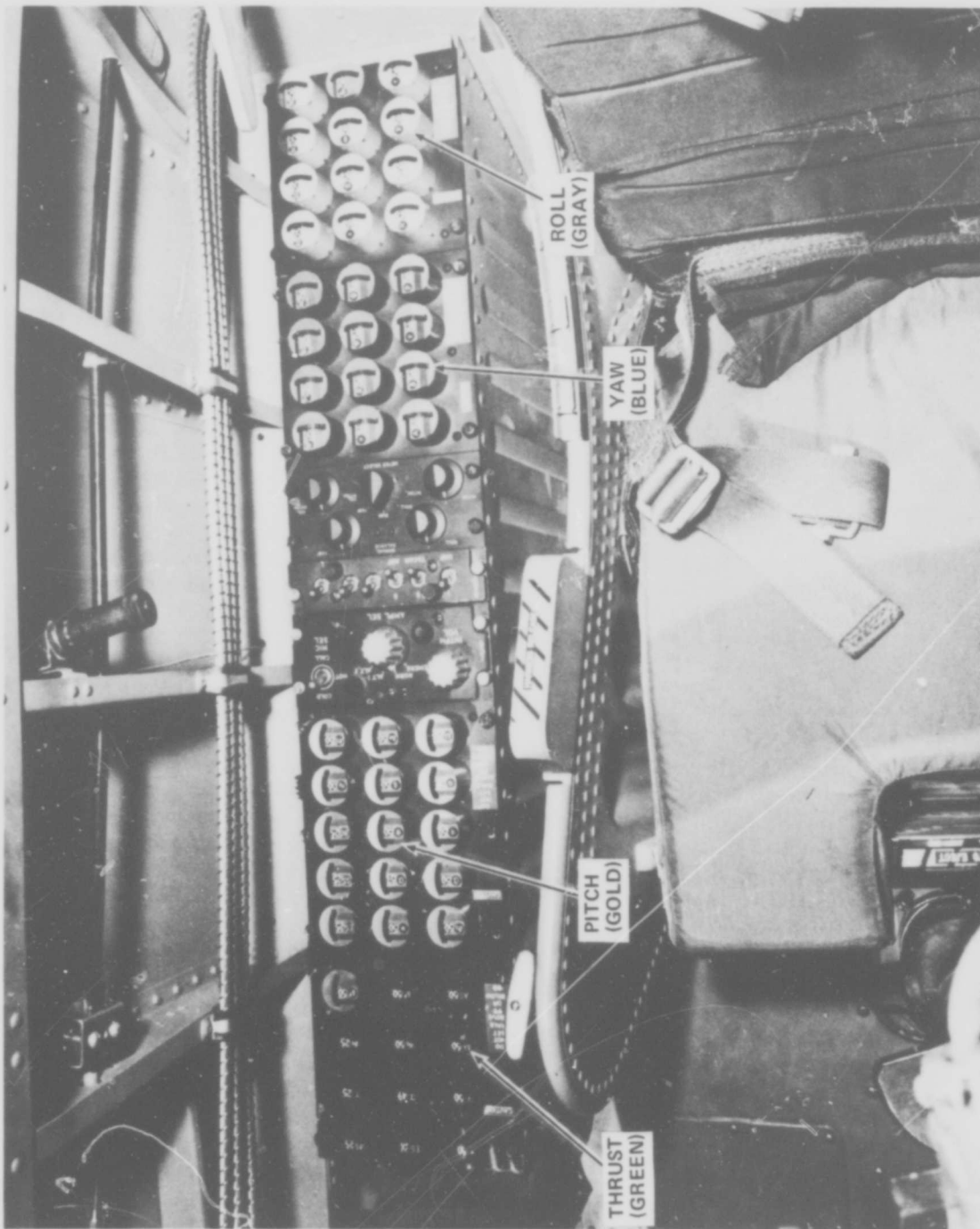
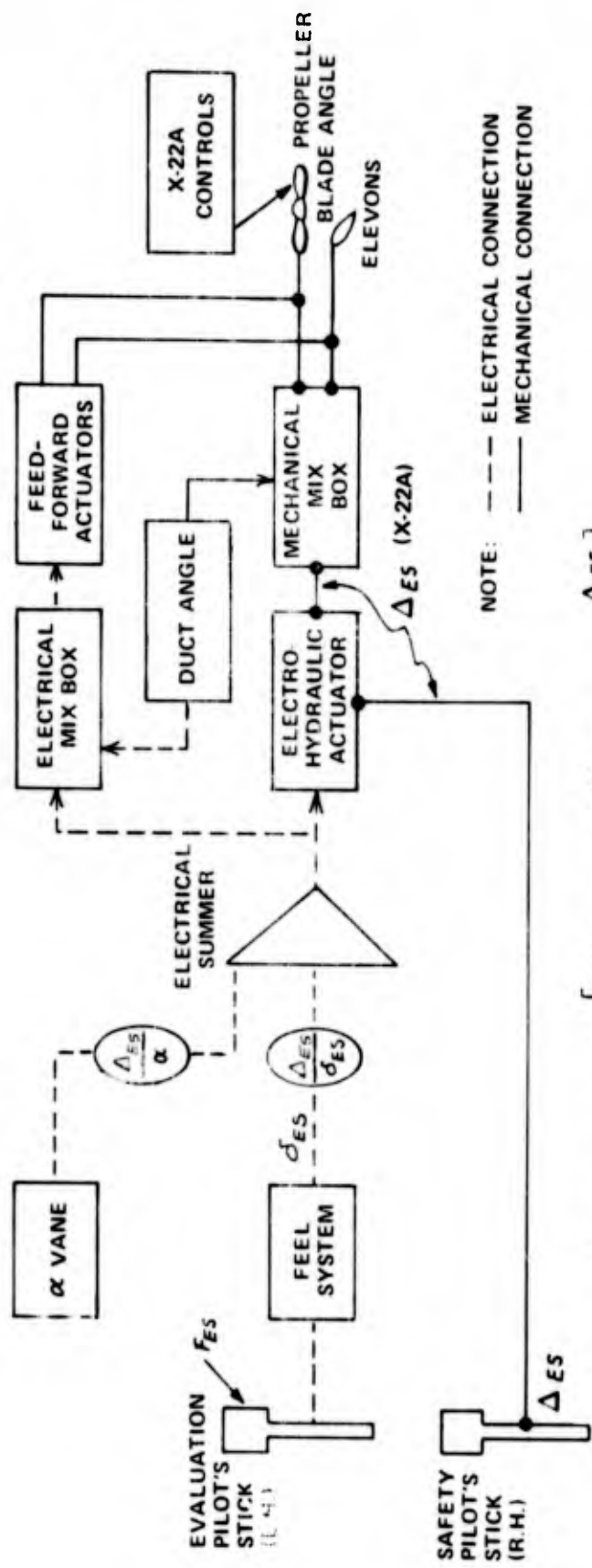


Figure I-8 VSS GAIN CONTROLS IN X-22A COCKPIT



$$M_{\alpha} \text{ (SIMULATED)} = \left[M_{\alpha(X-22A)} \pm M_{\Delta ES(X-22A)} \frac{\Delta ES}{\alpha} \right]$$

$$M_{\delta ES} \text{ (SIMULATED)} = \left[M_{\Delta ES(X-22A)} \frac{\Delta ES}{\delta ES} \right]$$

Figure 1-9 SIMPLIFIED EXAMPLE OF THE X-22A VARIABLE STABILITY SYSTEM MECHANIZATION

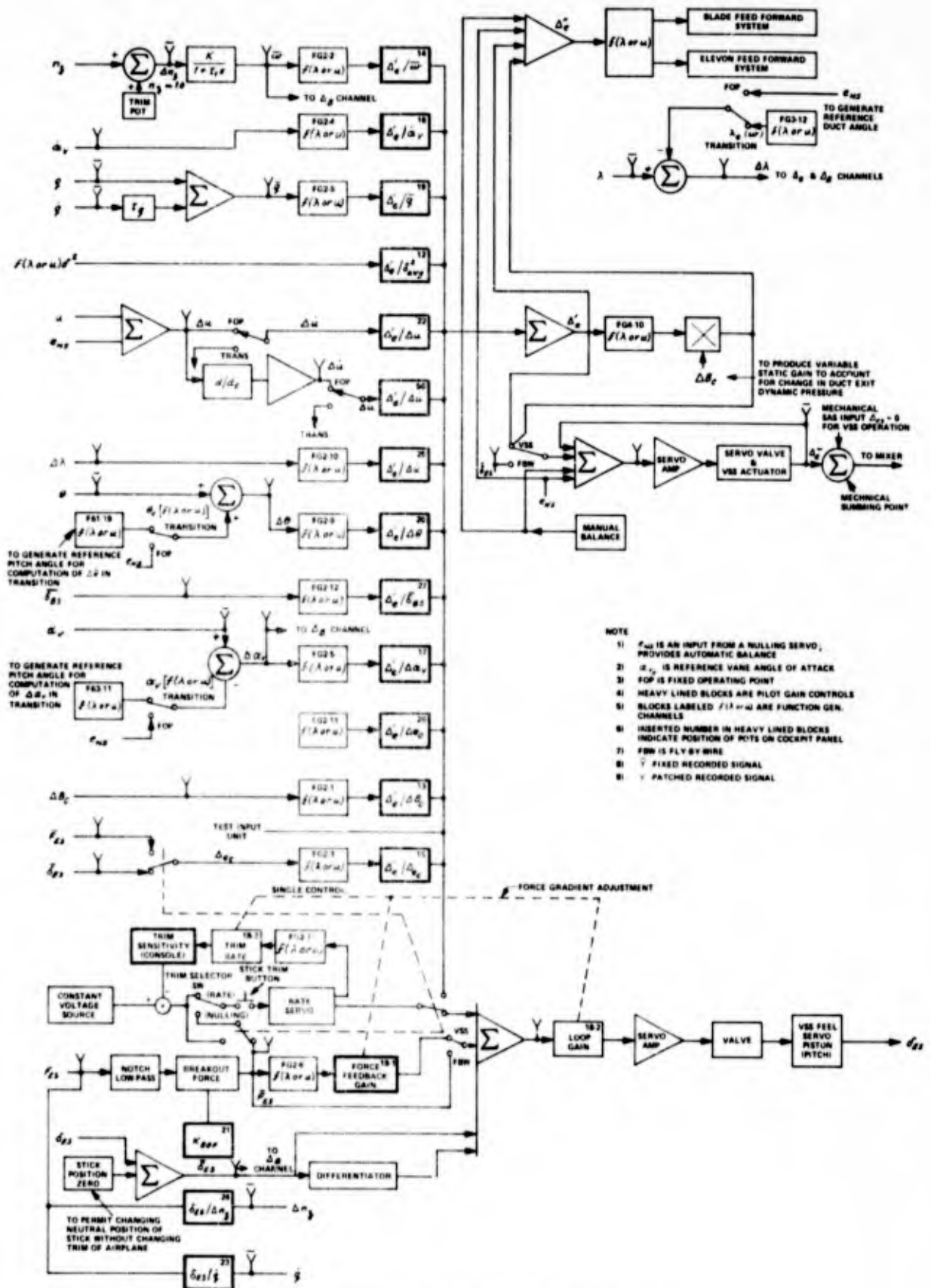


Figure I-10 X-22A VSS BLOCK DIAGRAM - PITCH

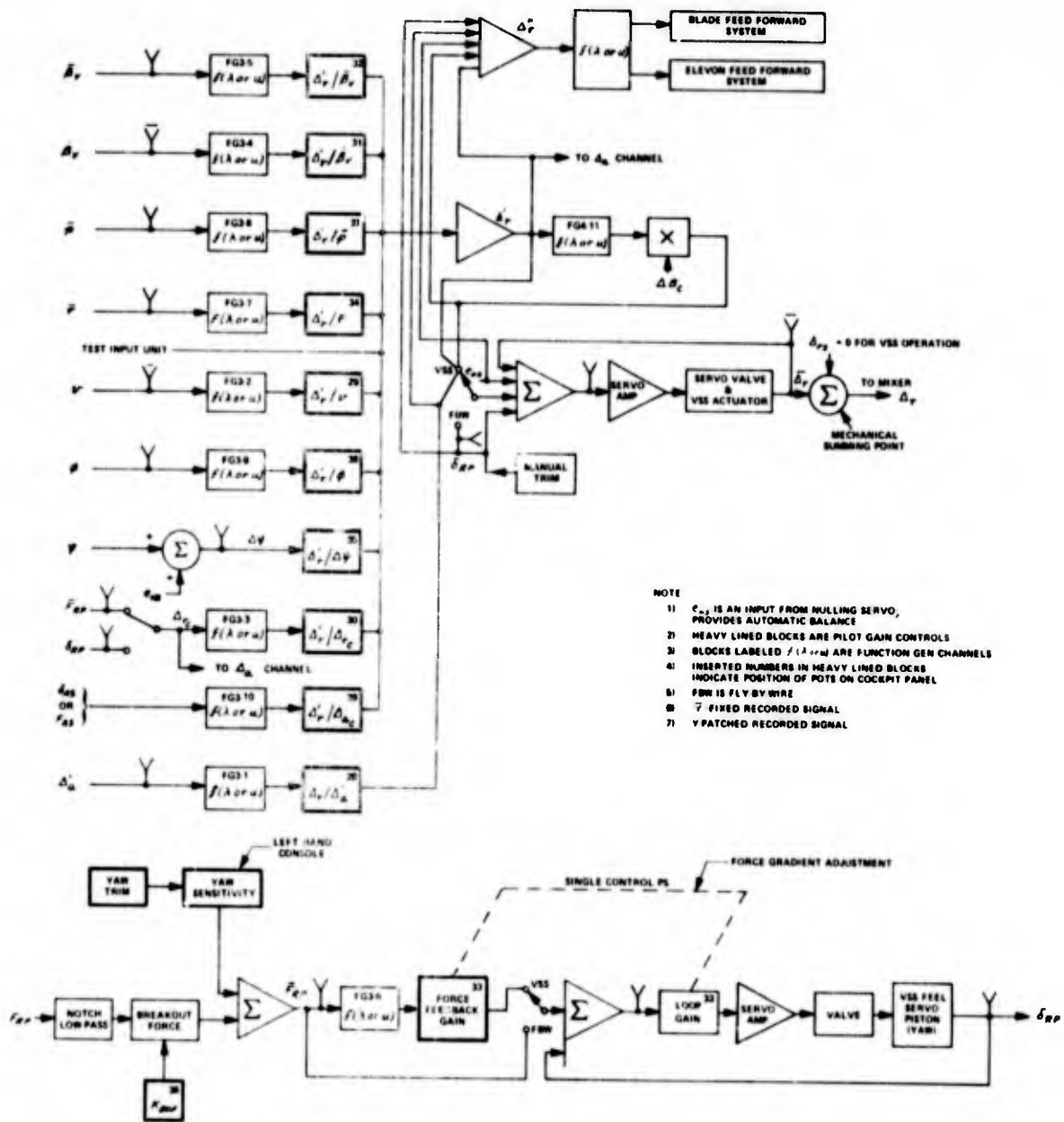


Figure I-12 X-22A VSS BLOCK DIAGRAM - YAW

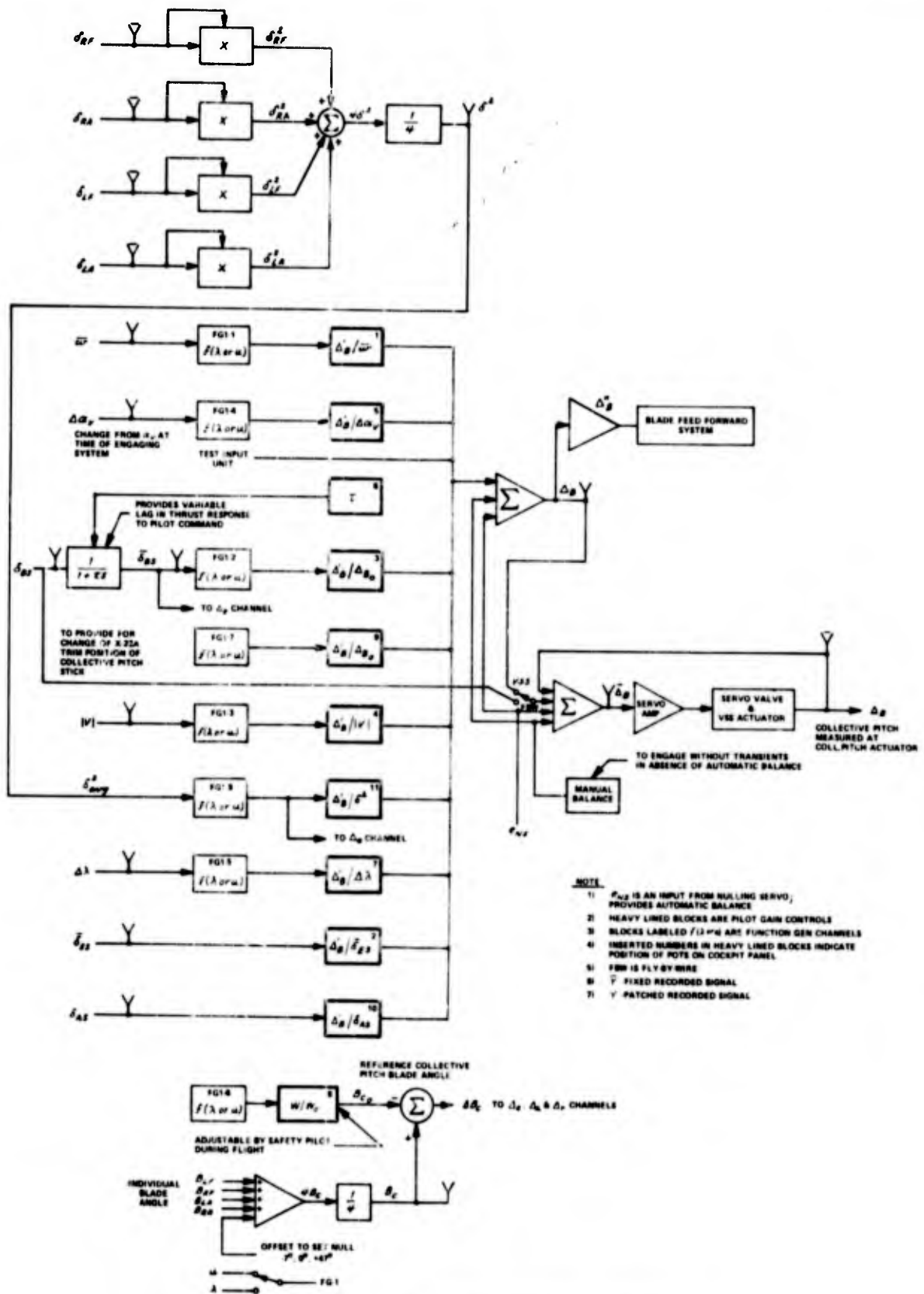


Figure I-13 X-22A VSS BLOCK DIAGRAM - THRUST

Unique Features of the X-22A VSS

One unique feature of the X-22A VSS is that the response feedback gains are programmable with velocity throughout the full range of airspeeds, from -30 knots rearward through zero to 150 knots forward airspeed. This is accomplished by a multi-channel function generator which receives its longitudinal airspeed input from the LORAS (Linear Omnidirectional Resolving Airspeed System, Figure I-14). LORAS was developed by Calspan specifically for the X-22A. Recently, a second LORAS - much smaller than the original - was added to the nose boom to measure the vertical component of airspeed (Figure I-15), specifically for VSS work in the hover. This figure also shows angle of attack (α_v) and sideslip (β_v) vanes mounted on the nose boom.

Another unique feature of the X-22A is the Feedforward Flight Control System (FFCS), shown schematically in Figure I-9. This is a limited authority, precision control system which acts like a vernier on the basic X-22A flight control system during VSS operation. The FFCS makes it possible to achieve extremely high precision in positioning the actuators for the X-22A aerodynamic controls - propeller pitch and elevon angle. Such control system precision is required for the satisfactory operation of the "closed-loop" VSS airplane.

A special Test Input Unit (TIU), which is a part of the X-22A VSS, greatly facilitates in-flight calibration procedures. This unit generates electrical step, doublet, or pulse inputs (whose magnitude and time scale are selectable) which can be inserted into any of the four VSS channels. Thus calibration records can be taken with repeatable, easily controlled, inputs.

VSS Gain Controls

The following tables summarize the command and feedback gains which can be used in the pitch, roll, yaw and thrust control channels of the variable stability system along with a brief description of the primary function of each gain control. Only the primary gain controls are listed in the table but, in fact, any desired electrical signal can be fed back to modify the response of the aircraft. Either position or force commands can be used in pitch, roll and yaw and all the feedback gains can be changed by both positive and negative increments.

Pitch

Gain	Primary Change
Δ_{ES}/δ_c	M_{δ_c} , decoupled basic X-22A
Δ_{ES}/δ_{ES} or F_{ES}	$M_{\delta_{ES}}$ or $M_{F_{ES}}$ control gearing
$\Delta_{ES}/\alpha_{\dot{v}}$	M_{α} , short period frequency
$\Delta_{ES}/\dot{\alpha}_{\dot{v}}$	$M_{\dot{\alpha}}$, short period damping
Δ_{ES}/q	M_q , pitch damping
Δ_{ES}/θ	M_{θ} , phugoid damping, short period frequency, pitch attitude stabilization
Δ_{ES}/u	M_u , phugoid frequency
δ_{ES}/F_{ES}	Force gradient
B_0	Adjustable breakout force
$F_{ES}/m_{\dot{v}}$	Bobweight effect

Roll

Gain	Primary Change
Δ_{AS}/r	L_r , at low speed
Δ_{AS}/δ_{AS} or F_{AS}	$L'_{\delta_{AS}}$ or $L'_{F_{AS}}$, control gearing
Δ_{AS}/β	L'_{β} , dihedral effect, $ \phi/\beta _d$
Δ_{AS}/p	L'_p , roll damping
Δ_{AS}/ϕ	L'_{ϕ} , roll attitude stabilization
Δ_{AS}/r	L'_r , spiral and $ \phi/\beta _d$
Δ_{AS}/δ_{RP}	$L'_{\delta_{RP}}$, cross coupling
δ_{AS}/F_{AS}	Force gradient
B_0	Adjustable breakout force

Yaw

Gain	Primary Change
$\Delta_{RP} / \delta_{RP} \quad F_{RP}$	$N'_{\delta_{RP}}$, or $N'_{F_{RP}}$, control gearing
$\Delta_{RP} / \beta_{\gamma}$	N'_{β} , directional stability
$\Delta_{RP} / \dot{\beta}_{\gamma}$	$N'_{\dot{\beta}}$, directional damping
Δ_{RP} / r	N'_{r} , directional damping
Δ_{RP} / p	N'_{p} , ϕ / δ_{AS} pole-zero displacement
Δ_{RP} / ν	N'_{ν} , low speed
Δ_{RP} / ψ	N'_{ψ} , heading hold, low speed
$\Delta_{RP} / \delta_{AS}$	$N'_{\delta_{AS}}$, ϕ / δ_{AS} pole-zero placement
δ_{RP} / F_{RP}	Force gradient
BO	Adjustable breakout force

Thrust

Gain	Primary Change
Δ_{BS} / δ_c	Collective gearing
Δ_{BS} / ω	Z_w at low speed with $\lambda = 90^\circ$, height damping
τ	Thrust lag, variable



Figure I-14 LONGITUDINAL VELOCITY LORAS INSTALLATION



Figure I-15 VERTICAL VELOCITY LORAS INSTALLATION ON NOSE BOOM
WITH α AND β VARIES

X-22A Flight Summary

The X-22A flight history from March 1966 to February 1973 can be summarized as follows:

No. of flights	320
Flight hours	232
Takeoffs Short	369
Vertical	457
Landings Short	317
Vertical	509 (2 on the VSS)
Transitions (Inbound and Outbound)	498 (25 on the VSS)

Of the total flight hours, 105 were flown at Calspan during the two research programs discussed in Section 2.1. The purpose in reviewing these statistics is to illustrate that the X-22A, although clearly a complex vehicle, has a substantial flight history behind it. In addition, the excellent reliability and operational readiness of the aircraft and the associated systems were evident during both flight programs. For example, of the 54 flights flown during the Task II program, only 3 were terminated due to aircraft problems and the last 14 evaluation flights were completed during a 17 day period.

Appendix II

DATA ACQUISITION AND PROCESSING SYSTEM

The X-22A aircraft and variable stability system are extremely complex systems, requiring monitoring during flight of many more variables than can be easily scanned by the pilot. A sophisticated system for data telemetry, acquisition, and processing was therefore designed for the X-22A system, and will be briefly described in this appendix. A complete description is given in Reference 2.

X-22A Telemetry System

All data pertinent to the flight of the X-22A is telemetered to the ground via a pulse-code-modulated "L-band" telemetry link. The nominal power of the transmitter is 6 watts at 1441.5 MHz. The basic pulse-code-modulator operates at a bit rate of 144 kHz - 80 channels sampled at a 200 Hz rate and encoded into 9-bit words. Five channels are required for time and synchronization, leaving 75 data channels. One of these 75 data channels is subcommutated to 64 channels; another one is required to identify the subcommutated channel; thus a total of 137 (73 + 64) channels are available for continuous data transmission. (The 73 main-frame channels are sampled 200 times per second and the 64 subcommutated channels are sampled 200/64 times per second.)

Patch panels in the X-22A permit selection of the 137 variables to be transmitted on a given flight from approximately 200 available variables. For the present flight test programs, approximately 80 of the transmitted variables are monitored purely from flight safety considerations. Another group of 51 variables are purely related to flying qualities research experiments. The remaining 16 transmitted variables are of interest to both flight safety and the research experiment.

Experience to date indicates that very good telemetry coverage, with few "drop-outs", is obtained up to about 15 to 20 miles between the X-22A and the van.

Equipment

The data are telemetered to a ground station and experiment control center housed in a mobile van (Figures II-1, 2). The van contains the following equipment:

- (a) an omnidirectional antenna and a steerable, directional antenna
- (b) a telemetry receiver
- (c) a PCM decommutator and signal simulator
- (d) a tape recorder for recording the complete data stream
- (e) a 32-channel digital-to-analog converter (DAC)



Figure II-1 MOBILE VAN, EXTERNAL VIEW



Figure II-2 MOBILE TELEMETRY VAN, INTERNAL VIEW

- (f) four 6-channel chart recorders
- (g) a panel of 9 meters for continuous display of a fixed set of flight safety variables
- (h) a patch panel to select a desired set of 32 variables for the DAC's
- (i) a paper printer
- (j) a mini-computer with 24K storage capacity, 800 nanosecond effective cycle time, 36 channels of Digital-to-Analog converters and 12 channels of Analog-to-Digital converters
- (k) a teletypewriter
- (l) a high-speed paper tape unit
- (m) a 9-channel digital tape recorder
- (n) a 360 channel VHF transceiver
- (o) a voice-actuated magnetic tape recorder
- (p) a weather station
- (q) two 5 kW 115-volt, 60 Hz generators

A simplified block diagram of the functions of this equipment during a flight is shown in Figure II-3. The primary purposes of the equipment include flight safety monitoring, experiment control, and data processing, each of which is briefly described below.

Functions of the Mobile Van/Experiment Control Center

As has been discussed, the complexity of the X-22A aircraft requires constant monitoring of a large number of flight safety variables. This function is performed by the mini-computer in the mobile van. High and/or low limit values for the variables are stored in the computer; the telemetered data is processed through the computer on-line and compared continuously with these limits. In the event of a variable exceeding these preset limits, the teletypewriter unit immediately prints out the variable in question and its value. The high speed paper tape unit acts as an independent backup by printing out on command the values of all of the telemetered variables.

During a flight, the mobile van is the experiment control center in which all the pilot input and aircraft response variables are monitored on-line with chart recorders. The flight test director is in continuous communication with the aircraft, and, on the advice of the engineers monitoring the flight variables, can, for example, request the repeat of a calibration record. In addition, although this capability has not been used, it is possible to program the desired equations of motion on the mini-computer, drive these equations with the telemetered control inputs to the aircraft, and compare the desired responses with the actual aircraft responses. This capability allows iteration of the VSS gains on-line to achieve the desired configuration dynamics.

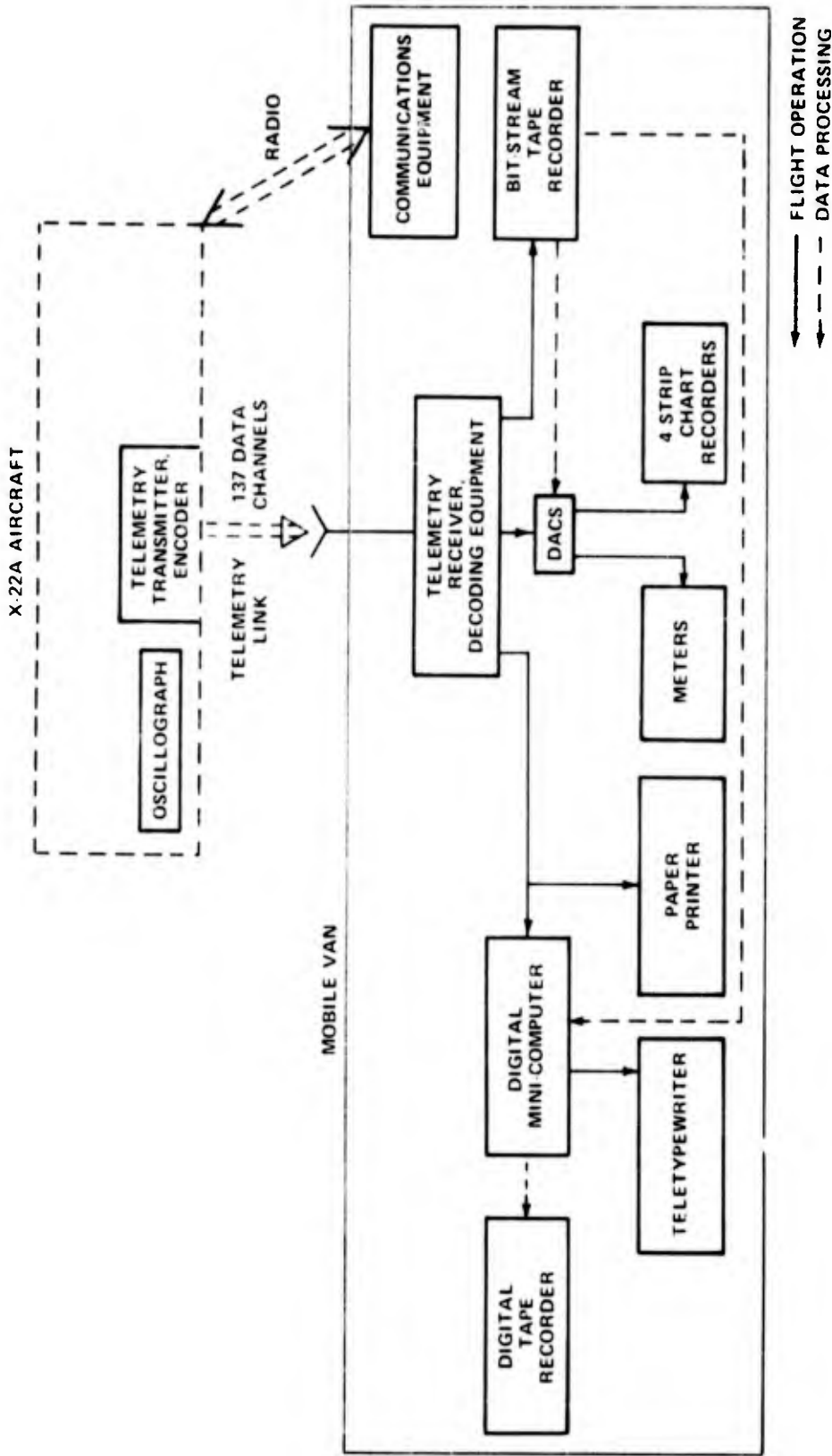


Figure III-3 SCHEMATIC DIAGRAM OF DIGITAL DATA ACQUISITION SYSTEM

The equipment in the van also serves to process the flight data digitally "off-line" after a flight. All telemetered data during a flight are recorded continuously on the bit-stream recorder. For digital data analysis, the appropriate portions of the appropriate channels are selected from the bit-stream recorder, and the format changed to be compatible with the IBM 370/165 computer used for the analyses. This is accomplished through use of the van computer and equipment to produce the required digital tape which is then processed by the IBM 370/165 computer. In this form the flight data can be processed as desired. For example, statistical measures of control usage and task performance can be quickly obtained on a semi-production basis in any required format including probability density functions and power spectral densities. The digital parameter identification technique used to identify the evaluation configurations from the flight data is discussed in Appendix IV.

Appendix III

IDENTIFICATION OF SIMULATED CHARACTERISTICS

The conduct of flying qualities experiments using response-feedback variable stability aircraft is strongly dependent on the capability to estimate dynamic characteristics from flight data. This capability is required both during the calibration phase of the flight program, in which the feedback gains to achieve the desired configurations are ascertained, and during the evaluation phase to verify the achieved dynamics. The estimation or identification problem is particularly difficult for lateral-directional flying qualities programs, in which all of the moment derivatives are varied to achieve modal characteristics which are highly nonlinear functions of these derivatives. It is mandatory in flying qualities research that the identification be performed carefully and with as accurate a method as possible.

This appendix discusses in some detail the digital identification technique used in support of X-22A research programs, and presents typical results for both longitudinal and lateral-directional simulated characteristics. Included in the discussion is a brief review of the digital identification technique used, a summary of the data processing required, a documentation of the input information required by the identification algorithm, and a review of the flight test and data analysis procedures that are appropriate.

Kalman Filter Digital Identification Technique

The primary method used on X-22A flight programs to identify the simulated stability derivatives is the locally iterated Kalman filter technique developed by Calspan for the X-22A. The development of this technique is presented in Reference 3, and its characteristics are summarized in References 1, 4 and 5. A schematic diagram of the identification process using this technique is given in Figure III-1, and is reviewed briefly below.

The Kalman filter technique is an advanced method which is capable of treating both process and measurement noises for systems that may be described by general nonlinear equations. Referring to Figure III-1, the method employs a three-stage refining process to perform the identification.

- (1) Initial estimates of the parameters, and their variances, in the assumed equations are obtained by a method that is essentially an equation-error technique. Since the variances obtained by this method are somewhat underestimated, an improved variance estimate, employing the parameters estimated above, may be obtained by a Cramer-Rao lower bound computation if desired.

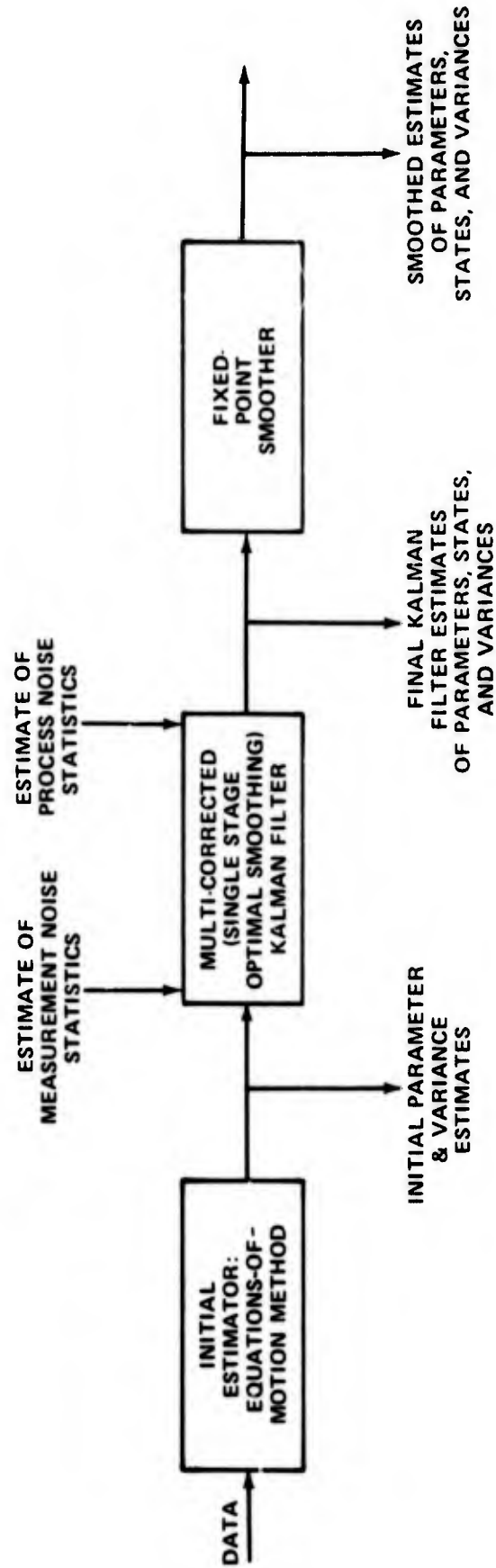


Figure III -1 SCHEMATIC DIAGRAM OF KALMAN FILTER DIGITAL IDENTIFICATION PROCESS

- (2) An extended Kalman filter, utilizing a "local iteration" or "multi-correction" algorithm, is used to refine the initial estimates of the parameters. Although the extended Kalman filter gives biased estimates when applied to a nonlinear problem, which is inherent to parameter identification, it can be shown that the multi-correction scheme reduces biases due to nonlinearities by improving the reference trajectory between data points.
- (3) A fixed-point smoothing algorithm, which actually works in conjunction with the multi-corrector at each data point, may be used to further refine the parameter estimates and separate out the effects of process noise. This step is extremely important as a first attempt at determining the mathematical modeling error, as well as improving the parameter estimates. Also, a more accurate variance computation of the parameter estimate is obtained.

As originally developed, the technique was only applicable to the three-degree-of-freedom longitudinal equations of motion but has since been extended to handle the lateral-directional equations of motion.

Digital Data Processing

To perform digital identification with the Kalman filter using the equations given above, a fairly extensive data processing procedure is required to transform the recorded flight data into a suitable format. A description of the general process is given in Appendix II, and those details pertinent to the identification procedure are summarized below.

For use with the assumed equations, the digital data are transformed from measured variables to equations-of-motion variables at the center of gravity. These transformations are not strictly required for the identification algorithms, but result in more efficient (i.e., less costly) identification. The primary transformations required are on the aerodynamic motions, since angle of attack and sideslip angle are measured on a boom in front of the aircraft. In addition, the linear accelerometer package is displaced above the aircraft center of gravity, and hence the η_y measurement must be corrected.

$$\beta = \frac{\beta_m}{K_\beta} - r_m \frac{l_x}{V_0}$$

$$\alpha = \frac{\alpha_m}{K_\alpha} - q_m \frac{l_x}{V_0} - \alpha_0$$

$$\eta_y = \eta_{ym} - \dot{x}_m Z_y \quad (\text{units of } \eta_y \text{ are deg/rad} \times \text{ft/sec}^2)$$

where $l_x = 22.5 \text{ ft}$

$y = 1 \text{ ft}$

$K_\beta = 1.1$

$K_\alpha = 1.12$

$\alpha_0 = 3.1 \text{ deg}$

()_m is measured value

The data processing procedure may therefore be summarized as follows. The flight data of interest that are recorded on-line by the "bit-stream" recorder are edited and placed into IBM 370/65 compatible format by the mini-computer and re-recorded on to digital tape (see Appendix II for a description of these units). In this form, the data are transformed to the appropriate variables as described above, edited to be compatible with the Kalman filter identification computer programs, and again re-recorded into a final data tape.

Input Information

The final data tape discussed above is now used for the identification procedure. In common with any technique based on Kalman filter theory, the following input information is required to start up the algorithm:

1. Initial estimates of the parameters.
2. Variances of the initial estimates.
3. Reference conditions of the states.
4. Measurement noise variances.
5. Process noise variances.

The initial parameter estimates are obtained from a conventional least-squares equation error method, which also produces estimates of the parameter variances. It has been observed experimentally that the variance estimates obtained by this method do not correctly represent either the absolute or the relative accuracy of the initial parameter estimates. Operational considerations dictated use of an arbitrary multiplication factor to correct these deficiencies, although this option was less appealing from a theoretical viewpoint. Experience has shown that this more direct method is adequate.

The measurement noise statistics are obtained by visual examination of the flight records. Generally, the "hash" on the records is assumed to equal the variance of the measurement noise, which provides a conservative value. This estimate is then checked qualitatively by comparing plots of the residual sequences of the filter operation with the assumed noise statistics, and readjusting the statistics if required. The X-22A data acquisition system provides data with excellent signal-to-noise ratios in general, and therefore this method of estimating the measurement noise variances is sufficiently precise. In the interests of rapid and efficient identification procedures, it is generally desirable to use the same statistics for all data records; on the other hand, these statistics also are weighting factors which can help to improve the filter performance and should therefore be chosen carefully. In addition to selecting the measurement noise statistics from visual examination of the data, the reference (or initial) conditions of the states are chosen to be the first datum points ($t = 0$) on each record tape. Since calibration identification records of the evaluation configurations are usually obtained about trimmed flight, the first point on the data tape is generally a valid reference condition. The fixed point smoother may be used to obtain an estimate of the initial conditions if necessary, but this computation is not generally required for the X-22A data.

The most difficult choice of required input information is that of the process noise statistics. To some degree, the process noise covariance matrix Q is a "fiddle parameter" in the algorithm which may be used to improve its performance for a given data record. On the other hand, the requirement for rapid post-flight identification as nearly automatic as possible leads to a desire to hold these statistics at a fixed value for all flight records. To make this tradeoff, then, it is important to define precisely what the sources of process noise might be. For the X-22A data, there are essentially three sources of process noise:

1. Gust or turbulence inputs.
2. The variable stability system.
3. Modeling errors.

Of these, the gust inputs are of the least significance for the records that are analyzed, because the majority of calibration identification records are obtained in turbulence-free air to facilitate rapid checks on the frequency and damping of prevalent rigid-body modes of motion. The variable stability system is the source of "noise" both as a result of its dynamics not being included in the model and through its operation on noisy measurement signals.

The primary source of modeling errors, however, is the fundamental restriction that we seek the best linear model for the aircraft dynamics that will fit the data, as most flying qualities parameters are defined in terms of linear systems.

With regard to the choice of process noise statistics, therefore, the following considerations are relevant. For simulated aircraft that are highly augmented with regard to the X-22A (e.g., higher rigid body frequencies and dampings), the assumption of a linear model becomes increasingly valid, but the process noise added by the variable stability system increases. For simulated aircraft whose rigid body motions are similar to the X-22A (very little augmentation), the effects of the variable stability system are reduced but nonlinearities may start to become important. The magnitude of the process noise in these two cases may be considered approximately the same. The worst case is one in which the X-22A must be highly de-augmented, as linear aerodynamic terms may approach zero, thereby accentuating nonlinearities, and the variable stability system effects again become larger. For this case, it may be necessary to assume more process noise, particularly if the configuration is sensitive to turbulence (high $|\phi/\beta|_d$).

For identification of the X-22A data, it is assumed that the one set of process noise statistics is acceptable for all configurations save those which involve the de-augmentation of several stability derivatives, and this set is used for the rapid processing of the data. The values of the statistics are selected primarily by iteration on early data sets to achieve adequate performance, and then held constant.

Control Inputs

It is well known that the control input can significantly affect the identifiability of a data record (Reference 3, for example). Design of the optimum input for the identification of a given set of dynamics is a complex theoretical problem and generally yields inputs which are difficult to implement in a flight program. Hence approximations that provide at least some benefit to identifiability are sought.

In flying qualities experiments, inputs for identification records have historically been simple analytically and chosen to accentuate some particular features of the response. Examples include rudder doublets for the Dutch roll characteristics, and aileron steps for roll mode time constants and ϕ/S_{as} transfer function characteristics. It is easy to demonstrate that these inputs do indeed provide large sensitivities for the stability derivatives which have the primary influence on the characteristics of interest, but that other derivatives may not be identifiable with any accuracy at all. The usual procedure that is followed is to obtain several records with different inputs tailored heuristically to certain characteristics and thereby obtain in a composite fashion the total identification; this procedure may be quite valid if the basic aircraft characteristics are well known and not too many derivatives are varied.

On programs such as one involving variations in lateral-directional characteristics, where a majority of stability derivatives are varied to achieve the desired dynamic configurations a single input does not provide sufficient identifiability.

It was decided, therefore, to have the pilot attempt to put in switching inputs in both rudder and aileron for the calibration records in this experiment to enhance the identifiability of the records. Analysis of a simple example (see Reference 4) for a first-order system shows that the switching period should be 6-9 times the time constant of the system; although a second-order system was not considered, intuitively one can say that the input switching frequency should be approximately the natural frequency in order to correctly pick out the damping ratio. The advantages of using the pilot instead of some preprogrammed input are that he can maintain the aircraft responses within the linear constraints and, to some extent sense the natural frequencies of the aircraft to initiate the switching. The disadvantages include his tendency to act as a feedback controller, which decreases the linear independence of the sensitivity functions and, strangely, a tendency to switch inputs at frequencies about twice the Dutch roll frequency, which masks the Dutch roll damping ratios.

Identification Results

Examples of time history matches and identified derivatives for selected dynamic characteristics from previous X-22A flying qualities programs are given in Figures III-2 and III-5. In all cases, the crosses are the flight data, and the solid lines the computed responses using the identified derivatives.

These results were all obtained with the control derivatives fixed, in order to more accurately determine the stability derivatives. The values for the control derivatives were obtained by averaging the values identified from a large number of records in which the normalized covariances indicated good identifiability of them. The resulting control derivatives for the basic X-22A airplane are:

$$\begin{aligned}
 N'_{\Delta AS} &= .041 \quad \left(\frac{\text{rad/sec}^2}{\text{in.}} \right) \\
 L'_{\Delta AS} &= .343 \\
 N'_{\Delta RP} &= .215 \\
 L'_{\Delta RP} &= -.135 \\
 M_{\Delta ES} &= .32
 \end{aligned}$$

These values were therefore used in conjunction with the appropriate gearings for each of the records to calculate the simulated control derivatives, which were held fixed at the correct values for each configuration.

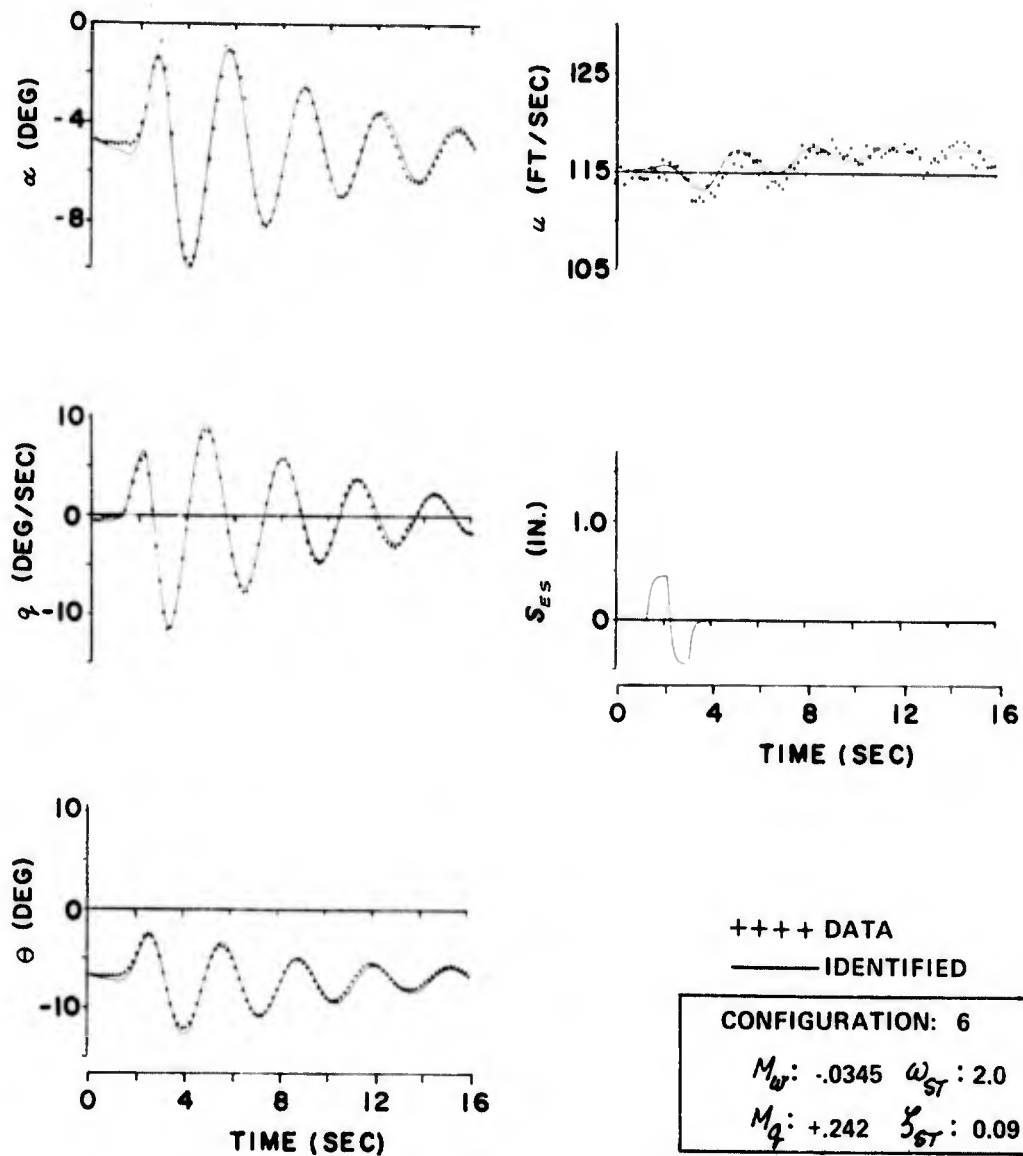


Figure III-2 IDENTIFICATION OF CONFIGURATION 6, LONGITUDINAL
(Reference 1)

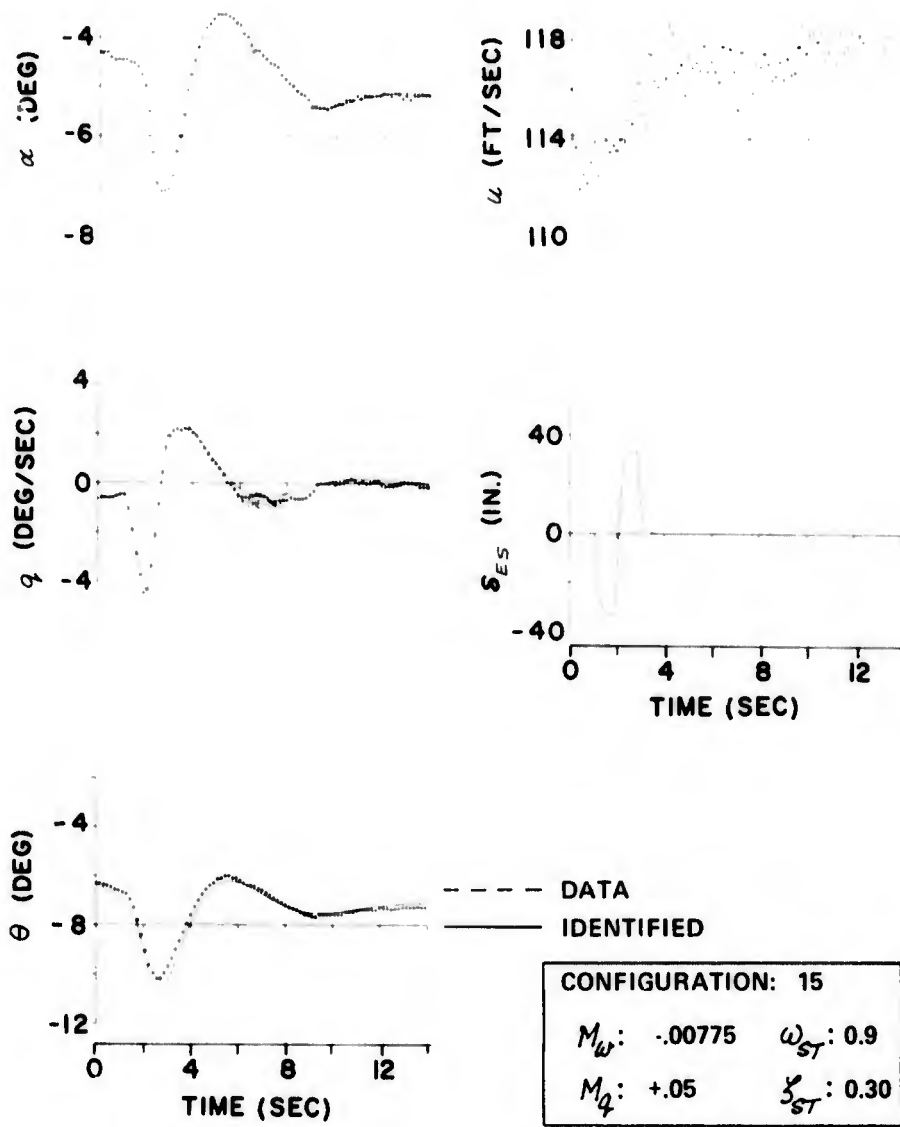


Figure III-3 IDENTIFICATION OF CONFIGURATION 15, LONGITUDINAL
(Reference 1)

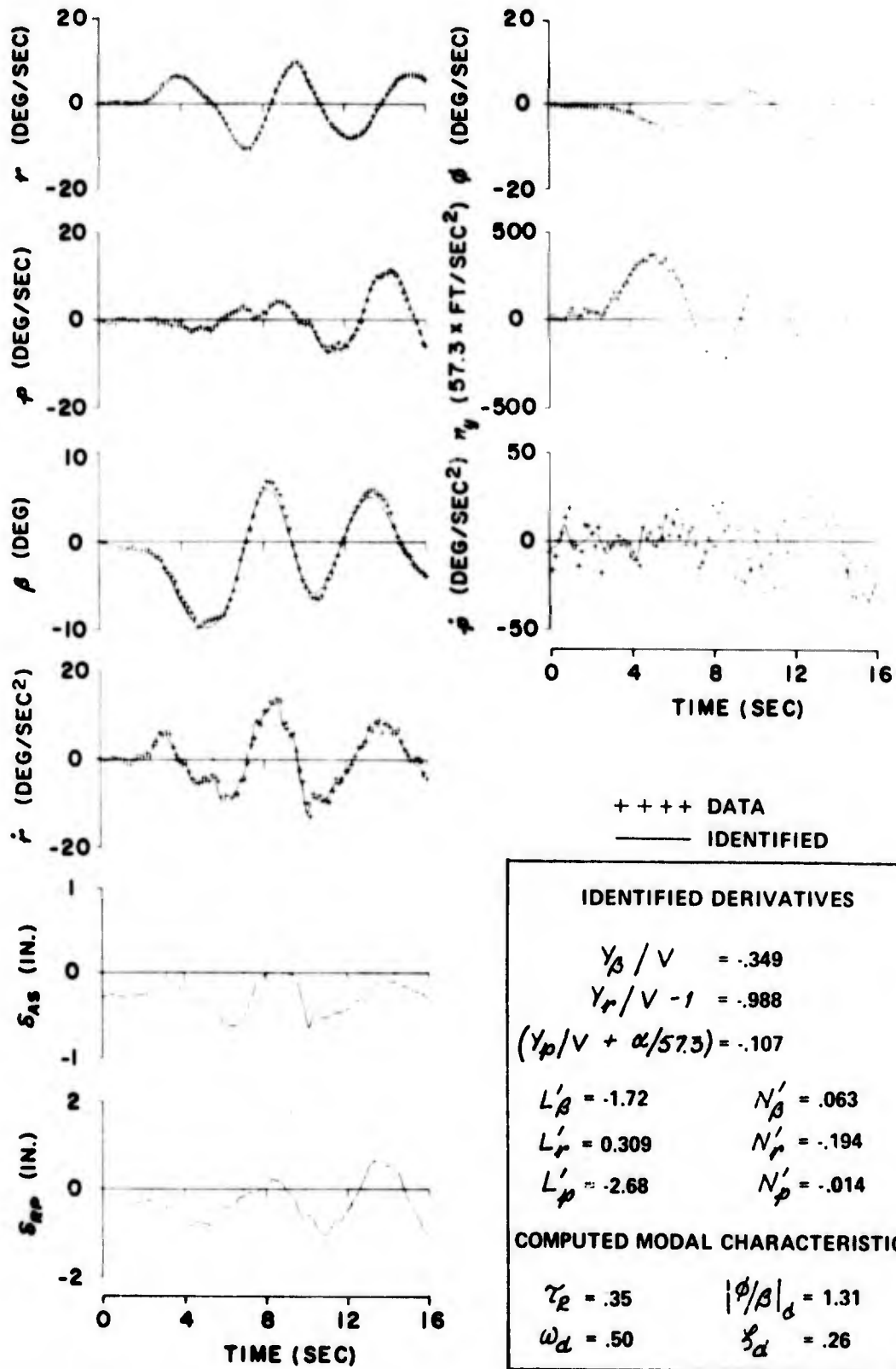


Figure III-4 IDENTIFICATION OF CONFIGURATION 1, LATERAL-DIRECTIONAL (Reference 5)

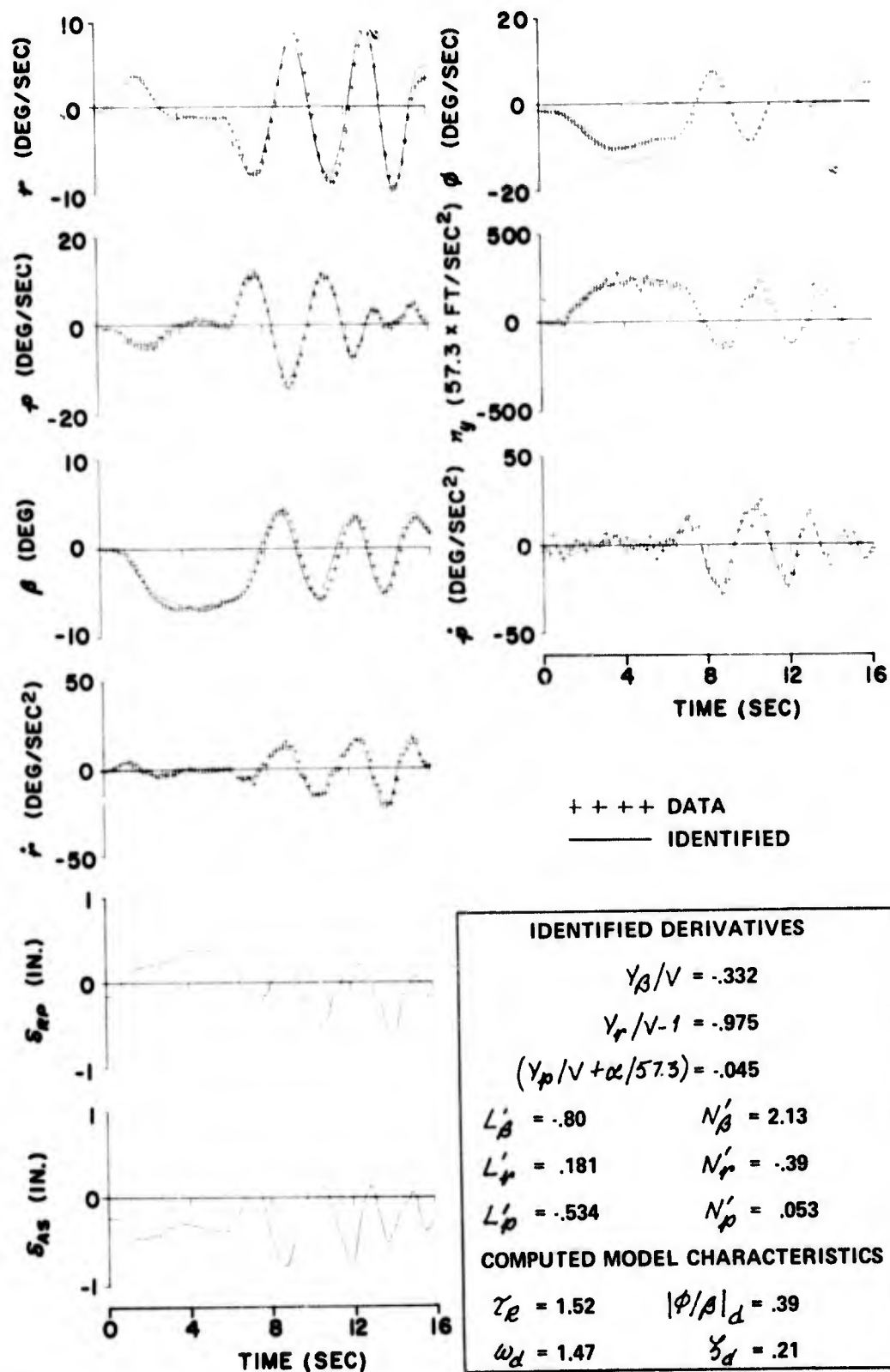


Figure III-5 IDENTIFICATION OF CONFIGURATION 6, LATERAL-DIRECTIONAL (Reference 5)

The good agreement between the computed and measured data apparent in the four examples presented in this appendix is characteristic of the identification results achieved in the first two X-22A flight programs (References 1 and 4). This fact, in conjunction with the generally low normalized covariances, indicates quite accurate identification. In addition, the digital results were generally in good agreement with hand and analog matching results of $|\phi/\delta|_d$ and Dutch roll frequency and damping, thereby providing further validation.

Appendix IV

FLIGHT DEMONSTRATIONS

This appendix presents an example of the flight plan that has been used to demonstrate the variable stability capability of the X-22A aircraft. During these demonstrations, the basic X-22A characteristics are shown first by having the evaluation pilot control the aircraft through the fly-by-wire (FBW) system of the aircraft; this system duplicates the safety pilot's control of the aircraft, but through a better feel system. With this background, the many different characteristics which can be obtained with the variable stability system (VSS) are then demonstrated. In the following listings, the summary of the flight and the actual flight test plan for a sample demonstration (Flight F-52 for Cmdr. C. Berthe, USN) are given.

SUMMARY OF X-22A DEMONSTRATIONS

1. SP performs normal $30^\circ \lambda$ STOL takeoff and climb to 3500 ft MSL. Engage FBW system at 80 KIAS, $30^\circ \lambda$ and EP samples basic X-22A response characteristics (SAS ON and OFF).
2. Disengage FBW and engage VSS with high frequency, well-damped longitudinal characteristics and good lateral directional response characteristics. EP samples aircraft with a variety of longitudinal gearings and force gradients. (Use Test Input Unit as desired).
3. Demonstrate high frequency, neutral damping longitudinal characteristics. Change longitudinal short-term response to low frequency, medium damping. EP samples aircraft.
4. Engage FBW. EP performs transition from 80 KIAS, $\lambda = 30^\circ$ to 110 KIAS, $\lambda = 15^\circ$, and back to 65 KIAS, $\lambda = 50^\circ$. EP investigates trim attitude/duct angle tradeoff at 65 KIAS, $\lambda = 45^\circ, 40^\circ$.
5. Engage VSS at 65 KIAS, $\lambda = 50^\circ$ with good configuration. If desired, EP performs transition to 80 KIAS, $\lambda = 30^\circ$ and back to 65 KIAS, $\lambda = 50^\circ$.
6. Change lateral-directional characteristics, varying ζ_α , $|\phi/\beta|_\alpha$, and yaw due to lateral control. Sample variations in lateral gearing, and demonstrate reduced control power using stick limiting.
7. EP performs approaches at 65 KIAS, $\gamma = -9^\circ$ with high frequency, well-damped longitudinal characteristics using mirror and TALAR for guidance. Repeat approaches with low-frequency, medium damping characteristics if desired.
8. Disengage VSS. SP performs transition to hover and back to $\lambda = 30^\circ$, and makes STOL landing at 80 KIAS, $\lambda = 30^\circ$.

TEST PROCEDURE

1. Perform "Pre-Start", "Engine Start", and "Pre-Taxi" checklists.
2. Taxi to appropriate runway and perform "Pre-Takeoff" checklist.
3. SP performs STOL takeoff ($\lambda = 30^\circ$, 80-90 KIAS), climb to safe altitude (~ 4000 feet AGL).
4. Engage FBW at $\lambda = 30^\circ$, 80 KIAS (LORAS). EP samples A/C (FBW is basic X-22A as flown in right hand seat). Demonstrate 1/2 SAS, SAS-OFF.
5. Disengage FBW. Engage VSS with:

Gold α = 22	Blue β = 74	Grey β = 70
Gold q = 20	Blue r = 30	Grey r = 50
Gold u = 50	Blue p = 50	Grey p = 36
Gold SS = 18 (7.5 lb/in)	Blue AC = 55	Grey SS = 50
Gold ES = 15	Blue RP = 26	Grey AS = 18
		Grey SL = 00

(High frequency, well damped: $\omega_{ST} \approx 2.5$ rad/sec, $\zeta_{ST} \approx .4$)

6. EP samples A/C. Demonstrate gearing (ES) and gradient (SS). If desired, use TIU.
7. Demonstrate zero damping:
 - Gold $\alpha \Rightarrow 16$
 - Gold q $\Rightarrow 55$
8. Demonstrate low frequency ($\omega_{ST} \approx 0.9$ rad/sec, $\zeta_{ST} \approx .3$):
 - Gold α = 55
 - Gold q = 62
 - Gold u = 72

If desired, vary gearing (ES).

9. Disengage VSS. Engage FBW. EP transitions to $\lambda = 15^\circ$, $V = 110$ KIAS, and then transitions to $\lambda = 50^\circ$, $V = 65$ KIAS (LORAS). Investigate trade-off of duct angle and trim pitch attitude by maintaining $V = 65$ KIAS, moving λ to 45° , 40° , back to 50° .
10. Disengage FBW. Engage VSS with gains as per #5 (reset Gold $\alpha = 22$, Gold q = 20, Gold u = 50, Gold SS = 18, Gold ES = 15). If desired, EP performs transition to $\lambda = 30^\circ$ to return to field, then transitions back to $\lambda = 50^\circ$.
11. EP samples A/C as SP varies Dutch roll damping (Blue r $\Rightarrow 50$), K_{osc}/K_{av} (Blue AC), and roll-to-sideslip ratio (Grey $\beta \Rightarrow 80, 60$: vary Grey r if required). Demonstrate gearings (AS) and stick limiting (Grey SL $\Rightarrow 99$, decrease AS to ~ 10 if necessary).

12. EP performs approaches from 2500 feet MSL at $\gamma = -9^\circ$, using mirror and/or TALAR for guidance information, performing wave-offs above 200 feet AGL.

13. Change longitudinal characteristics to:

Gold $\alpha = 55$

Gold $q = 62$

Gold $u = 72$

EP performs approaches from 2500 feet AGL using mirror and/or TALAR.

14. Disengage VSS. SP performs transition to hover and back to $\lambda = 30^\circ$, 80 KIAS. Return to field and perform STOL landing.

15. Perform "Post-Landing" and "Shutdown" checklists.

REFERENCES

1. Smith, R.E., Lebacqz, J.V., and Schuler, J.M.: "Flight Investigation of Various Longitudinal Short-Term Dynamics for STOL Landing Approach Using the X-22A Variable Stability Aircraft," CAL Report No. TB-3011-F-2, January 1973.
2. Beilman, J.L.: "An Integrated System of Airborne and Ground-Based Instrumentation for Flying Qualities Research with the X-22A Airplane," paper presented at the 28th Annual National Forum of the American Helicopter Society, May, 1972.
3. Chen, R.T.N., Eulrich, B.J., and Lebacqz, J.V.: "Development of Advanced Techniques for the Identification of V/STOL Aircraft Stability and Control Parameters," CAL Report No. BM-2820-F-1, August, 1971.
4. Smith, R.E., Lebacqz, J.V., and Radford, R.C.: "Flight Investigation of Lateral-Directional Flying Qualities and Control Power Requirements for STOL Landing Approach Using the X-22A Aircraft," draft submitted to NASC, June 20, 1973.
5. Lebacqz, J.V.: "Application of a Kalman Filter Identification Technique to Flight Data From the X-22A Variable Stability V/STOL Aircraft," paper presented at NASA Symposium on Parameter Estimation, April 24-25, 1973.
6. Gavin, T.J., and Till R.D.: "X-22A Fixed-Base Ground Simulator Facility," CAL Report No. AK-5113-F-1, January, 1973.
7. Aiken, E.W., and Schuler, J.M.: "A Fixed-Base Ground Simulator Study of Control and Display Requirements for VTOL Instrument Landings With a Decelerating Approach to a Hover," draft submitted to NASC, June 30, 1973.
8. Anon.: "LORAS II: Linear Omnidirectional Resolving Airspeed System - Manual of Installation and Operating Instructions," LORAS Instruments, Inc.
9. Scheuren, W.J., and Traskos, R.L.: "Phase II Military Preliminary Evaluation of the X-22A Variable Stability Research Aircraft; Final Report" Report No. FT-47R-69, 28 May 1969.
10. Anon.: "X-22A Tri-Service V/STOL Aircraft--Final Progress Report," Bell Aerospace Company, Report No. 2127-933073, December, 1969.

GLOSSARY OF SYMBOLS

AND ABBREVIATIONS

Symbol

F_{AS}	roll control stick force, positive right, lb
F_{Bo}	breakout force, lbs
F_{ES}	pitch control stick force, positive aft, lb
F_{RP}	rudder pedal control force, positive right, lb
h	rate of climb (or descent), ft/sec or ft/min
I_x	moment of inertia about body x -axis, ft-lb sec ²
I_y	moment of inertia about body y -axis, ft-lb sec ²
I_z	moment of inertia about body z -axis, ft-lb sec ²
I_{xz}	product of inertia in body axes, ft-lb sec ²
L	total aerodynamic rolling moment in body axes, ft-lb
L'	total aerodynamic rolling moment in primed axes, ft-lb $= (1 - I_{xz}^2 / I_x I_z)^{-1} (L + \frac{I_{xz}}{I_x} N)$
$L'_{()}$	$= (1 - I_{xz}^2 / I_x I_z)^{-1} (L_{()} + \frac{I_{xz}}{I_x} N_{()})$, (rad/sec ²) / ()
M	total aerodynamic pitching moment in body axes, ft-lb
$M_{()}$	$= \frac{1}{I_y} \frac{\partial M}{\partial ()}$, dimensional pitching moment derivative, (rad/sec ²) / ()
N	total aerodynamic yawing moment in body axes, ft-lb
N'	$= (1 - I_{xz}^2 / I_x I_z)^{-1} (N + \frac{I_{xz}}{I_z} L)$, total aerodynamic yawing moment in primed axes, ft-lb
$N'_{()}$	$= (1 - I_{xz}^2 / I_x I_z)^{-1} (N_{()} + \frac{I_{xz}}{I_z} L_{()})$, (rad/sec ²) / ()
$n_{()}$	body axes (x , y or z) acceleration, ft/sec ²
n_z/α	steady-state normal acceleration per angle of attack, g's/rad
p	body axes roll rate, deg/sec, rad/sec
q	body axes pitching rate, deg/sec, rad/sec
r	body axes yaw rate, deg/sec or rad/sec
s	Laplace transform variable, rad/sec

GLOSSARY OF SYMBOLS
AND ABBREVIATIONS (cont.)

<u>Symbol</u>	
t	time, seconds
u_0	trim velocity in body x -axis, ft/sec
u	velocity (also perturbation from trim) along body x -axis, ft/sec
u_L	velocity along body x -axis measured by u-LORAS, ft/sec
v	velocity (also perturbation from trim) along body y -axis, ft/sec
v_0	trim velocity, ft/sec or kts
w_0	trim velocity along body z -axis, ft/sec
w	velocity (also perturbation from trim) along z -axis, ft/sec
w_L	velocity along body z -axis measured by w-LORAS, ft/sec
X	total aerodynamic force along body x -axis, lb
$X_{()}$	$= \frac{1}{m} \frac{\partial X}{\partial ()}$, dimensional X-force derivative, ft/sec ² /()
Y	total aerodynamic force along body y -axis, lb
$Y_{()}$	$= \frac{1}{m} \frac{\partial Y}{\partial ()}$, dimensional Y-force derivative, ft/sec ² /()
Z	total aerodynamic force along body z -axis, lb
$Z_{()}$	$= \frac{1}{m} \frac{\partial Z}{\partial ()}$, dimensional Z-force derivative, ft/sec ² /()
α	angle of attack, degrees or radians
α_v	angle of attack measured by vane, degrees
β	angle of sideslip, degrees or radians
β_v	angle of sideslip measured by vane, degrees
$\beta_{()}$	average propeller blade angle in () duct
θ	glide slope angle, degrees
Δ_{ES}	displacement of safety pilot's pitch control, positive aft, inches
Δ_{RS}	displacement of safety pilot's roll control, positive right, inches

GLOSSARY OF SYMBOLS
AND ABBREVIATIONS (cont.)

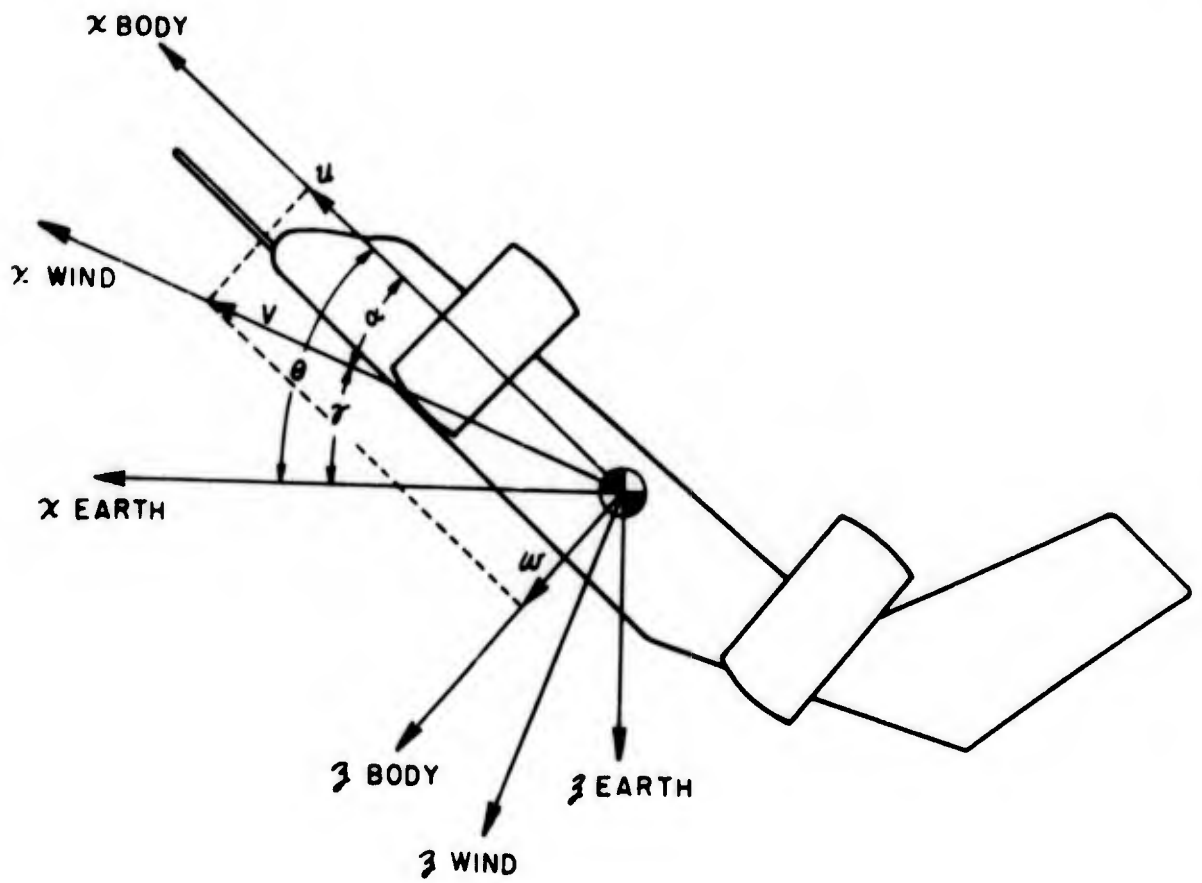
Symbol

Δ_{RP}	displacement of safety pilot's yaw control, positive right, inches
$\Delta'_{()}$	summation of VSS electrical command in () channel, inches
δ_C	collective control stick position, degrees
δ_{AS}	rolling moment control stick position, positive right, inches
δ_{ES}	pitching moment control stick position, positive aft, inches
δ_{RP}	yawing moment control pedal position, positive right, inches
ζ_d	damping ratio of Dutch roll characteristic roots
ζ_{FS}	damping ratio of feel system
ζ_{ST}	damping ratio of short period characteristic roots
θ	pitch attitude, degrees or radians
λ	X-22A duct angle, measured from horizontal, degrees
τ_R	roll mode time constant, sec
ϕ	roll angle, degrees or radians
ϕ/δ_{AS}	roll to aileron transfer function
$ \phi/\beta _d$	magnitude of roll-to-sideslip ratio in Dutch roll component
ω_d	undamped natural frequency of Dutch roll mode, rad/sec
ω_{FS}	undamped natural frequency of feel system, rad/sec
ω_p	undamped natural frequency of phugoid mode, rad/sec
ω_{ST}	undamped natural frequency of short period mode, rad/sec
$\dot{(\)}$	time rate of change of (), ()/sec
$()_0$	initial or trim value of (), ()
$()_L$	value measured by LORAS of (), ()

GLOSSARY OF SYMBOLS
AND ABBREVIATIONS (cont.)

Abbreviations

AGL	above ground level
CTOL	conventional takeoff and landing
IFR	instrument flight rules
ILS	instrument landing system
LORAS	low range airspeed system
SAS	stability augmentation system
VAA	visual approach aid
VFR	visual flight rules
VSS	variable stability system
deg	degrees (angle)
fpm	feet per minute
kt	knots (airspeed)
rms	root-mean-square
Hz	frequency (1 Hertz - 1 cycle per second)



BODY AXIS SYSTEM